DRBEM SOLUTIONS OF CAUCHY PROBLEM FOR THE MAGNETOHYDRODYNAMIC DUCT FLOW

A THESIS SUBMITTED TO
THE GRADUATE SCHOOL OF NATURAL AND APPLIED SCIENCES
OF
MIDDLE EAST TECHNICAL UNIVERSITY

BY

CEMRE AYDIN

IN PARTIAL FULFILLMENT OF THE REQUIREMENTS
FOR
THE DEGREE OF DOCTOR OF PHILOSOPHY
IN
MATHEMATICS

JANUARY 2020

Approval of the thesis:

DRBEM SOLUTIONS OF CAUCHY PROBLEM FOR THE MAGNETOHYDRODYNAMIC DUCT FLOW

submitted by **CEMRE AYDIN** in partial fulfillment of the requirements for the degree of **Doctor of Philosophy in Mathematics Department, Middle East Technical University** by,

Prof. Dr. Halil Kalıpçılar
Dean, Graduate School of **Natural and Applied Sciences** _____

Prof. Dr. Yıldıray Ozan
Head of Department, **Mathematics** _____

Prof. Dr. Münevver Tezer-Sezgin
Supervisor, **Department of Mathematics, METU** _____

Examining Committee Members:

Prof. Dr. Canan Bozkaya
Department of Mathematics, METU _____

Prof. Dr. Münevver Tezer-Sezgin
Department of Mathematics, METU _____

Prof. Dr. Nevzat Güneri Gençer
Department of Electrical and Electronics Engineering, METU _____

Prof. Dr. Tanıl Ergenç
Department of Mathematics, Atılım University _____

Prof. Dr. Selçuk Han Aydın
Department of Mathematics, Karadeniz Technical University _____

Date:

I hereby declare that all information in this document has been obtained and presented in accordance with academic rules and ethical conduct. I also declare that, as required by these rules and conduct, I have fully cited and referenced all material and results that are not original to this work.

Name, Surname: Cemre Aydın

Signature :

ABSTRACT

DRBEM SOLUTIONS OF CAUCHY PROBLEM FOR THE MAGNETOHYDRODYNAMIC DUCT FLOW

Aydın, Cemre
Ph.D., Department of Mathematics
Supervisor: Prof. Dr. Münevver Tezer-Sezgin

January 2020, 132 pages

In this thesis, the direct and inverse problems of the MHD flow in rectangular ducts are solved in terms of the velocity of the fluid and the induced magnetic field by using the Dual Reciprocity Boundary Element Method (DRBEM). The two-dimensional, steady flow of a viscous, incompressible, and electrically conducting fluid is considered under the effect of an externally applied mangetic field. The duct wall conditions for the MHD flow ranges from the no-slip to slip and insulated to perfectly conducting. In the DRBEM application, the fundamental solution of the Laplace equation is made use of transform the integral equations into boundary integral equations eliminating domain integral resulting from the inhomogeneity. The terms other than Laplacian are treated as inhomogeneity and they are approximated by using the radial basis functions which are related with the particular solution of the PDE through the Laplace operator.

The boundary inverse and parameter identification problems are considered as the two types of inverse problems for the MHD duct flow. In the boundary type inverse formulation, the aim is to calculate the slip length on the slipping boundary and the

conductivity constant on the variably conducting boundary. In the parameter identification, the parameter Hartmann number in the MHD flow equations is going to be redetermined for a preassigned velocity and induced magnetic field in the problem region. Since the inverse problems are ill-posed, the DRBEM is accompanied with three regularization techniques, namely, Tikhonov regularization, the direct-inverse iterations, and the well-posed iterations for obtaining the solution of the Cauchy MHD duct flow. The originality of this thesis lies in the construction and solution of the MHD duct flow problems as inverse problems.

Keywords: Magnetohydrodynamics, Dual Reciprocity Boundary Element Method, Slip Boundary Condition, Inverse Problems, Cauchy Problems

ÖZ

MAGNETOHİDRODİNAMİK KANAL AKIŞI İÇİN CAUCHY PROBLEMİNİN KARŞILIKLI SINIR ELEMANLARI METODU İLE ÇÖZÜMÜ

Aydın, Cemre
Doktora, Matematik Bölümü
Tez Yöneticisi: Prof. Dr. Münevver Tezer-Sezgin

Ocak 2020 , 132 sayfa

Bu tezde, kanallardaki MHD akış probleminin direkt ve ters formülasyonları sıvının hızı ve indüklenen manyetik alan cinsinden karşılıklı sınır elemanları metodu (DRBEM) kullanılarak çözülmüştür. İki boyutlu, zamandan bağımsız, yoğunluğu fazla olan, sıkıştırılamaz, elektriksel iletkenliği olan sıvının akışı uygulanan dış manyetik alan etkisinde incelenmiştir. Kanalın sınır koşulları kaymayandan kayana ve yalıtkandan iletkene olacak şekilde değişmektedir. DRBEM uygulamasında, integral denklemlerinin sınır integral denklemlerine dönüştürülmesi için Laplace denkleminin temel çözümü kullanılmıştır. Laplace haricindeki terimlere özel çözümlere Laplace operatörü ile bağlantılı olan radyal baz fonksiyonları kullanılarak yaklaşılmıştır.

Sınır tipinde ve parametre belirleme tipinde ters problemler, MHD kanal akış problemlerinde ters problem inşa etmede göz önünde bulundurulmuştur. Sınır tipindeki ters problemlerde, amaç kayan duvarlarda kayma uzunluğunu hesaplamak ve değişken iletken duvarlarda iletkenlik kat sayısını bulmaktır. Parametre tipindeki ters problemlerde, MHD diferansiyel denklemlerindeki Hartmann sayısı belirlenmiş hız ve in-

düklenen manyetik alan değerleri için hesaplanmıştır. Ters problemler kötü koşullu olduğundan; DRBEM, Tikhonov düzenlileştirmesi, direkt-ters iterasyonlar ve iyi tanımlı iterasyonlar ile kullanılarak Cauchy MHD kanal akış problemleri çözülmüştür. Bu tezdeki orjinallik, MHD akış problemlerini ters problemler olarak inşa etmek ve çözmektir.

Anahtar Kelimeler: Magnetohidrodinamik, Karşılıklı Sınır Elemanları Metodu, Kayma Sınır Koşulu, Ters Problemler, Cauchy Problemleri

To my family

ACKNOWLEDGMENTS

First, I would like to express my deepest gratitude to my research supervisor Prof. Dr. Münevver Tezer-Sezgin for her precious guidance, encouragement, and patience during this research period. Her enthusiastic motivation and support make this thesis possible. I will always remember her suggestions and guidance during my life.

I would also like to thank my defense committee members Prof. Dr. Canan Bozkaya, Prof. Dr. Nevzat Güneri Gençer, Prof. Dr. Tanıl Ergenç, and Prof. Dr. Selçuk Han Aydın for their valuable suggestions. My gratitude is extended to Assoc. Prof. Dr. Mehmetçik Pamuk and Assist. Prof. Dr. Semra Pamuk for their wortful advices and motivation throughout my studies.

I am deeply indebted to my friends Cansu Aktepe İlter, Hakan Genç, Gülden Budak, Murat Burhan İlter, and Sura İmren for their kind friendship and making my life more colorful. I especially thank Merve Gürbüz and Elif Ebren Kaya for their honest companionship and their help while writing process of the thesis.

My sincerest thanks belong to my mother Saliha and my father Mehmet for their endless love and motivation which provide me success and happiness in my whole life. They were always with me in all the stages of my academic and social life. I also thank to my grandmother Asiye for her support from my childhood to now.

I want to show my heartfelt gratitude to my fiance Mahmut for his continous encouragement, understanding, and being always with me.

TABLE OF CONTENTS

ABSTRACT v

ÖZ vii

ACKNOWLEDGMENTS x

TABLE OF CONTENTS xi

LIST OF TABLES xiv

LIST OF FIGURES xv

LIST OF ABBREVIATIONS xxi

CHAPTERS

1 INTRODUCTION 1

1.1 MHD Duct Flow with Slipping Velocity and Variable Conductivity Condition 4

1.2 Literature Survey 8

1.3 Originality in the Thesis 17

1.4 Plan of the Thesis 18

2 THE DUAL RECIPROCITY BOUNDARY ELEMENT METHOD FOR THE DIRECT AND INVERSE PROBLEMS 21

2.1 BEM Solution of Poisson's Equation $\nabla^2 u = b(x, y)$ 22

2.2 DRBEM Solution of Poisson's Equation $\nabla^2 u = b(x, y)$ 24

2.3 DRBEM Solution of Cauchy Problem 32

2.3.1 DRBEM Solution of Poisson's Equation as an Inverse Problem 33

2.4 Regularization Techniques 34

2.4.1 Tikhonov Regularization 34

2.4.2 Direct-Inverse Iterations for Poisson's Equation 35

2.4.3 The Well-posed Iterations for Poisson's Equation 36

3 DRBEM SOLUTION OF DIRECT AND INVERSE MHD DUCT FLOW PROBLEMS 39

3.1 MHD Direct and Cauchy Problems 39

3.2 DRBEM Solution of Direct MHD Duct Flow Problem 39

3.3 DRBEM Solution of MHD Duct Flow Equations as an Inverse Problem 43

3.4 Parameter Identification for the MHD Duct Flow 45

3.5 Regularization Techniques for Cauchy MHD Duct Flow 46

3.5.1 The Direct-Inverse Iterations for Cauchy MHD Duct Flow . . 46

3.5.2 The Well-posed Iterations for Cauchy MHD Duct Flow 48

3.6 DRBEM Application to the Cauchy MHD Flow with a Slip Velocity Duct Wall 48

3.7 DRBEM Application to the Cauchy MHD Flow with a Slipping and Variably Conducting Duct Wall 53

3.8 DRBEM Application to the Cauchy MHD Flow in a Duct with a Slipping Perturbed Upper Boundary 55

3.8.1 Asymptotic Analysis 56

3.8.2 The inverse formulations 59

3.9 Application of the DRBEM to Parameter Identification in MHD Duct Flow Cauchy Problem 60

3.9.1 Parameter Identification - Problem 1 60

3.9.2 Parameter Identification - Problem 2 61

3.9.3 Parameter Identification - Problem 3 62

3.9.4 Parameter Identification - Problem 4 63

3.9.5 Parameter Identification - Problem 5 63

3.9.6 Solution Procedure 64

4 NUMERICAL RESULTS OF THE DIRECT AND CAUCHY MHD DUCT FLOW WITH SLIP AND VARIABLE CONDUCTIVITY CONDITIONS . 67

4.1 The Cauchy MHD Flow With Slipping and Variably Conducting Duct Walls 68

4.1.1 MHD duct flow - Problem 1 69

4.1.2 MHD duct flow - Problem 2 77

4.1.3 MHD duct flow - Problem 3 84

4.2 The Cauchy MHD Duct Flow with a Slipping Perturbed Upper Boundary, Problem 4 94

4.3 Parameter Identification in MHD Duct Flow Cauchy Problem 105

4.3.1 Parameter Identification - Problem 1 106

4.3.2 Parameter Identification - Problem 2 109

4.3.3 Parameter Identification - Problem 3 111

4.3.4 Parameter Identification - Problem 4 114

4.3.5 Parameter Identification - Problem 5 116

5 CONCLUSION 119

REFERENCES 121

CURRICULUM VITAE 131

LIST OF TABLES

TABLES

Table 4.1 MHD duct flow - Problem 3: Velocity and induced magnetic field values from the inverse solution at the point $(-1, 0)$, $Ha = 10, \beta = \frac{\pi}{2}, \alpha = 0.2, c = 0.3$. 92

Table 4.2 Parameter Identification - Problem 1: The maximum errors in Ha, $\alpha = c = 0$. 108

Table 4.3 Parameter Identification - Problem 2: The maximum errors in Ha, $\alpha = 0$, c is large on Hartmann walls. 110

Table 4.4 The maximum errors in Ha, $\alpha = 0$, $c = 0.3$ Prob. 3 112

Table 4.5 Parameter Identification - Problem 3: The maximum errors in Ha, $\alpha = 0$, $c = 1$. 113

Table 4.6 Parameter Identification - Problem 3: The maximum errors in Ha, $\alpha = 0$, $c = 2$. 113

Table 4.7 Parameter Identification - Problem 3: The maximum errors in Ha, $\alpha = 0$, $c = 5$. 113

Table 4.8 Parameter Identification - Problem 4: The maximum errors in Ha, $\alpha = 0.2$, $c = 0$. 115

Table 4.9 Parameter Identification - Problem 5: The maximum errors in Ha, $\alpha = 0.2$, $c = 5$. 117

LIST OF FIGURES

FIGURES

Figure 2.1 Constant boundary elements 26

Figure 3.1 Boundary Conditions for the Direct MHD Duct Flow 40

Figure 3.2 Problem 1. Left wall is slipping. Boundary conditions for the direct (left) and the Cauchy (right) problems. 49

Figure 3.3 Problem 2. Bottom wall is slipping. Boundary conditions for the direct (left) and the Cauchy (right) problems. 50

Figure 3.4 Problem 3. Left wall is both slipping and variably conducting. Boundary conditions for the direct (left) and the Cauchy (right) problems. $\tilde{V}$, $\tilde{B}$ denote direct problem solution. 53

Figure 3.5 Problem 4. Upper wall is perturbed and slipping. Boundary conditions for the direct problem. 56

Figure 3.6 Problem 1. Boundary conditions for the direct (left) and the inverse (right) problems. 61

Figure 3.7 Problem 2. Boundary conditions for the direct (left) and the inverse (right) problems. 62

Figure 3.8 Problem 3. Boundary conditions for the direct (left) and the inverse (right) problems. 62

Figure 3.9 Problem 4. Boundary conditions for the direct (left) and the inverse (right) problems. 63

Figure 3.10 Problem 5. Boundary conditions for the direct (left) and the inverse (right) problems. 64

Figure 4.1 Fluid flow configuration under the applied uniform magnetic field. 68

Figure 4.2 MHD duct flow - Problem 1: Boundary conditions for the direct (left) and the Cauchy (right) problems. Left wall is slipping. 69

Figure 4.3 MHD duct flow - Problem 1: Velocity and induced magnetic field profiles from direct problem, $\alpha = 0.2$, $k = 0$ 70

Figure 4.4 MHD duct flow - Problem 1: Velocity and induced magnetic field profiles from direct problem, $\alpha = 0.2$, $k = 1$. 70

Figure 4.5 MHD duct flow - Problem 1: Velocity profiles from inverse solution, $k = 0$. 72

Figure 4.6 MHD duct flow - Problem 1: Velocity profiles from inverse solution, $k = 1$. 73

Figure 4.7 MHD duct flow - Problem 1: Induced magnetic field profiles from inverse solution, $k = 0$. 74

Figure 4.8 MHD duct flow - Problem 1: Induced magnetic field profiles from inverse solution, $k = 1$. 75

Figure 4.9 MHD duct flow - Problem 1: Slip lengths, Ha=10, $k = 0$, $k = 1$. 76

Figure 4.10 MHD duct flow - Problem 1: Error in slip length, Ha=10, $k = 0$, $k = 1$. 76

Figure 4.11 MHD duct flow - Problem 2: Boundary conditions for the direct (left) and the Cauchy (right) problems. 77

Figure 4.12 MHD duct flow - Problem 2: Velocity and induced magnetic field profiles from direct problem, $\alpha = 0.2$, $k = 0$. 78

Figure 4.13 MHD duct flow - Problem 2: Velocity and induced magnetic field profiles from direct problem, $\alpha = 0.2$, $k = 1$. 78

Figure 4.14 MHD duct flow - Problem 2: Velocity profiles from inverse solution, $k = 0$. 80

Figure 4.15 MHD duct flow - Problem 2: Velocity profiles from inverse solution, $k = 1$. 81

Figure 4.16 MHD duct flow - Problem 2: Induced magnetic field profiles from inverse solution, $k = 0$. 82

Figure 4.17 MHD duct flow - Problem 2: Induced magnetic field profiles from inverse solution, $k = 1$. 83

Figure 4.18 MHD duct flow - Problem 2: Slip lengths, Ha=10, $k = 0$, $k = 1$. 84

Figure 4.19 MHD duct flow - Problem 3: Boundary conditions for the direct (left) and the Cauchy (right) problems. $\tilde{V}$, $\tilde{B}$ denote direct problem solution. 85

Figure 4.20 MHD duct flow - Problem 3: Velocity and induced magnetic field from direct solution, $\beta = \frac{\pi}{2}, \alpha = 0.2, c = 0.3, Ha = 10$. 87

Figure 4.21 MHD duct flow - Problem 3: Velocity and induced magnetic field from direct problem, $\beta = 0, \alpha = 0.2, c = 0.3$. 87

Figure 4.22 MHD duct flow - Problem 3: Velocity and induced magnetic field from inverse solution, $\beta = 0$ 88

Figure 4.23 MHD duct flow - Problem 3: Velocity and induced magnetic field from direct problem, $\beta = \frac{\pi}{2}, \alpha = 0.2, c = 0.3$. 88

Figure 4.24 MHD duct flow - Problem 3: Velocity and induced magnetic field from inverse solution, $\beta = \frac{\pi}{2}$ 89

Figure 4.25 MHD duct flow - Problem 3: Velocity and induced magnetic field from direct problem, $\beta = \frac{\pi}{4}, \alpha = 0.2, c = 0.3$. 90

Figure 4.26 MHD duct flow - Problem 3: Velocity and induced magnetic field from inverse solution, $\beta = \frac{\pi}{4}$ 90

Figure 4.27 MHD duct flow - Problem 3: Velocity and induced magnetic field from direct problem, $\beta = \frac{\pi}{3}, \alpha = 0.2, c = 0.3$. 91

Figure 4.28 MHD duct flow - Problem 3: Velocity and induced magnetic field from inverse solution, $\beta = \frac{\pi}{3}$ 91

Figure 4.29 MHD duct flow - Problem 3: $\beta = 0$, $x = -1$. 93

Figure 4.30 MHD duct flow - Problem 3: $\beta = \frac{\pi}{4}$, $x = -1$. 93

Figure 4.31 MHD duct flow - Problem 3: $\beta = \frac{\pi}{3}$, $x = -1$. 94

Figure 4.32 MHD duct flow - Problem 3: $\beta = \frac{\pi}{2}$, $x = -1$. 94

Figure 4.33 MHD Duct Flow-Problem 4, Boundary conditions for the direct problem. Upper wall is perturbed and slipping. 96

Figure 4.34 MHD Duct Flow-Problem 4, Boundary conditions for the inverse problem. Upper wall is perturbed and slipping. 96

Figure 4.35 Problem 4. Velocity , $Ha = 5$, $\alpha = 0$, $\epsilon = 0.1$, $f(x) = -cos(\frac{\pi x}{4})$, $f(r) = 1 + r$. 97

Figure 4.36 Problem 4. Velocity and induced magnetic field from direct problem, $Ha = 5$, $\alpha = 0$, $f(x) = -cos(\frac{2\pi x}{3})$, $\epsilon = 0.1$, $f(r) = 1 + r$. . 98

Figure 4.37 Problem 4. Velocity and induced magnetic field from direct problem, $Ha = 5$, $\alpha = 0.2$, $f(x) = -cos(\frac{2\pi x}{3})$, $f(r) = 1 + r$. 98

Figure 4.38 Problem 4. Velocity and induced magnetic field from inverse formulation, $Ha = 5$, $f(x) = -cos(\frac{2\pi x}{3})$, $f(r) = 1 + r$. 100

Figure 4.39 Problem 4. Velocity and induced magnetic field from inverse formulation, $Ha = 5$, $\alpha = 0.2$, $f(x) = -cos(\frac{2\pi x}{3})$, $f(r) = 1 + r + r^2$. 100

Figure 4.40 Problem 4. Velocity and induced magnetic field from inverse formulation, $Ha = 5$, $\alpha = 0.2$, $\epsilon = 0.1$, $f(x) = -cos(\frac{2\pi x}{3})$. 101

Figure 4.41 Problem 4. Velocity and induced magnetic field from direct problem, $Ha = 10$, $\alpha = 0.2$, $f(x) = -cos(\frac{2\pi x}{3})$, $f(r) = 1 + r$. 101

Figure 4.42 Problem 4. Velocity and induced magnetic field from inverse formulation, $Ha = 10$, $f(x) = -cos(\frac{2\pi x}{3})$, $f(r) = 1 + r$. 102

Figure 4.43 Problem 4. Velocity and induced magnetic field from direct problem, $Ha = 5$, $\alpha = 0.2$, $f(x) = -(1 - x^2)cos(2\pi x)$, $f(r) = 1 + r$. . 102

Figure 4.44 Problem 4. Velocity and induced magnetic field from inverse formulation, $Ha = 5$, $f(x) = -(1 - x^2)cos(2\pi x)$, $f(r) = 1 + r$. 103

Figure 4.45 Problem 4. Velocity and induced magnetic field from direct problem, $Ha = 5$, $\alpha = 0.2$, $f(x) = -cos(\frac{\pi x}{4})$, $f(r) = 1 + r$. 103

Figure 4.46 Velocity and induced magnetic field from inverse formulation, $Ha = 5$, $\alpha = 0.2$, $f(x) = -cos(\frac{\pi x}{4})$, $f(r) = 1 + r$. 104

Figure 4.47 Reseized slip lengths, $Ha = 5$, $f(x) = -cos(\frac{2\pi x}{3})$ 104

Figure 4.48 Parameter Identification - Problem 1: Boundary conditions for the direct (left) and the inverse (right) problems. 107

Figure 4.49 Parameter Identification - Problem 1: Velocity and induced magnetic fiel, $\alpha = c = 0$ (direct solution). 108

Figure 4.50 Problem 2: Boundary conditions for the direct (left) and the inverse (right) problems. 109

Figure 4.51 Parameter Identification - Problem 2: Velocity and induced magnetic field, $\alpha = 0$, c is large on the Hartmann walls(direct solution). . . . 110

Figure 4.52 Problem 3: Boundary conditions for the direct (left) and the inverse (right) problems. 111

Figure 4.53 Parameter Identification - Problem 3: Velocity and induced magnetic field for $Ha = 10$, $\alpha = 0$ (direct solution). 112

Figure 4.54 Problem 4: Boundary conditions for the direct (left) and the inverse (right) problems. 114

Figure 4.55 Parameter Identification - Problem 4: Velocity and induced magnetic field for $Ha = 10$, $c = 0$ (direct solution). 115

Figure 4.56 Problem 5: Boundary conditions for the direct (left) and the inverse (right) problems. 116

Figure 4.57 Parameter Identification - Problem 5: Velocity and induced magnetic field profiles, $\alpha = 0.2$, $c = 1$. 116

LIST OF ABBREVIATIONS

ABBREVIATIONS

BEM	Boundary element method
DRBEM	Dual reciprocity boundary element method
MHD	Magnetohydrodynamics
$\boldsymbol{B}$	induced magnetic field
B_0	magnetic field intensity
c	conductivity parameter
E	electric field intensity
J	electric current density
$\boldsymbol{\mathcal{H}}$	Magnetic field intensity
H, G	BEM matrices
F	coordinate matrix
f	radial basis functions
Ha	Hartmann number
$\boldsymbol{n}$	unit outward normal to the boundary
L_0	characteristic length
p	pressure
$\boldsymbol{V}$	velocity of the fluid
λ	regularization parameter
α	slip length
β	angle with the y-axis
ϵ	perturbation parameter
σ	electrical conductivity
μ	dynamic viscosity

μ_ϵ	magnetic permeability
ν	kinematic viscosity
Ω	problem domain
Γ	boundary of the problem domain
x, y, z	Cartesian coordinates

CHAPTER 1

INTRODUCTION

Ordinary and partial differential equations with suitable boundary information represent the mathematical model of some engineering and physical problems. In general, obtaining the analytical or the close-form solutions of PDEs is possible only for some simple problems in simplified geometries. On the other hand, the numerical solutions can be obtained for partial differential equations due to their complexity.

The most common and popular numerical techniques for the approximate solutions of PDEs are Finite Difference Method (FDM), Finite Element Method (FEM), the Boundary Element Method (BEM), and the Dual Reciprocity Boundary Element Method (DRBEM). The type of the approximation of the variables, the discretization of the domain of the problem, and the computational cost of the technique are the main differences between the numerical methods.

In the Finite Difference Method, the derivatives of the unknowns in the governing differential equations are represented with the truncated Taylor series expansions. A system of algebraic equations are obtained when the derivatives of the unknowns are replaced with the finite differences by inserting the given boundary informations. In general, the usage of the Finite Difference Method is easy for the discretization of the internal region. On the other hand, the main difficulty of the method occurs while discretizing the curved boundaries and inserting boundary conditions which involve derivatives. However, the Finite Difference Method is still used to get approximate solutions of many problems since coding the FDM is a simple and practical procedure to generate the system of algebraic equations and also, it has an economical cost.

Finite Element method presents a better representation of the geometry of the prob-

lem region and eases inserting the boundary conditions. In FEM, the domain of the problem is divided into small portions called as elements. By using the polynomial interpolation functions, the terms in the governing differential equations are approximated over the small portions of the region. A global matrix for the equations is obtained by assembling the influence matrices which includes the properties of each element. Evaluating the boundary integrals yields the insertion of boundary conditions. Consequently, inserting the boundary conditions in the Finite Element method is easier than the Finite Difference Method. However, there are some disadvantages of FEM in discretizing the domain of the problem region which increases the size of the system of algebraic equations causing higher computational cost although the system matrix is sparse. In addition, some difficulties occur when the domain of the problem is infinite.

The boundary element method which is a well-established numerical technique has crucial advantages over the domain type discretization techniques, FEM and FDM which are mentioned above. The starting point of the method is transforming the partial differential equation which is related to unknown in the problem domain and on its boundary into the corresponding integral equation which is defined only on the boundary. This boundary integral equation includes the values of the unknown solution and their normal derivatives on the boundary. The boundary-only nature is the primary advantage of the Boundary Element Method. This means that only the boundary is discretized and hence the dimension of the problem is reduced to one-dimension giving a smaller size system of algebraic equations but not sparse when compared to other domain type discretization methods. Solving the BEM resulting system of equations gives the unknown values and their normal derivatives on the boundary. In addition, the solution in the interior of the domain can be calculated by using these boundary values. Also, the BEM is suitable for the problems having infinite domain and moving boundaries.

The Boundary Element Method dates back to 1960's. A small group of researchers worked on some applications of boundary integral equations to stress analysis and the potantial flow. Then, the BEM became an excellent alternative to the domain type discretization methods, such as FDM and FEM. In 1978, Brebbia and his colleagues [1, 2, 3] introduced the today's definition of the boundary element method. Baner-

jee and Butterfield [4] represent the first comprehensive study on the BEM and its applications in the engineering science in their book. The BEM has been a popular technique in many applications of engineering such as fluid mechanics, inelastic problems, elastodynamics, electrodynamics, and magnetohydrodynamics. The Boundary Element Method is a very advantegous numerical technique in the case of the availability of the fundamental solution of the partial differential equation. On the other hand, because of some nonhomogenous, nonlinear, and convection-reaction terms of the governing differential equation, it may be needed to evaluate domain integrals which requires an extra domain discretization. In this case, the boundary-only nature property which is the main advantage of the BEM is destroyed. Hence, another approach should be used to overcome the computation of the domain integrals. The Fourier expansions technique, Galerkin vector method, the multiple reciprocity and the Dual Reciprocity Boundary Element Method are the most common techniques to deal with the domain integrals [5].

In this thesis, the Dual Reciprocity Boundary Element Method is used as a numerical solution technique. Nardini and Brebbia [6] introduced the DRBEM, and this method was broadened by Brebbia, Wrobel, and Partridge [7, 8]. The DRBEM uses a fundamental solution of the simpler equation, and the other terms are treated as an inhomogeneity. Hence, this method is useful in solving the nonhomogenous, nonlinear, and also time-dependent problems. In the DRBEM, the crucial point is to determine the simple form of the governing differential equation whose fundamental solution is available. In general, the DRBEM uses the fundamental solution of Laplace equation to obtain the Poisson's equation. There are applications of DRBEM by using fundamental solutions of Helmholtz and modified Helmholtz equations [9, 10]. Here, all the terms other than the Laplacian term of the corresponding differential equation are considered as inhomogeneity. Also, to decrease the interpolation error in the computations, the inhomogenous part of the governing partial differential equation should contain simple components such as linear terms.

In the thesis, some Magnetohydrodynamics (MHD) duct flow direct and inverse problems are solved by employing the DRBEM for the direct and inverse formulations. The governing equations of the MHD duct flow problems are of convection-diffusion type. The fundamental solution of Laplace equation is used in the application of

the DRBEM by considering the convection-diffusion terms as inhomogeneity in the governing equations. The most general boundary conditions as the slip-velocity and variably conducting induced magnetic field imposed for both the direct and inverse MHD duct flow as explained in the next section together with the construction of the MHD duct flow equations.

1.1 MHD Duct Flow with Slipping Velocity and Variable Conductivity Condition

Magnetohydrodynamic flow has many industrial and biological applications such as MHD pumps, MHD generators, cooling of nuclear fusion apparatus, flow meters, and measuring the blood flow pressure. The analytical solutions of MHD equations are available only for some special geometries of problem region and boundary conditions [11].

In this thesis, the governing equations of magnetohydrodynamic flow are derived in the 2D or two-dimensional cross-section of long channels which are named as rectangular ducts. The MHD duct flow equations are accompanied with the duct wall conditions ranging from no-slip to slipping and insulated to conducting. Hence, the derivation of the equations for the MHD duct flow problems are given as in Dragoş [11] and Shercliff [12].

A fully developed, steady, and pressure driven fluid flow is considered in a rectangular duct. The fluid is taken as viscous, incompressible and having uniform electrical conductivity. A uniform magnetic field of intensity $\mathcal{H}_0$ is applied perpendicular to the channel axis forming an angle β with the y-axis. Since the flow is fully-developed, there is no variation of the fluid movement and induced magnetic field in the channel axis direction but they are subjected to change on the cross-section of the channel which is a rectangular region in the xy- plane.

All of the physical quantities (except pressure), are independent of z, and the velocity $\boldsymbol{V}$ and the induced magnetic field have only z-components. Thus $\boldsymbol{V} = (0, 0, V_z(x, y))$ and $\boldsymbol{\mathcal{H}} = (\mathcal{H}_x, \mathcal{H}_y, \mathcal{H}_z(x, y))$ where $\mathcal{H}_x = \mathcal{H}_0 sin\beta$ and $\mathcal{H}_y = \mathcal{H}_0 cos\beta$. In addition, we assume that displacement currents are negligible.

In the steady-state case, on neglecting displacement currents, Maxwell's equations corresponding to the electrodynamic field are stated as [11]

$$\nabla \times \mathbf{E} = 0 \tag{1.1}$$

$$\nabla \times \boldsymbol{\mathcal{H}} = \mathbf{J} \tag{1.2}$$

$$\nabla . \boldsymbol{\mathcal{H}} = 0 \tag{1.3}$$

where $\mathbf{E}$ is the electric field intensity and $\mathbf{J}$ is the electric current density.

By taking the curl of the Ohm's law, which is given as

$$\mathbf{J} = \sigma(\mathbf{E} + \mu_\epsilon \boldsymbol{V} \times \boldsymbol{\mathcal{H}}) \tag{1.4}$$

where σ is the electrical conductivity and μ_ϵ is the magnetic permeability. Since σ and μ_ϵ are uniform, using equations (1.1) and (1.2), we get the following equation

$$\nabla \times \mathbf{J} = \nabla \times (\nabla \times \boldsymbol{\mathcal{H}}) = \sigma \mu_\epsilon \nabla \times (\mathbf{V} \times \boldsymbol{\mathcal{H}}). \tag{1.5}$$

By using the following two vector identities

$$\nabla \times (\nabla \times \boldsymbol{\mathcal{H}}) = \nabla(\nabla . \boldsymbol{\mathcal{H}}) - \nabla^2 \boldsymbol{\mathcal{H}} \tag{1.6}$$

and

$$\nabla \times (\boldsymbol{V} \times \boldsymbol{\mathcal{H}}) = (\boldsymbol{\mathcal{H}} . \nabla)\boldsymbol{V} - (\boldsymbol{V} . \nabla)\boldsymbol{\mathcal{H}} + \boldsymbol{V} \nabla . \boldsymbol{\mathcal{H}} - \boldsymbol{\mathcal{H}} \nabla . \boldsymbol{V} \tag{1.7}$$

and noting that the divergences of $\boldsymbol{\mathcal{H}}$ and $\boldsymbol{V}$ vanish since μ_e is constant and the fluid is incompressible, the following equation for the induced magnetic field

$$\nabla^2 \boldsymbol{\mathcal{H}} + \sigma \mu_\epsilon [(\boldsymbol{\mathcal{H}} . \nabla)\boldsymbol{V} - (\boldsymbol{V} . \nabla)\boldsymbol{\mathcal{H}}] = 0 \tag{1.8}$$

is obtained.

The steady Navier-Stokes equation for the steady-state in the lack of the body forces is defined as (since $\nabla . \boldsymbol{V} = 0$) [12]

$$\boldsymbol{F}^{em} - \nabla p + \mu \nabla^2 \boldsymbol{V} = \rho (\boldsymbol{V} . \nabla)\boldsymbol{V}. \tag{1.9}$$

where the electromagnetic force $\boldsymbol{F}^{em}$ is reduced to the Lorentz force $\boldsymbol{J}\times\mu_\epsilon\boldsymbol{\mathcal{H}}$ when the medium is simple. From equations (1.7) and (1.9), the following equation is obtained as

$$\mu_\epsilon(\nabla\times\boldsymbol{\mathcal{H}})\times\boldsymbol{\mathcal{H}}-\nabla p+\mu\nabla^2\boldsymbol{V}=\rho(\boldsymbol{V}.\nabla)\boldsymbol{V} \tag{1.10}$$

where μ is the coefficient of viscosity and ρ is the density of the fluid, and p is the pressure.

The equation (1.10) can be rewritten as

$$\mu_\epsilon(\boldsymbol{\mathcal{H}}.\nabla)\boldsymbol{\mathcal{H}}-\mu_\epsilon\frac{1}{2}\nabla|\boldsymbol{\mathcal{H}}|^2-\nabla p+\mu\nabla^2\boldsymbol{V}=\rho(\boldsymbol{V}.\nabla)\boldsymbol{V} \tag{1.11}$$

since

$$(\nabla\times\boldsymbol{\mathcal{H}})\times\boldsymbol{\mathcal{H}}=(\boldsymbol{\mathcal{H}}.\nabla)\boldsymbol{\mathcal{H}}-\frac{1}{2}\nabla|\boldsymbol{\mathcal{H}}|^2. \tag{1.12}$$

When equation (1.11) is differentiated with respect to z, $\nabla(\partial p/\partial z)$ vanishes, due to the invariant condition in the z-direction. Therefore $\partial p/\partial z$ is constant.

We have $J_z=0$, $\boldsymbol{\mathcal{H}}.\nabla=\boldsymbol{\mathcal{H}}_x\dfrac{\partial}{\partial x}+\boldsymbol{\mathcal{H}}_y\dfrac{\partial}{\partial y}$, and $\boldsymbol{V}.\nabla=0$. Since $V_x=0$, $V_y=0$, $\mathcal{H}_x=\boldsymbol{\mathcal{H}}_0 sin\beta$, $\boldsymbol{\mathcal{H}}_y=\boldsymbol{\mathcal{H}}_0 cos\beta$ where $\boldsymbol{\mathcal{H}}_0$ is a constant.

Hence, the z-components of equations (1.11) and (1.8) become

$$\begin{aligned}&\mu\nabla^2V_z+\mu_\epsilon\mathcal{H}_0 sin\beta\frac{\partial\mathcal{H}_z}{\partial x}+\mu_\epsilon\mathcal{H}_0 cos\beta\frac{\partial\mathcal{H}_z}{\partial y}=\frac{\partial p}{\partial z}\\&\nabla^2\mathcal{H}_z+\sigma\mu_\epsilon\mathcal{H}_0 sin\alpha\frac{\partial V_z}{\partial x}+\sigma\mu_\epsilon\mathcal{H}_0 cos\beta\frac{\partial V_z}{\partial y}=0.\end{aligned} \tag{1.13}$$

By taking $\eta=\dfrac{1}{\sigma\mu_\epsilon}$, which is called as magnetic diffusivity and using the relationships

$$\mathbf{B}=\mu_\epsilon\boldsymbol{\mathcal{H}},\quad \mathbf{B}_0=\mu_0\boldsymbol{\mathcal{H}_0} \tag{1.14}$$

equation (1.13) can be written in terms of induced magnetic field **B**

$$\begin{aligned}&\mu\nabla^2V_z+\mu_\epsilon\mathcal{H}_0 sin\beta\frac{\partial\mathcal{H}_z}{\partial x}+\mu_\epsilon\mathcal{H}_0 cos\beta\frac{\partial\mathcal{H}_z}{\partial y}=\frac{\partial p}{\partial z}\\&\eta\nabla^2\mathcal{H}_z+\mathcal{H}_0 sin\beta\frac{\partial V_z}{\partial x}+\mathcal{H}_0 cos\beta\frac{\partial V_z}{\partial y}=0\end{aligned} \tag{1.15}$$

and

$$\begin{aligned}\mu\nabla^2 V_z + \frac{B_0}{\mu_\epsilon} sin\beta \frac{\partial B_z}{\partial x} + \frac{B_0}{\mu_\epsilon} cos\beta \frac{\partial B_z}{\partial y} = \frac{\partial p}{\partial z} \\ \eta\nabla^2 B_z + B_0 sin\beta \frac{\partial V_z}{\partial x} + B_0 cos\beta \frac{\partial V_z}{\partial y} = 0\end{aligned} \tag{1.16}$$

where B_0 is the intensity of the imposed magnetic field.

Introducing non-dimensional variables as

$$V = \frac{1}{V_0} V_z, \quad B = \frac{1}{V_0 \mu_\epsilon} (\sigma\mu)^{-1/2} B_z, \quad x' = \frac{x}{L_0}, \quad y' = \frac{y}{L_0} \tag{1.17}$$

where

$$V_0 = -L_0^2 (\frac{\partial p}{\partial z})/\mu \tag{1.18}$$

is the characteristic velocity and L_0 is the characteristic length and dropping 'prime' sign, we arrive at

$$\begin{aligned}\nabla^2 V + Hasin\beta \frac{\partial B}{\partial x} + Hacos\beta \frac{\partial B}{\partial y} = -1 \\ \nabla^2 B + Hasin\beta \frac{\partial V}{\partial x} + Hacos\beta \frac{\partial V}{\partial y} = 0\end{aligned} \tag{1.19}$$

In equations (1.19)

$$Ha = \frac{B_0 L_0 \sqrt{\sigma}}{\sqrt{\mu}} \tag{1.20}$$

is the Hartmann number which represents the ratio of the electromagnetic force to the viscous force [16].

The Hartmann number Ha is the magnitude of the vector $Ha = (Ha_x, Ha_y)$ where

$$\begin{aligned}Ha_x = Hasin\beta \\ Ha_y = Hacos\beta.\end{aligned} \tag{1.21}$$

Then, equation (1.19) can be rewritten as follows

$$\begin{aligned}\nabla^2 V + Ha_x \frac{\partial B}{\partial x} + Ha_y \frac{\partial B}{\partial y} = -1 \\ \nabla^2 B + Ha_x \frac{\partial V}{\partial x} + Ha_y \frac{\partial V}{\partial y} = 0.\end{aligned} \tag{1.22}$$

These equations describe coupled MHD flow equations which are second order linear convection-diffusion type partial differential equations. For each problem considered

in this thesis as direct or inverse problem, the geometry, the related boundary conditions and the direction of the applied magnetic field are explained in Section 3.

If the mixed (or Robin) type boundary condition is specified for the velocity of the fluid as

$$V + \alpha \frac{\partial V}{\partial n} = 0, \tag{1.23}$$

this means that this wall is slipping and α denotes the dimensionless slip length.

In the case of $\alpha = 0$, there is no-slip on that wall and $V = 0$. Here, the slip length α is described as the distance between the fluid to the solid surface where the velocity of the fluid vanishes [13]. Without the slip effect, some special boundary layers are exhibited near the boundary. The walls which are perpendicular to the externally applied magnetic field are called as Hartmann walls and Hartmann layers have the thickness of δ_{Ha} in scaling as $1/Ha$. The side walls are parallel to the externally applied magnetic field and the thickness of side layers is scaled as $1/\sqrt{Ha}$.

The conductivity considition of the walls can also be expressed with the mixed type boundary condition for the induced magnetic field on the walls as

$$B + c \frac{\partial B}{\partial n} = 0 \tag{1.24}$$

where c is the conductivity parameter.

The conductivity constant $c = 0$ represents the electrically insulated wall and the induced magnetic field becomes $B = 0$ there. In the case of $1/c \to 0$, the relation (1.24) becomes $\dfrac{\partial B}{\partial n} = 0$ which represents the perfectly conducting duct wall.

For all the direct and inverse problem formulations in the thesis, equations (1.22) are used with the most general case of boundary conditions as slipping and variably conducting duct walls by choosing several values for α and c in (1.23) and (1.24), respectively.

1.2 Literature Survey

Magnetohydrodynamics (MHD) deals with the conducting fluid flow under the effect of an externally applied magnetic field. It combines the fluid mechanics and elec-

trodynamics. The magnetic field affects the behaviour of the fluid flow through the Ohm's law, and with the interaction of the electrically conducting fluid and applied magnetic field, an induced magnetic field is generated inside the fluid [11]. The MHD has many applications in engineering, industry, and biology such as MHD pumps, MHD flow meters, accelerators, generators, metallurgy, chemical industry, nuclear energy, the process of material, and measuring the blood flow pressure, etc. Rectangular or circular channels, flow between parallel plates are the most common components of MHD phenomena. Thus, the MHD flow of conducting fluids in channels under the effect of an externally applied magnetic field has a considerable importance [14].

In 1836, Faraday makes the investigations of the fluid flow in the presence of externally applied magnetic field for the first time. In 1937, Hartmann studied the liquid metal channel flow under an externally applied magnetic field. The work on MHD was initially established by Alfven who received the Nobel Prize in 1970 [15].

The conducting fluid motion is described with the system of MHD differential equations including the Navier-Stokes equations for the movement of incompressible viscous fluid with the Lorentz force and the Maxwell's Equations [16]. Because of the nonlinearity of the differential equations, the analytical solutions of MHD flow problems can be obtained for some specific geometries of the problem region with some special boundary conditions such as insulated or perfectly conducting or two opposite insulated walls where the other walls are conducting [11, 17, 18, 19, 12]. Hence, for obtaining approximate values of the MHD duct flow solutions, some numerical techniques such as Finite Difference Method, Finite Element Method, Differential Quadrature Method, Boundary Elements Method, Dual Reciprocity Boundary Elements Method, etc. have been used.

Singh and Lal [20, 21, 22, 23, 24] have obtained the numerical solutions of the MHD flow through pipes having several types of cross-section where Hartmann number is less than 10. In their study, they have used Finite Difference Method and Finite Element Method. Yagawa and Masuda [25] studied and simulated MHD flow in the design of liquid lithium blanket of any fusion reactor by using an incremental FEM. They concern the forced convection problems through Navier Stoke's equation with

finite Reynold numbers. They solve the poblem in terms of magnetic field and velocity iteratively in a coupled form. The fluid behaviour is well obtained if the Reynolds number ≤ 200. Ramos and Winowich [26] employed the FEM to deal with the MHD channel flow including the Reynolds number, the wall conductivity, and electrode length variations. It was observed that the velocity of axial profile was deformed into M-shapes by the effect of applied electromagnetic field and as the Reynolds number increases, the deformation increases. In the paper of Hua and Walker [27], the steady and laminar fluid flow of a liquid metal in a circular duct including insulated wall under a strong transverse nonuniform field. In this study, the magnetic Reynolds number was small while the Hartmann number and the interaction parameter were large. Sterl [28] investigated the effect of Hartmann number, wall conductance ratio, interaction parameter and variable magnetic field on the fluid flow by employing FDM. In their calculations, if the two dimensional flow is considered, Hartmann number can be increased to 1000, although the limitation for Ha is 100 in three dimensional problem. Gardner and Gardner [29] employed a two-dimensional bi-cubic B-spline FEM to obtain the solutions for Hartmann number values less than 10 in arbitrary cross-section of channels. Also, this technique was used within a Galerkin approach in modelling the Magnetohydrodynamic duct flow. Further, Tezer-Sezgin and Köksal [30] broadened these researches to increase the Hartmann numbers to 100 by using the FEM using linear and quadratic elements. Then, Demendy and Nagy [31] obtained the numerical solutions of the governing equations of steady magnetohydrodynamic duct flows up to Hartmann number $Ha = 1000$ by employing the analytical Finite Element Method. Meir [32] has been studied on the MHD flow in pipes of arbitrary cross-section and wall conductivities under a transverse magnetic field by using the FEM. He investigated the existence and uniqueness of steady-state MHD flow solution with arbitrary boundary informations. Barret [33] used the FEM to determine the flow motion in a straight duct with various types of wall conductivities under a uniform magnetic field which is applied perpendicularly to the direction of flow. However, he stated that this method is not effective since it is time and memory consuming and also computationally expensive. Shakeri and Dehghan [34] combined the other two domain type discretization techniques. Finite Volume Method and Spectral Element Technique, which were improved from the Hermit interpolation for obtaining numerical solutions of the coupled MHD flow equations in terms of the velocity

and the induced magnetic field. Their results are compared with the solutions of other numerical techniques and the exact solutions (if exist), and it was shown that the solutions are approached to analytical results. Neslitürk and Tezer-Sezgin [35, 36] used a stabilized FEM employing the residual free buble functions (RFB) to solve the governing equations of MHD flow in rectangular ducts with general wall conductivities. Thus, the Hartmann number was able to be increased to $Ha = 1000$. Tezer-Sezgin [37] has also investigated MHD flow of an incompressible viscous, electrically conducting fluid in a rectangular channel under an externally applied transverse magnetic field by interpreting the solution from the dual infinite series for partly insulated and partly conducting boundaries. She developed the numerical solution for the velocity and magnetic field by converting the problem to the solution of a Fredholm integral equation of the second kind [37].

Due to the computational difficulties in dealing with the large system of equations and the cost in the FEM because of the need of domain discretization of the problem region, another technique has been developed which is called the Boundary Element Method (BEM). Singh and Agarwal [38] obtained the solutions for the velocity and the induced magnetic field of the MHD flow in a rectangular pipe having perfectly conducting electrodes. The MHD equations are reduced to a singular integral equation which was solved numerically by employing the BEM. Tezer-Sezgin [9] solved the MHD flow equations in a rectangular duct with conducting and insulated walls under an external magnetic field by using the BEM with constant elements for Hartmann number values $Ha \leq 10$. In the study of Carabineanu [39], the BEM was developed to investigate the viscous, incompressbile, and electrically conducting fluid flow in a cylindrical duct. It was observed that the numerical solutions for the circular channel with insulated boundary are very close the solutions which are obtained analytically. Tezer-Sezgin and Han Aydın [40] implemented the BEM in order to get the numerical solution of MHD flow in a duct having various cross-sections. Firstly, they transformed the coupled MHD equations into the decoupled inhomogenous convection-diffusion type equations. The fundamental solutions of the decoupled MHD differential equations include the Ha through the exponential and modified Bessel functions so that the solutions can be obtained for large values of Hartmann number as $Ha \leq 300$. Then, Bozkaya and Tezer-Sezgin [41, 42] es-

tablished the fundamental solution for the coupled convection-diffusion MHD flow equations to be able to solve them as a whole. Hence, it was possible to apply the BEM to the MHD equations with the most general form of wall conductivities.

The main restriction of the Boundary Element Method is that the fundamental solution of the original PDE is needed to get the equivalent boundary integral equation. In addition, non-homogenous terms in the PDE results in some domain integrals which destroys the main advantage of the BEM, the boundary-only character. To deal with these problems, the Dual Reciprocity Boundary Element Method has been developed. The main idea is to use a fundamental solution of a simpler equation and treat the other terms as an inhomogeneity by employing some approximating functions and reciprocity rules. Tezer-Sezgin ad Han Aydın [43] investigated the MHD flow in a rectangular duct with insulating walls by employing the DRBEM for Hartmann number value $Ha \leq 10$. They transformed the MHD differential equations into Poisson equations and the right hand side terms in the equations are approximated by using radial basis functions. In the study of Bozkaya and Tezer-Sezgin [44], the time derivatives were considered as inhomogeneity and they were approximated by using an implicit backward difference and the convection terms were approximated by using radial basis functions. The numerical results were obtained for different values of problem parameters. Han Aydın [45] presented the DRBEM solutions for magnetohydrodynamic pipe flow under the effect of a transverse magnetic field with the electrically conducting outside medium. In his study, it was observed that the velocity and the magnetic field demonstrates the MHD flow properties as Reynolds number increases. If Reynolds number is high, the fluid flow is obtained in a similar way as in the case of insulated boundary. Pekmen [46] obtained the numerical solution of incompressible MHD flow by using the DRBEM satisfying the divergence free conditions for the velocity and induced magnetic field. It was shown that circulations for the magnetic potential are obtained at the core region when magnetic Reynolds number is high. Also, when Reynolds number increases, symmetric vortices are streched to the channel, while an increase in Hartmann number weakens this stretchiness. In the study of Pekmen [47], the dual reciprocity boundary element has been proposed for the solutions of MHD equations in a lid-driven cavity where the MHD equations were coupled with the heat transfer equation. She stated that the velocity of the fluid

decreases as Hartmann number increases. In addition, increasing values of Rayleigh number leads to strong temperature gradient close to moving lid. Fendoglu, Bozkaya and Tezer-Sezgin [48] studied the unsteady MHD flow in a rectangular duct having a perturbed boundary on the upper part of the boundary. Coupled MHD equations are solved for the velocity and the induced magnetic field in a duct where the side walls are insulated and the Hartmann walls are perfectly conducting. In the spatial discretization, the domain boundary element method (DBEM) and the DRBEM were used by employing the fundamental solution odf modified Helmholtz equation or the steady state convection-diffusion equation. For the time integration, backward finite difference scheme was used.

In the most of the applications such as cooling where the fluid is interacted with the solid wall, it is assumed that a good wettability is set at the liquid solid interface. In this case, no-slip boundary condition is generally applied. This means that the velocity of the fluid tends to become zero relative to the solid at the the solid fluid interface. Although many experimental studies support the no-slip bounday condition, in some applications such as nanofluidic and the microfluidic devices where the surface-volume ratio is large, the slip hydrodynamic condition is typical [49], that was proposed by Navier firstly. The slip length is defined as the distance between the liquid and the solid surface where the extrapolated fluid flow velocity vanishes. The slip length may change from microns to nanometers and also it depends on some physical and chemical factors [13]. The slip boundary condition is written as a linear relation between slipping velocity and tangential stress. Smolentsev [13] studied three main MHD flow problems with a slip boundary condition which are Hartmann flow, fully developed flow in a rectangular channel, and the quasi two-dimensional turbulent flow. He solved the first two problems analytically. He observed that Hartmann layers are developed near the duct wall with slip velocity condition as in the no-slip case. Also, he performed numerical simulations for two dimensional quasi turbulent flow where the fluid flow becomes irregular. In the paper of Ligere, Dzenite ,and Matvejevs [14], an analytical solution of the MHD flow for a fully developed conducting fluid flow was presented. Also, the MHD flow equations in this study were solved by employing integral transforms, however, firstly the kernels of integral transformations was derived and used in the solution procedure. Rivero and Cuevas

[50] explored the analytical and numerical solutions with slip in MHD micropumps. They investigated several combinations of slip and no-slip boundary conditions on the walls and also, the effect of the slip length on the flow rate was analyzed. In their study, it was stated that the solution of the MHD flow cannot be obtained analytically if all the boundary has the slip velocity condition. Here, they used the collocation-Tau-Chebyshev method [51]. Makinde and Chinyoka [52] studied the unsteady dusty fluid flow and heat transfer between two parallel plates with electrical conductivity and variable viscosity. The governing equations of the problem were solved numerically by employing a semi-implicit finite difference scheme. They discussed the effect of the slip, electrical conductivity and viscosity. Senel and Tezer-Sezgin [53, 54] used the DRBEM to obtain the numerical solutions of MHD flow equations in circular and rectangular pipes with slip velocity condition. They demonstrated that the fluid flow speeds up and the Hartmann and side layers are weakened when slip length increases. In the paper of Tezer-Sezgin and Senel [55], the MHD flow between two parallel conducting and slipping infinite plates including electrodes which were placed symmetrically was solved numerically with the DRBEM. An important point in their study lies in the discretization of the finite region and obtaining the solution in an infinite region near the electrodes.

All of the studies mentioned above have the direct problem formulations, i.e, the boundary conditions and the problem parameters are known and the only unknowns are the solutions of the problems in the interior of the problem domain and may be on the boundary depending on the given boundary informations. But then, inverse (Cauchy) problems start to become popular among many researchers. There are many applications of inverse problems in science and engineering such as tomography, radar, acoustics, astronomy, optics, signal processing, geophysics, oceanography and also many other applications. In the inverse problems, the solution of the problem itself is known on the problem region but the boundary conditions or some problem parameters are considered as the unknowns. Mainly, inverse problems can be categorized as boundary inverse problems and parameter identification problems. In many engineering applications, the boundary informations are generally incomplete, i.e, they are underspecified or overspecified on different parts of the boundary or the solution is given at the interior of the problem region but some problem pa-

rameters are unknown. It is very well known that such problems are mostly ill-posed that the existence, uniqueness, and stability of the solution cannot be always guaranteed [56]. Due to the ill-posedness, for obtaining the numerical solutions of inverse problems some regularization techniques such as the Tikhonov regularization, the singular value decomposition (SVD), the conjugate gradient method, or some iterative techniques should be used in addition to numerical solution methods. In the study of Aydin and Tezer-Sezgin [57], the MHD flow direct and Cauchy problems have been solved in a rectangular duct with a perturbed, curved, and slip upper boundary. The aim is to recompute the slipping velocity and the slip length by using the asymptotic analysis with respect to the perturbation parameter and solving MHD flow equations for the first order and the corrector solutions in the rectangular duct. The dual reciprocity boundary element method (DRBEM) with the Tikhonov regularization was utilized for solving the coupled MHD equations as a whole in that study.

In the last decade, many researchers have studied on the inverse problems related with the Helmholtz type equations. Bai [58] reconstructed sound fields which are generated by the irregularly shaped resources by using the BEM-based acoustic holography method with the SVD. In his study, to deal with the ill-posed property in the reconstruction of the field, singular value decomposition is used. Also, the analytical solutions and results obtained from holographically show a vey well agreement. Kim and Ih [59] used the BEM with the SVD to reconstruct the acoustic power, the vibrational velocity, and sound pressure in the inverse solution of the least-squares sense. Their method promotes the reconstructed field resolution. Consequently, vibro acoustic parameters are evaluated with a good accuracy. Marin et al. [60, 61] solved the Cauchy problem corresponding to the Helmholtz type differential equation by using the BEM with an alternating iterative technique including the well-posed boundary value problems and the conjugate gradient method (CGM). Their numerical solutions show that for increasing number of boundary elements, the BEM with iterations and conjugate gradient method yields a stable and convergent technique. Later on, Martin et al. [62] compared these techniques with the SVD and the Tikhonov regularization. In addition, the same researchers developed an iterative technique which is based on the Landweber method combined with the BEM [63]. However, they stated that singular value decomposition and Tikhonov regularization give more accurate results.

Marin and Lesnic [64] and Marin [65] employed the method of fundamental solutions and the Tikhonov regularization to get the numerical solution of the Cauchy problem for two and three dimensional Helmholtz equations. Their findings express that for increasing count of source nodes and decreasing quantity of noise in data, their technique is both convergent and stable. Cauchy problems for the convection-diffusion type equations were studied in [66, 67, 68]. The reaction-diffusion and advection-diffusion type Cauchy problems were investigated in [69, 70], respectively. Alsoy-Akgün and Lesnic [71] studied the inverse natural magneto-convection problems including boundary temperature and heat flux data with the DRBEM. They formulate the boundary value problem as an inverse problem. They obtain stable numerical solutions for several values of Hartmann and Rayleigh numbers with a good precision in the case of uniform boundary temperature and discontinous time dependent heat flux, seperately.

In recent years, both of the numerical and theoretical techniques for the inverse problems in parameter identification have been considered. Chen et al. [72] proposed an improved asymptotic regularization technique to identify the coefficient in the Helmholtz-type equation. They prove that their regularization technique for the Helmholtz equation with the coefficient determination problem is convergent by expressing that it is possible to use this technique in real problems. Gylys-Colwell [73] determined the parameters which are sufficiently close to constant in the anisotropic and isotropic wave equations. Burger and Mühlhuber [74] developed sequential quadratic programming techniques as an iterative regularization method for the parameter identification problems. They stated that stable saddle poblems and SQP problems are equivalent to each other. Also, it is expressed as new approaches for the approximate solutions of the inverse problems are offered through the saddle point problems. Marin et al. [75] determined the constant ratio of the convective heat transfer and the thermal conductivity by employing the BEM with a constrained non-linear minimisation technique. It is seen from the approximate results their numerical technique is robust, convergent, stable, and accurate. Similarly, Marin et al. [75] recovered a space-dependent coefficient in two dimensional Helmholtz equations by using the DRBEM combined with a constrained non-linear minimisation technique. Tezer-Sezgin and Aydin [76] identified the Hartmann number in the MHD duct flow

equations through the inverse formulation by using the DRBEM with the Tikhonov regularization. In their study, The velocity and the induced magnetic field profiles are simulated from the direct solution depicting the well-known MHD characteristics. In addition, the Hartmann number is reconstructed from the inverse problem with an accuracy of 10^{-4} and 10^{-6}.

1.3 Originality in the Thesis

In this thesis, the direct and Cauchy MHD duct flow problems with no-slip to slip and insulated to perfectly conducting wall conditions are solved by using the DRBEM. The governing equations of the MHD flow are converted into the boundary integral equations by using the fundamental solution of the Laplace equation. All the terms other than Laplacian are considered as an inhomogeneity and they are approximated with the use of some radial basis functions. In all the problems considered in this thesis, the constant boundary elements are used in the application of the DRBEM to discretize the boundary of the problem region.

In this thesis, two types of inverse (Cauchy) problems such as boundary inverse problem and the parameter identification problem are considered. In the boundary inverse problems, our aim is to recover the slip length on the slipping wall and the conductivity constant on variably conducting wall for several values of Hartmann numbers. On the other hand, in the parameter idetification problems, the parameter Hartmann number in the MHD differential equations is going to be determined for a preassigned velocity and induced magnetic field. Due to the incompleteness of the boundary conditions, Cauchy problems are ill-posed. Therefore, three regularization methods which are the Tikhonov regularization method, a direct-inverse iterations, and the well-posed iterations are used to obtain the solutions for the Cauchy problems. These three regularization methods are compared in terms of the accuracy. In the literature, there are many studies on the direct MHD duct flow problems with various types of boundary conditions. On the other hand, the boundary inverse and parameter identification formulations of the MHD duct flow constitutes the original part of this thesis. The recomputation of the slip length and the Hartmann number through the boundary inverse and parameter identification formulations, respectively, is a newly carried

study in the MHD flow research area.

Another originality in this thesis is the discretization of the curved boundary of the duct for the MHD flow and solving the equations with the use of asymptotic analysis. In this way, the problem is solved in a rectangular duct with straight boundaries which is a subset of the original problem domain by using the Taylor series near the curved part. Then, by utilizing the first order approximation and the corrector for the solutions, it is possible to obtain the solution in the problem region having curved part. Thus, the difficulties in the discretization of the curved boundary of the duct has been eliminated.

1.4 Plan of the Thesis

The aim of this thesis is to obtain the solutions of direct and inverse formulations of the MHD duct flow problems by using the DRBEM. Therefore, in Chapter 1, the governing equations of the MHD flow are described. The nondimensionalization of the equations is also carried. Section 1.3 and Section 1.4 give a literature survey on the solutions of MHD flow and the original contributions of the thesis study, respectively.

In Chapter 2, the BEM and the DRBEM solutions of Poisson's Equation, the DRBEM solution of Poisson's Equation as an inverse problem are introduced since the governing operator in the MHD equations is Laplacian. Also, the three regularization techniques, namely, the Tikhonov regularization method, the direct-inverse iterations and the well-posed iterations are explained which are needed in the solutions of the inverse MHD flow problems.

In Chapter 3, MHD direct and Cauchy problems are introduced. The DRBEM solution of direct and inverse MHD duct flow problems are given in detail. Then, parameter identification formulation for the MHD duct flow is explained. Regularization techniques which are introduced in Chapter 2, are again explained for the Cauchy MHD duct flow problems. Later, the DRBEM application to the Cauchy MHD flow with slipping and variably conducting duct walls is given. Also, the DRBEM application to the Cauchy MHD flow in a duct with a slipping perturbed upper boundary is shown. Here, the asymptotic expansion technique due to the upper perturbed bound-

ary is introduced for discretizing only the rectangular region. Lastly, application of the DRBEM to parameter identification (Hartmann number) in the MHD duct flow Cauchy problem is given with several boundary conditions.

In Chapter 4, the numerical results for each problem introduced in Chapter 3 are given for several values of Hartmann number, slip length, and conductivity constants. The velocity and induced magnetic field values are simulated together with detailed discussions giving the effects of problem parameters and recovering the slip length and Hartmann number from the inverse MHD flow solutions.

Chapter 5 summarizes all the carried studies and findings in the thesis.

CHAPTER 2

THE DUAL RECIPROCITY BOUNDARY ELEMENT METHOD FOR THE DIRECT AND INVERSE PROBLEMS

The Boundary Element Method (BEM) is a well-established numerical technique which supplies many advantages over domain based solutions of PDEs. Discretizing only the boundary of the problem region rather than the domain and providing the whole problem solution using the boundary conditions only are the most important features of BEM. The use of BEM provides smaller discretized systems in size and less computational effort than domain type discretization techniques, such as Finite Difference Method (FDM) or Finite Element Method (FEM). In the boundary element method, by using the fundamental solution of the original PDE, a boundary integral equation is derived and it is solved discretizing only the boundary. Using the fundamental solution to the original PDE is a limitation of the BEM. Therefore, this technique is most suitable for the solution of homogenous PDEs. On the other hand, when the BEM is applied to non-homogeneous PDEs, the integral equation contains a domain integral which destroys the advantages of BEM.

The Dual Reciprocity Boundary Element Method (DRBEM) is one of the most beneficial numerical technique to prevail over these drawbacks. In DRBEM, it is possible to transform the integral equations into boundary integral equations without any domain integral by treating all the terms other than the Laplacian as inhomogeneity in a PDE. This involves approximation of inhomogeneties by radial basis functions related with the particular solution of PDE through the Laplacian operator. Non-linear equations, convection-diffusion type PDEs, and time dependent PDEs can be solved through the DRBEM considering all these terms as inhomogeneity.

The DRBEM is mostly employed for the solution of direct problems, however, it can

be used for the inverse problems as well. In this Chapter, the theory and application of DRBEM formulation on the direct and inverse solutions of the Poisson's equation is provided in Section 2.2 and Section 2.3, respectively.

The discretization of Cauchy problems results in an ill-conditioned system of linear algebraic equations, hence a regularization technique is necessary to solve these problems [69]. In this thesis, the Tikhonov regularization, the direct-inverse and the well-posed iterations which are explained in Section 2.4 are used to obtain the solution of the Cauchy MHD duct flow problems in Chapter 3.

2.1 BEM Solution of Poisson's Equation $\nabla^2 u = b(x, y)$

In this section, boundary integral equation is derived for the Poisson's equation as in [2]. The two dimensional Poisson's equation

$$\nabla^2 u = b(x, y), \qquad (x, y) \in \Omega \tag{2.1}$$

is considered with the Dirichlet and/or Neumann type boundary conditions

$$\begin{aligned} u(x, y) &= \bar{u}(x, y), \qquad (x, y) \in \Gamma_1 \\ q(x, y) &= \bar{q}(x, y), \qquad (x, y) \in \Gamma_2 \end{aligned} \tag{2.2}$$

where $\nabla^2 = \dfrac{\partial^2}{\partial x} + \dfrac{\partial^2}{\partial y}$ is the Laplace operator, $b(x, y), \bar{u}(x, y), \bar{q}(x, y)$ are known functions, $\Gamma_1 + \Gamma_2 = \Gamma$ is the piecewisely smooth boundary of the problem region $\Omega \in R^2$, $q = \dfrac{\partial u}{\partial n}$ with the unit outward normal vector $\boldsymbol{n}$ to the boundary Γ.

In order to get a boundary integral equation for the Poisson's equation, firstly, equation (2.1) is multiplied with the fundamental solution of Laplace equation

$$u^* = \frac{1}{2\pi} ln(\frac{1}{r}) = \frac{1}{2\pi} ln|\vec{r} - \vec{r_i}| \tag{2.3}$$

where r denotes the distance between the source $\vec{r_i} = (x_i, y_i)$ and the field points $\vec{r} = (x, y)$. Then, one can get the following domain integral equation

$$\int_\Omega (\nabla^2 u - b) u^* d\Omega = 0. \tag{2.4}$$

Applying integration by parts twice, i.e., Green's theorem results in

$$\int_\Omega (u \nabla^2 u^* - b u^*) d\Omega + \int_\Gamma \frac{\partial u}{\partial n} u^* d\Gamma - \int_\Gamma \frac{\partial u^*}{\partial n} u d\Gamma = 0. \tag{2.5}$$

After inserting the boundary conditions (2.2), the following integral equation is obtained as

$$\int_{\Omega} u\nabla^2 u^* d\Omega - \int_{\Omega} bu^* d\Omega + \int_{\Gamma_2} \bar{q}u^* d\Gamma + \int_{\Gamma_1} qu^* d\Gamma - \int_{\Gamma_2} uq^* - \int_{\Gamma_1} \bar{u}q^* = 0 \tag{2.6}$$

where $q^* = \dfrac{\partial u^*}{\partial n} = \dfrac{1}{2\pi}\dfrac{(\vec{r}-\vec{r_i}).\vec{n}}{|\vec{r}-\vec{r_i}|^2}$ is the normal derivative of the fundamental solution.

In the above equations, u^* is the fundamental solution satisfying

$$\nabla^2 u^* + \Delta^i = 0. \tag{2.7}$$

Here, Δ^i denotes Dirac delta function which is defined as

$$\Delta^i(x) = \begin{cases} 0 & \text{if } x \neq x_i \\ \infty & \text{if } x = x_i. \end{cases} \tag{2.8}$$

The integral of Δ^i over the domain is equal to one. In addition, the integral property of the Dirac delta function gives [2]

$$c_i u_i = -\int_{\Omega} u\nabla^2 u^* d\Omega = -\int_{\Omega} u(-\Delta^i) d\Omega \tag{2.9}$$

where $u_i = u(x_i, y_i)$, and $c_i = \begin{cases} \dfrac{1}{2} & \text{if } (x_i, y_i) \in \Gamma \\ 1 & \text{if } (x_i, y_i) \in \Omega. \end{cases}$

To simplify equation (2.6), the following notation is introduced

$$\tilde{u} = \begin{cases} u & \text{on} \quad \Gamma_2 \\ \bar{u} & \text{on} \quad \Gamma_1 \end{cases} \tag{2.10}$$

and

$$\tilde{q} = \begin{cases} q & \text{on} \quad \Gamma_1 \\ \bar{q} & \text{on} \quad \Gamma_2. \end{cases} \tag{2.11}$$

Then, combining the equations (2.6) and (2.9) gives

$$c_i \tilde{u}_i + \int_{\Omega} bu^* d\Omega + \int_{\Gamma} \tilde{u}q^* d\Gamma = \int_{\Gamma} \tilde{q}u^* d\Gamma. \tag{2.12}$$

Here, although b is a known function and the integral over the domain Ω gives no new unknowns, this domain integral needs to be carried out as well as the integrals on the boundary. Integration regions which are called as cells are used to calculate the domain integral in (2.12), and a numerical integration technique is generally applied. The domain integral in (2.12) can be written as

$$\int_{\Omega} bu^* d\Omega = \sum_{e=1}^{M} (\sum_{k=1}^{r} w_k (bu^*)_k) \Omega_e \tag{2.13}$$

where e represents the cells in the discretized region, M is the total number of cells, w_k is the integration weight, r is the integration point on each cell, and Ω_e is the area of the cell e. One can note that the domain integral in (2.13) has to be computed, and hence BEM loses its own advantage which is discretizing only the boundary of the problem region. To deal with this drawback, DRBEM can be used to transform all the domain integrals into equivalent boundary integrals.

2.2 DRBEM Solution of Poisson's Equation $\nabla^2 u = b(x, y)$

In order to convert the domain integral, due to the function $b(x, y)$ on the right hand side of the Poisson's equation, into the boundary integral equation, the dual reciprocity boundary element method is going to be applied. The DRBEM is going to be explained on the Poisson's equation (2.1) in this section as given in [5].

The solution of equation (2.1)

$$\nabla^2 u = b(x, y), \qquad (x, y) \in \Omega \tag{2.14}$$

with the boundary conditions

$$\begin{aligned} u(x, y) &= \bar{u}(x, y), \qquad (x, y) \in \Gamma_1 \\ q(x, y) &= \bar{q}(x, y), \qquad (x, y) \in \Gamma_2 \end{aligned} \tag{2.15}$$

is expressed as the summation of the solution of Laplace equation and the particular solution $\hat{u}$ such that

$$\nabla^2 \hat{u} = b(x, y). \tag{2.16}$$

In general, determining the particular solution $\hat{u}$ satisfying the equation (2.16) is troubling. In DRBEM, it is suggested to take a series of particular solutions $\hat{u}_j$ rather than a single particular solution $\hat{u}$. Thus, the right hand side function $b(x, y)$ considered as an inhomogeneity is approximated as

$$b \approx \sum_{j=1}^{N+L} \alpha_j f_j \tag{2.17}$$

where α_j's are initially unknown coefficients, N and L are the number of boundary elements and interior nodes, respectively, and f_j's are the approximating functions related with the particular solutions $\hat{u}_j$'s through the relation

$$\nabla^2 \hat{u}_j = f_j. \tag{2.18}$$

Substituting equation (2.18) into (2.17), the approximation for $b(x, y)$ is obtained as follows

$$b = \sum_{j=1}^{N+L} \alpha_j \nabla^2 \hat{u}_j. \tag{2.19}$$

When this form of b in equation (2.19) is substitued into equation (2.14), one can get

$$\nabla^2 u = \sum_{j=1}^{N+L} \alpha_j \nabla^2 \hat{u}_j. \tag{2.20}$$

Having the Laplacian operator on both sides of equation (2.20), one can apply the BEM procedure to both sides.

Multiplying equation (2.20) with the fundamental solution of Laplace equation which is $u^* = \dfrac{1}{2\pi} ln(\dfrac{1}{r})$ and integrating over the domain Ω,

$$\int_\Omega \big(\nabla^2 u\big) u^* d\Omega = \sum_{j=1}^{N+L} \alpha_j \int_\Omega \big(\nabla^2 \hat{u}_j\big) u^* d\Omega \tag{2.21}$$

is obtained.

Applying integration by parts twice to the above equation yields the following integral equation for each source node i

$$c_i \tilde{u}_i + \int_\Gamma \tilde{u} q^* d\Gamma - \int_\Gamma \tilde{q} u^* d\Gamma = \sum_{j=1}^{N+L} \alpha_j \big(c_i \hat{u}_{ij} + \int_\Gamma \hat{u}_j q^* d\Gamma - \int_\Gamma \hat{q}_j u^* d\Gamma\big) \tag{2.22}$$

where $\hat{u}_{ij} = \hat{u}_j(x_i, y_i)$, and $\hat{q}_j$ is the normal derivative of $\hat{u}_j$ defined as

$$\hat{q}_j = \frac{\partial \hat{u}_j}{\partial n} = \frac{\partial \hat{u}_j}{\partial x}\frac{\partial x}{\partial n} + \frac{\partial \hat{u}_j}{\partial y}\frac{\partial y}{\partial n}. \tag{2.23}$$

To simplify the notation, 'u' and 'q' will be used instead of '$\tilde{u}$' and '$\tilde{q}$' in the rest of the DRBEM formulation.

The equation (2.22) is going to be discretized to get the system of equations for obtaining the boundary values. The boundary of the problem domain is divided into N boundary elements, and the points whose values are considered as unknown which are placed on the boundary elements are called as "boundary nodes". If each element has a node in the middle of it , the elements are called as "constant boundary elements". If two nodes are located at the ends of an element, the elements are called as "linear boundary elements". In addition, if each element has two nodes at the ends and a node at the center, the elements are called as "quadratic boundary elements". In a similar way, we can increase the number of boundary nodes. In this thesis, the constant boundary elements are used to discretize the boundary Γ which is shown in Figure 2.1.

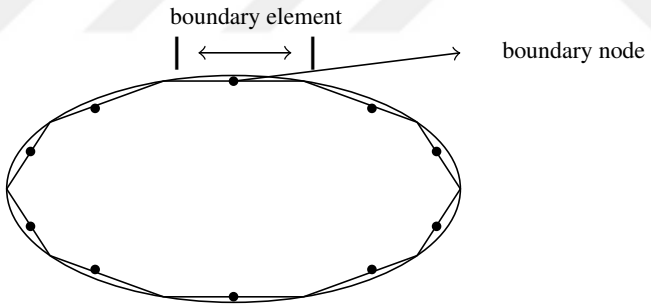


Figure 2.1: Constant boundary elements

For the constant boundary elements, u and q values are supposed to be constant over each boundary element and equal to the nodel value since each element is always smooth. The approximate values of u and q everywhere on the boundary element are taken as $u \approx u_k$ and $q \approx q_k$ on Γ_k which is k-th boundary element where $k \in \{1, N\}$.

When the boundary Γ in equation (2.22) is discretized into N constant boundary

elements, the following equation is obtained

$$\begin{aligned} &c_i u_i + \sum_{k=1}^{N} [\int_{\Gamma_k} u q^* d\Gamma - \int_{\Gamma_k} q u^* d\Gamma] = \\ &\sum_{j=1}^{N+L} \alpha_j [c_i \hat{u}_{ij} + \sum_{k=1}^{N} \int_{\Gamma_k} \hat{u}_j q^* d\Gamma - \sum_{k=1}^{N} \int_{\Gamma_k} \hat{q}_j u^* d\Gamma], \quad i = 1, ..., N \end{aligned} \tag{2.24}$$

where index k denotes the constant boundary nodes. After taking the constant values of u and q out of the boundary integrals, we get

$$\begin{aligned} &c_i u_i + \sum_{k=1}^{N} u_k \int_{\Gamma_k} q^* d\Gamma - \sum_{k=1}^{N} q_k \int_{\Gamma_k} q^* d\Gamma = \\ &\sum_{j=1}^{N+L} \alpha_j [c_i \hat{u}_{ij} + \sum_{k=1}^{N} \hat{u}_{jk} \int_{\Gamma_k} q^* d\Gamma - \sum_{k=1}^{N} \hat{q}_{jk} \int_{\Gamma_k} u^* d\Gamma], \quad i = 1, ..., N. \end{aligned} \tag{2.25}$$

Here, there are two integrals which are going to be evaluated over the boundary elements as

$$\int_{\Gamma_k} q^* d\Gamma$$

and

$$\int_{\Gamma_k} u^* d\Gamma.$$

The integration of q^* and u^* over each boundary element yields the following system of equations

$$c_i u_i + \sum_{k=1}^{N} \bar{H}_{ik} u_k - \sum_{k=1}^{N} G_{ik} q_k = \sum_{j=1}^{N+L} \alpha_j [c_i \hat{u}_i j + \sum_{k=1}^{N} \bar{H}_{ik} \hat{u}_{kj} - \sum_{k=1}^{N} G_{ik} \hat{q}_{kj}], \quad i = 1, ..., N. \tag{2.26}$$

The entries of $\bar{\boldsymbol{H}}$ and $\boldsymbol{G}$ matrices are computed as [1]

$$\begin{aligned} \bar{H}_{ik} &= \int_{\Gamma_k} q^* d\Gamma_k = \frac{1}{2\pi} \int_{\Gamma_k} \frac{(r - r_i).\boldsymbol{n}}{|r - r_i|^2} d\Gamma_k \qquad \text{when} \qquad i \neq k, \\ G_{ik} &= \int_{\Gamma_k} u^* d\Gamma_k = \frac{1}{2\pi} \int_{\Gamma_k} ln(\frac{1}{|r - r_i|}) d\Gamma_k \qquad \text{when} \qquad i \neq k \end{aligned} \tag{2.27}$$

where $\boldsymbol{n}$ is the unit outward normal vector to the boundary Γ_k, $r = (x, y)$ and $r_i = (x_i, y_i)$ are the vectors specifying the field and the source points, respectively.

There are singularities in $\bar{H}_{ii}$ and G_{ii} since the distance between the field and source points becomes zero when $i = k$. However, the diagonal entries of **H** and **G** matrices

can be evaluated analytically for constant boundary elements. H_{ii} entries can be taken as zero since the normal vector $\boldsymbol{n}$ is always perpendicular to the distance $|r - r_i|$,i.e, $\boldsymbol{n}.(r - r_i) = 0$. The components of G_{ii} are taken as [1]

$$G_{ii} = \frac{A}{2\pi}(ln\frac{2}{A} + 1) \tag{2.28}$$

where A is the length of the boundary element.

The constant c_i is taken as

$$c_i = \begin{cases} \frac{1}{2} & \text{if } (x_i, y_i) \in \Gamma \\ 1 & \text{if } (x_i, y_i) \in \Omega. \end{cases} \tag{2.29}$$

On the boundary, the equation (2.26) is rewritten as

$$\frac{1}{2}u_i + \sum_{k=1}^{N} \bar{H}_{ik}u_k - \sum_{k=1}^{N} G_{ik}q_k = \sum_{j=1}^{N+L} \alpha_j[\frac{1}{2}\hat{u}_{ij} + \sum_{k=1}^{N} \bar{H}_{ik}\hat{u}_{kj} - \sum_{k=1}^{N} G_{ik}\hat{q}_{kj}] \tag{2.30}$$

where $i = 1, 2, ..., N$.

Rearranging the entries of the coefficient matrices yields the matrix-vector form

$$\mathbf{Hu} - \mathbf{Gq} = \sum_{j=1}^{N+L} \alpha_j(\mathbf{H}\hat{u}_j - \mathbf{G}\hat{q}_j) \tag{2.31}$$

where **u** and **q** are $N \times 1$ vectors, **H** and **G** are $N \times N$ matrices and also

$$H_{ik} = \bar{H}_{ik} + \frac{1}{2}\delta_{ik} \tag{2.32}$$

where δ_{ik} is the Kronecker delta operator

$$\delta_{ik} = \begin{cases} 1 & \text{if} \quad i = k \\ 0 & \text{if} \quad i \neq k. \end{cases} \tag{2.33}$$

The vectors $\hat{u}_j$ and $\hat{q}_j$ are considered as the columns of the matrices $\hat{\boldsymbol{U}}$ and $\hat{\boldsymbol{Q}}$, respectively, resulting in the matrix-vector equation

$$\mathbf{Hu} - \mathbf{Gq} = (\mathbf{H}\hat{\boldsymbol{U}} - \mathbf{G}\hat{\boldsymbol{Q}})\boldsymbol{\alpha} \tag{2.34}$$

where $\hat{\boldsymbol{U}}$ and $\hat{\boldsymbol{Q}}$ are $N \times (N + L)$ matrices and $\boldsymbol{\alpha}$ is $(N + L) \times 1$ vector containing the undetermined coefficients α_j.

The unknown values of the solution **u** and its normal derivative **q** on the boundary are obtained from the solution of the equation (2.34) where the coefficients c_i's are taken as $c_i = \frac{1}{2}$ on the diagonal entries of the matrix **H**. The interior values are calculated from the equation (2.26) by taking $c_i = 1$ as

$$u_i = -\sum_{k=1}^{N} \bar{H}_{ik} u_k + \sum_{k=1}^{N} G_{ik} q_k + \sum_{j=1}^{N+L} \alpha_j [\hat{u}_{ij} + \sum_{k=1}^{N} \bar{H}_{ik} \hat{u}_{kj} - \sum_{k=1}^{N} G_{ik} \hat{q}_{kj}]. \quad (2.35)$$

In a matrix-vector form, the equation (2.35) is written as

$$\mathbf{I}\boldsymbol{u}^i = \mathbf{G}\mathrm{q} - \mathbf{H}\mathrm{u} + (\mathbf{I}\hat{\boldsymbol{U}}^i + \mathbf{H}\hat{\boldsymbol{U}} - \mathbf{G}\hat{\boldsymbol{Q}})\boldsymbol{\alpha} \quad (2.36)$$

where $\boldsymbol{u}^i$ is a $L \times 1$ vector containing the computed values at interior nodes, $\hat{\boldsymbol{U}}^i$ matrix is of size $L \times (N + L)$, and **I** is an $L \times L$ identity matrix. The $(N \times 1)$ vectors **u** and **q** include the known boundary points, and $\boldsymbol{\alpha}$ is a $(N + L) \times 1$ vector.

Combining the systems (2.34) and (2.36) with enlarging the matrices yields the whole system as [5]

$$\begin{bmatrix} \mathbf{H^b} & \mathbf{0} \\ \mathbf{H^i} & \mathbf{I} \end{bmatrix} \begin{Bmatrix} \mathbf{u^b} \\ \mathbf{u^i} \end{Bmatrix} - \begin{bmatrix} \mathbf{G^b} & \mathbf{0} \\ \mathbf{G^i} & \mathbf{0} \end{bmatrix} \begin{Bmatrix} \mathbf{q^b} \\ \mathbf{0} \end{Bmatrix} = \left(\begin{bmatrix} \mathbf{H^b} & \mathbf{0} \\ \mathbf{H^i} & \mathbf{I} \end{bmatrix} \begin{Bmatrix} \hat{\mathbf{U}}^{\mathbf{b}} \\ \hat{\mathbf{U}}^{\mathbf{i}} \end{Bmatrix} - \begin{bmatrix} \mathbf{G^b} & \mathbf{0} \\ \mathbf{G^i} & \mathbf{0} \end{bmatrix} \begin{Bmatrix} \hat{\mathbf{Q}}^{\mathbf{b}} \\ \mathbf{0} \end{Bmatrix} \right) \boldsymbol{\alpha} \quad (2.37)$$

where **I** is an $L \times L$, and **0** is a $N \times L$ matrix, b and i denote the boundary and interior nodes, respectively.

The compact form of equation (2.37) is given as

$$\mathbf{Hu} - \mathbf{Gq} = (\mathbf{H}\hat{\boldsymbol{U}} - \mathbf{G}\hat{\boldsymbol{Q}})\boldsymbol{\alpha}. \quad (2.38)$$

In the system (2.38), **H, G**, $\hat{\boldsymbol{U}}$ and $\hat{\boldsymbol{Q}}$ matrices are of size $(N+L) \times (N+L)$, and **u**, **q**, and $\boldsymbol{\alpha}$ vectors have size $(N + L) \times 1$ making the whole system of equations in (2.38) a square system. The same notations in the equation (2.34) are going to be used for the whole system to simplify the rest of the equations.

In equation (2.38), the $\boldsymbol{\alpha}$ vector is computed by using the approximation given in (2.17) and it gives a system

$$\boldsymbol{b} = \mathbf{F}\boldsymbol{\alpha} \quad (2.39)$$

where $\mathbf{F}$ is an $(N+L) \times (N+L)$ coordinate matrix, $\boldsymbol{b}$ is the vector obtained by collocating the function $b(x, y)$ at $(N+L)$ points.

The coordinate matrix $\mathbf{F}$ is constructed columnwise containing the values of the function f_j at $(N+L)$ points. When the equation (2.39) is inverted, $\boldsymbol{\alpha}$ is obtained as

$$\boldsymbol{\alpha} = \mathbf{F}^{-1}\boldsymbol{b} \tag{2.40}$$

where $\mathbf{F}$ is invertible since the leading diagonal of $\mathbf{F}$ is nonzero [5].

Combining the equations (2.38) and (2.40) results in

$$\mathbf{Hu} - \mathbf{Gq} = (\mathbf{H}\hat{\boldsymbol{U}} - \mathbf{G}\hat{\boldsymbol{Q}})\mathbf{F}^{-1}\boldsymbol{b} \tag{2.41}$$

where $\mathbf{H}$, $\mathbf{G}$, $\hat{\boldsymbol{U}}$, $\hat{\boldsymbol{Q}}$, $\mathbf{F}^{-1}$ and $\boldsymbol{b}$ values are known, and hence, the right hand side of (2.41) can be computed. After inserting the boundary conditions and arranging the known and unknown values of vectors, a linear system of algebraic equations is obtained in the form of

$$\boldsymbol{Ax} = \boldsymbol{y} \tag{2.42}$$

where the vector $\boldsymbol{x}$ contains the unknown values of u or q at N boundary points, and the unknown values of u at L interior points.

To get the matrices $\mathbf{F}$, $\hat{\boldsymbol{U}}$, and $\hat{\boldsymbol{Q}}$, we need to choose a suitable f_j function. Although several functions can be taken for f_j, it is necessary that $\mathbf{F}$ matrix is invertible. The simplest and accurate choices for the function f_j are the polynomials of the distance function r with the constant term.

We can choose f as a polynomial

$$f = 1 + r + r^2 + ... + r^m \tag{2.43}$$

where r denotes the distance between the source and the field points, and satisfying the equation

$$\nabla^2 \hat{u} = f. \tag{2.44}$$

From the equation (2.44), $\hat{u}$ and $\hat{q}$ are obtained as

$$\hat{u} = \frac{r^2}{4} + \frac{r^3}{9} + ... + \frac{r^{m+2}}{(m+2)^2} \tag{2.45}$$

$$\hat{q} = (r_x \frac{\partial x}{\partial n} + r_y \frac{\partial y}{\partial n})(\frac{1}{2} + \frac{r}{3} + ... + \frac{r^m}{m+2}) \tag{2.46}$$

where $r^2 = r_x^2 + r_y^2$ and $\dfrac{\partial r}{\partial n} = \dfrac{1}{r}(r_x \dfrac{\partial r_x}{\partial n} + r_y \dfrac{\partial r_y}{\partial n})$.

Any polynomial which is obtained as combination of the terms from equation (2.43) can be used as a radial basis function, however, the results will be almost the same. Hence, one can choose $f = 1 + r$, so that the computations become easier and less costly. In addition, different types of radial basis functions can be used in the application of the DRBEM, and corresponding particular solution and its normal derivative are obtained ($\hat{u}$ and $\hat{q} = \dfrac{\partial \hat{u}}{\partial n}$) as

$$f = 1 + r, \quad \hat{u} = \frac{r^2}{4} + \frac{r^3}{9}, \quad \hat{q} = (\frac{1}{2} + \frac{r}{3})(r_x \frac{\partial x}{\partial n} + r_y \frac{\partial y}{\partial n}) \tag{2.47}$$

$$f = 1 + r + r^2, \quad \hat{u} = \frac{r^2}{4} + \frac{r^3}{9} + \frac{r^4}{16}, \quad \hat{q} = (\frac{1}{2} + \frac{r}{3} + \frac{r^2}{4})(r_x \frac{\partial x}{\partial n} + r_y \frac{\partial y}{\partial n}) \tag{2.48}$$

$$f = r^2 lnr, \quad \hat{u} = \frac{r^4}{16}(lnr - \frac{1}{2}), \quad \hat{q} = (\frac{r^3}{4} lnr - \frac{r^3}{16}) \frac{\partial r}{\partial n}. \tag{2.49}$$

$$f = exp(-r^2), \quad \hat{u} = \frac{1}{4}(lnr^2 + E_1(r^2)), \quad \hat{q} = \frac{1}{2r}(1 - exp(-r^2)) \frac{\partial r}{\partial n}. \tag{2.50}$$

where E_1 is the exponential integral defined as [77]

$$E_1(x) = \int_x^\infty \frac{exp(-t)}{t} dt. \tag{2.51}$$

In the case that the function b on the right hand side of the equation (2.1) contains the spatial derivatives of the unknown u as u_x and u_y, a special approach is needed by the use of the coordinate matrix $\mathbf{F}$. In this case, the unknown u is also approximated as

$$\mathbf{u} = \mathbf{F}\boldsymbol{\beta} \tag{2.52}$$

where $\boldsymbol{\beta}$ includes the undetermined coefficients becoming different from α in equation (2.40). Then,

$$\frac{\partial \mathbf{u}}{\partial x} = \frac{\partial \mathbf{F}}{\partial x}\boldsymbol{\beta} \tag{2.53}$$

and

$$\frac{\partial \mathbf{u}}{\partial y} = \frac{\partial \mathbf{F}}{\partial y}\boldsymbol{\beta}. \tag{2.54}$$

By using the coordinate matrix $\mathbf{F}$ which is a function of nodal coordinates (r_x, r_y), the spatial derivatives of the unknown $\mathbf{u}$ can be approximated as

$$\frac{\partial \mathbf{u}}{\partial x} = \frac{\partial \mathbf{F}}{\partial x}\mathbf{F}^{-1}\mathbf{u} \tag{2.55}$$

and

$$\frac{\partial \mathbf{u}}{\partial y} = \frac{\partial \mathbf{F}}{\partial y}\mathbf{F}^{-1}\mathbf{u} \tag{2.56}$$

where $\mathbf{F}^{-1}$, $\frac{\partial \mathbf{F}}{\partial x}$, and $\frac{\partial \mathbf{F}}{\partial y}$ are of sizes $(N+L)\times(N+L)$. The entries of the matrices $\frac{\partial \mathbf{F}}{\partial x}$ and $\frac{\partial \mathbf{F}}{\partial y}$ are constructed in terms of the partial derivatives of the radial basis function f.

2.3 DRBEM Solution of Cauchy Problem

Direct problems which are also called as well-posed problems satisfy the properties of uniqueness, stability and existence of a solution of the corresponding mathematical problem. On the other hand, if a mathematical problem does not satisfy one of the above properties, then it is called as an ill-posed problem.

Cauchy (inverse) problems are the problems which consists of obtaining an unknown characteristic of a medium from the observation of reply of this medium to probing signal [78]. While the solutions of direct problems are well-posed, that of Cauchy problems are generally ill-posed. On the other hand, direct and Cauchy problems are very related to each other since the known data of the direct problem is unknown for the Cauchy problem. In direct problems, the aim is to determine the field variables. However, the main purpose of Cauchy problems is to specify the unknown term from the corresponding direct problem. In brief, it can be said that the main idea of the Cauchy problem is to determine the unknowns by using the extra information obtained from the direct problem.

In general, Cauchy problems can be grouped into three main classes. These are boundary inverse problems, parameter identification, and reconstruction of defects such as cracks, holes, etc [75]. In this thesis, we deal with the Cauchy problems in terms of boundary inverse formulation and parameter identification for MHD duct flow.

2.3.1 DRBEM Solution of Poisson's Equation as an Inverse Problem

In this section, the DRBEM solution is explained for the inverse formulation of Poisson's equation

$$\nabla^2 u = b(x,y), \qquad (x,y) \in \Omega \tag{2.57}$$

with the Dirichlet and Neumann boundary conditions

$$\begin{aligned} u(x,y) &= \bar{u}_1(x,y), \qquad (x,y) \in \Gamma_1 \\ q(x,y) &= \bar{q}_2(x,y), \qquad (x,y) \in \Gamma_2 \end{aligned} \tag{2.58}$$

where $b(x,y), \bar{u}_1(x,y), \bar{q}_2(x,y)$ are known functions, $\Gamma_1 + \Gamma_2 = \Gamma$ is the piecewisely smooth boundary of the problem region $\Omega \in R^2$, $q = \dfrac{\partial u}{\partial n}$ with the unit outward normal vector n to the boundary Γ.

In some cases, while one part of the boundary is overspecified since it contains both Dirichlet and Neumann type boundary conditions as u and q, the other part is underspecified since it has no boundary information. Such kind of problems are called as Cauchy or inverse problems.

An inverse formulation for the Poisson's equation can be defined as

$$\nabla^2 u = b(x,y), \qquad (x,y) \in \Omega \tag{2.59}$$

with the Dirichlet and Neumann type boundary conditions

$$\begin{aligned} u(x,y) &= \bar{u}_1(x,y), \quad q(x,y) = \bar{q}_1(x,y), \qquad (x,y) \in \Gamma_1 \\ u(x,y) &= \bar{u}_2(x,y) =?, \quad q(x,y) = \bar{q}_2(x,y) =?, \qquad (x,y) \in \Gamma_2 \end{aligned} \tag{2.60}$$

where the prescribed boundary informations of direct problem are taken as unknown for the inverse formulation. The overspecified boundary conditions for the inverse problem are obtained through the solution of the corresponding direct problem.

The DRBEM solution of the inverse formulation of Poisson's equation is obtained by using the same procedure which is explained in Section 2.2. After inserting the boundary conditions into the system and swapping the columns of the **H** and **G** matrices, the system of linear algebraic equations is obtained as

$$\boldsymbol{A}\boldsymbol{x} = \boldsymbol{b}. \tag{2.61}$$

One can construct the above system by using the known boundary informations of the inverse problem and extra informations from the direct problem. Since one part of the boundary is overspecified and the other part is underspecified, the DRBEM discretization results in an ill-posed system of equations. Hence, in addition to the DRBEM application, a regularization technique must be used to get the solution of the ill-posed system.

2.4 Regularization Techniques

For the solution of inverse problems in terms of boundary conditions or parameter identification, many numerical techniques such as BEM, DRBEM, and FEM yield a system of the form

$$\boldsymbol{Ax} = \boldsymbol{b} \tag{2.62}$$

where small changes in the vector b cause large changes in the solution vector x due to the overspecified and underspecified boundary conditions or more known information. Hence, without any regularization, the solution of the ill-conditioned system (2.62) may not be obtained correctly. There exist several regularization techniques to obtain an accurate close solution of an ill-conditioned system such as Tikhonov regularization which is the most common one, and some iterative methods as direct-inverse or well-posed iterations.

2.4.1 Tikhonov Regularization

The Tikhonov regularized solution x is given as the solution of the regularized equation

$$(\boldsymbol{A^T A} + \lambda \boldsymbol{I})\boldsymbol{x} = \boldsymbol{A^T b} \tag{2.63}$$

where $\boldsymbol{I}$ is the identity matrix, $\lambda > 0$ is the regularization parameter to be chosen, and the choice of this parameter is an important issue in solving the system.

When λ is taken as $\lambda = 0$, the solution of the system becomes simply the least-squares solution which is completely dominated by data and rounding errors. The norm of

the solution $||\boldsymbol{x}||_2$ of the system can be maintained in the reasonable size by adding regularization. If λ is taken as a large value, i.e, too much regularization, then the residual norm $||\boldsymbol{A}\boldsymbol{x} - \boldsymbol{b}||_2$ will be very large and it cannot fit the data $\boldsymbol{b}$ properly. If λ is small, $||\boldsymbol{x}||_2$ will be large since the solution is dominated by data errors although the solution fits tha data. In general, the regularization parameter λ is found from the L-curve method, Mozorov principle [62], etc.

2.4.2 Direct-Inverse Iterations for Poisson's Equation

Apart from classical regularization techniques such as Tikhonov regularization which is applied to solve an ill-posed problem, iterative methods can be developed to regularize some particular ill-posed problems.

In this section, the iterative procedure which includes the solution of direct and inverse problems is explained on the inverse formulation of the Poisson's equation [10]

$$\nabla^2 u = b(x,y), \qquad (x,y) \in \Omega \tag{2.64}$$

with the Dirichlet and Neumann type boundary conditions

$$\begin{aligned} &u(x,y) = \bar{u}_1(x,y), \qquad q(x,y) = \bar{q}_1(x,y), \qquad (x,y) \in \Gamma_1 \\ &u(x,y) = \bar{u}_2(x,y) = ?, \quad q(x,y) = \bar{q}_2(x,y) = ?, \qquad (x,y) \in \Gamma_2. \end{aligned} \tag{2.65}$$

The iterative algorithm consisting of the solutions of direct and inverse formulations of Poisson's equation includes the following steps:

Step 1. The direct formulation of Poisson's equation

$$\nabla^2 u = b(x,y), \qquad (x,y) \in \Omega \tag{2.66}$$

with the boundary conditions

$$\begin{aligned} u(x,y) &= \bar{u}(x,y), \qquad (x,y) \in \Gamma_1 \\ q(x,y) &= \bar{q}(x,y), \qquad (x,y) \in \Gamma_2 \end{aligned} \tag{2.67}$$

is solved to obtain $\dfrac{\partial u}{\partial n}(x,y) = q(x,y)$ on Γ_1 as an overspecified boundary condition. Here, the value of $q(x,y) = \bar{q}(x,y)$ on Γ_2 is taken as an initial assumption from the direct formulation of the problem.

Step 2. The inverse formulation of Poisson's equation (2.64) with the overspecified and underspecified boundary conditions (2.65) is solved by using Tikhonov regularization.

Step 3. The value of $\dfrac{\partial u}{\partial n}(x,y) = q(x,y)$ on Γ_2 in *Step 1* is replaced with the one which is found from *Step 2*.

Step 4. Repeat steps 1-3 until the value of q on Γ_2 converges to the direct solution of Poisson's problem.

2.4.3 The Well-posed Iterations for Poisson's Equation

In this section, an iterative algorithm which was advanced by Kozlov et al. [79] is explained for the inverse formulation of Poisson's equation. In this method, the main idea is alternating the given boundary informations on the overspecified boundary to reduce the ill-posed problem into a sequence of well-posed problems.

The well-posed iterations technique consists of the following steps:

Step 1. The direct Poisson's equation

$$\nabla^2 u = b(x,y), \qquad (x,y) \in \Omega \tag{2.68}$$

with the boundary conditions

$$\begin{aligned} u(x,y) &= \bar{u}(x,y), \qquad (x,y) \in \Gamma_1 \\ q(x,y) &= \bar{q}(x,y), \qquad (x,y) \in \Gamma_2 \end{aligned} \tag{2.69}$$

is solved to obtain $\dfrac{\partial u}{\partial n} = q$ on Γ_1 and u on Γ_2.

Step 2. Now, we have both $u = \bar{u}$ and $q = \bar{q}$ on Γ_1 as overspecified boundary conditions of the inverse formulation of Poisson's equation. The direct problem is solved with $q = \bar{q}$ on Γ_1 and $u = \bar{u}$ on Γ_2. Thus, new $u = \bar{u}$ on Γ_1 and $q = \bar{q}$ on Γ_2 are obtained.

Step 3. The values of $u = \bar{u}$ on Γ_1 and $q = \bar{q}$ on Γ_2 which were used in *Step 1* are replaced with the ones which are obtained from *Step 2*.

Step 4. Steps 1-3 are repeated until the value of q which is newly found in *Step 2.* converges to $q = \bar{q}$ on Γ_2 which is the boundary condition of direct Poisson's problem.

In Chapter 2, the boundary element method is shown in general for the Poisson's type partial differential equation and the DRBEM solutions of Poisson's equation are presented for both direct and inverse formulations. In addition, the regularization techniques which are the Tikhonov regularization, the direct-inverse iterations, and the well-posed iterations for the inverse formulation of Poisson's problem are explained. In Chapter 3, the applications of the DRBEM are going to be given for the direct and inverse formulations of MHD rectangular duct flow problem. The governing equations of the MHD flow can be considered in the form of $\nabla^2 u = b(x, y)$ and the DRBEM is the most suitable method for the direct and inverse formulations of MHD duct flow problems since it provides both the solution and its normal derivative which are used in boundary inverse type MHD problems. In the parameter identification MHD problems, the interior solution obtained from the DRBEM is made use of on the boundary.

CHAPTER 3

DRBEM SOLUTION OF DIRECT AND INVERSE MHD DUCT FLOW PROBLEMS

3.1 MHD Direct and Cauchy Problems

In this thesis, the MHD duct flow problem is formulated as direct and inverse problems. If the velocity of the fluid and the induced magnetic field or their normal derivatives are known on some parts of the duct boundary and the only unknowns are their values of them in the domain, this yields the direct formulation of the MHD flow. However, in some cases, one part of the boundary allows both the velocity slip and conductivity change depending on the material of the boundary. Thus, the slip length and conductivity constant are unknowns, which can be obtained through the inverse formulation of the MHD flow problem, i.e, inverse problem in terms of boundary conditions. Sometimes, the velocity of the fluid and the induced magnetic field are given on the boundary and also in the problem region, however, the Hartmann number in the MHD differential equations is unknown which leads to an inverse problem in terms of parameter identification.

3.2 DRBEM Solution of Direct MHD Duct Flow Problem

Governing equations of the MHD flow in a channel whose cross-section is a rectangle (duct) under externally applied oblique magnetic field are given in Chapter 1 as

$$\begin{aligned} \nabla^2 V + Ha_x \frac{\partial B}{\partial x} + Ha_y \frac{\partial B}{\partial y} &= -1 \\ \nabla^2 B + Ha_x \frac{\partial V}{\partial x} + Ha_y \frac{\partial V}{\partial y} &= 0 \end{aligned} \tag{3.1}$$

respectively. $V(x,y)$ is the velocity of the fluid and $B(x,y)$ is the induced magnetic field, and Ha is the Hartmann number resulted from the non-dimensionalization of the equations. Here,

$$\begin{aligned} Ha_x &= Hasin(\beta) \\ Ha_y &= Hacos(\beta) \\ Ha &= \sqrt{Ha_x^2 + Ha_y^2} \end{aligned} \tag{3.2}$$

where the magnetic field applies in the direction obtained with an angle β from the y-axis. When the angle β is taken as $\beta = 0$ or $\beta = \frac{\pi}{2}$, the externally applied magnetic field becomes parallel to the y-axis or x-axis, respectively.

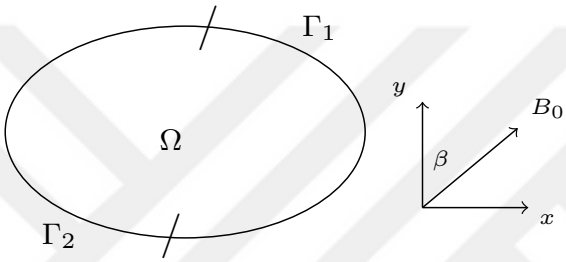


Figure 3.1: Boundary Conditions for the Direct MHD Duct Flow

For simplicity, in the rest of this chapter, the application of DRBEM is explained for the case of horizontally applied magnetic field by taking $\beta = \frac{\pi}{2}$. Hence, the term $Ha_x = Ha$ and $Ha_y = 0$, then the MHD equations in the domain Ω are obtained as

$$\begin{aligned} \nabla^2 V + Ha\frac{\partial B}{\partial x} &= -1 \\ \nabla^2 B + Ha\frac{\partial V}{\partial x} &= 0. \end{aligned} \tag{3.3}$$

The problem is considered with several boundary conditions varying from no-slip to slipping velocity and insulated to variably conducting walls.

The MHD differential equations (3.3) can be solved either in the decoupled or coupled form. In the solution of MHD flow problem in a rectangular duct, the decoupling of the MHD differential equations is performed with the change of variables [9]

$$U_1 = V + B, \qquad U_2 = V - B \tag{3.4}$$

which results in two convection-diffusion type equations in a domain Ω

$$\begin{aligned} \nabla^2 U_1 + Ha\frac{\partial U_1}{\partial x} &= -1 \\ \nabla^2 U_2 - Ha\frac{\partial U_2}{\partial x} &= -1. \end{aligned} \tag{3.5}$$

Taking the terms other than Laplacian in equation (3.5) as inhomogeneties and following the DRBEM procedure given in Chapter 2, the DRBEM discretized equations in matrix-vector form become

$$\begin{aligned} \mathbf{H}\boldsymbol{U}_1 - \mathbf{G}\frac{\partial \boldsymbol{U}_1}{\partial n} &= (\mathbf{H}\hat{\boldsymbol{U}} - \mathbf{G}\hat{\boldsymbol{Q}})\mathbf{F}^{-1}(-\mathbf{1} - Ha\frac{\partial \boldsymbol{U}_1}{\partial x}) \\ \mathbf{H}\boldsymbol{U}_2 - \mathbf{G}\frac{\partial \boldsymbol{U}_2}{\partial n} &= (\mathbf{H}\hat{\boldsymbol{U}} - \mathbf{G}\hat{\boldsymbol{Q}})\mathbf{F}^{-1}(-\mathbf{1} + Ha\frac{\partial \boldsymbol{U}_2}{\partial x}). \end{aligned} \tag{3.6}$$

Solving the matrix-vector equations (3.6) after converting them into the form $\boldsymbol{Ax} = \boldsymbol{b}$ by collecting the known and unknown values of $\boldsymbol{U}_1$ and $\boldsymbol{U}_2$ according to the corresponding boundary conditions gives all the unknown values of $\boldsymbol{U}_1$ and $\boldsymbol{U}_2$ on the boundary and in the interior of the domain. Then, using the given substitutions (3.4), the velocity $\boldsymbol{V}$ and the induced magnetic field $\boldsymbol{B}$ values on the boundary and in the interior of the problem region can be obtained.

In addition, instead of decoupling the MHD differential equations (3.3), they can be solved by constructing the coupled matrix-vector equations as a whole. Although the system size increases, the computational effort in the numerical solution through the DRBEM considerably decreases. The DRBEM discretized matrix-vector equations corresponding to the MHD differential equations (3.3) become then

$$\begin{aligned} \mathbf{H}\boldsymbol{V} - \mathbf{G}\frac{\partial \boldsymbol{V}}{\partial n} &= -(\mathbf{H}\hat{\boldsymbol{U}} - \mathbf{G}\hat{\boldsymbol{Q}})\mathbf{F}^{-1}(Ha\frac{\partial \boldsymbol{B}}{\partial x} + \mathbf{1}) \\ \mathbf{H}\boldsymbol{B} - \mathbf{G}\frac{\partial \boldsymbol{B}}{\partial n} &= -(\mathbf{H}\hat{\boldsymbol{U}} - \mathbf{G}\hat{\boldsymbol{Q}})\mathbf{F}^{-1}(Ha\frac{\partial \boldsymbol{V}}{\partial x}). \end{aligned} \tag{3.7}$$

The combination of the equations (3.7) by using the coordinate matrix $\mathbf{F}$ given in (2.39) to approximate the derivatives $\dfrac{\partial V}{\partial x}$ and $\dfrac{\partial B}{\partial x}$ yields

$$\begin{bmatrix} \mathbf{H} & \mathbf{0} \\ \mathbf{0} & \mathbf{H} \end{bmatrix} \begin{Bmatrix} \boldsymbol{V} \\ \boldsymbol{B} \end{Bmatrix} - \begin{bmatrix} \mathbf{G} & \mathbf{0} \\ \mathbf{0} & \mathbf{G} \end{bmatrix} \begin{Bmatrix} \dfrac{\partial \boldsymbol{V}}{\partial n} \\ \dfrac{\partial \boldsymbol{B}}{\partial n} \end{Bmatrix} = -Ha \begin{bmatrix} \mathbf{M} & \mathbf{0} \\ \mathbf{0} & \mathbf{M} \end{bmatrix} \begin{Bmatrix} \boldsymbol{B} \\ \boldsymbol{V} \end{Bmatrix} + \begin{bmatrix} \mathbf{D} & \mathbf{0} \\ \mathbf{0} & \mathbf{0} \end{bmatrix} \begin{Bmatrix} -1 \\ \mathbf{0} \end{Bmatrix} \tag{3.8}$$

where $\mathbf{D}=(\mathbf{H}\hat{\boldsymbol{U}}\text{-}\mathbf{G}\hat{\boldsymbol{Q}})\mathbf{F}^{-1}$ and $\mathbf{M}=\mathbf{D}\dfrac{\partial \mathbf{F}}{\partial x}\mathbf{F}^{-1}$.

The equation (3.8) can be rewritten as

$$\begin{bmatrix} \mathbf{H} & \mathbf{0} \\ \mathbf{0} & \mathbf{H} \end{bmatrix} \begin{Bmatrix} \boldsymbol{V} \\ \boldsymbol{B} \end{Bmatrix} - \begin{bmatrix} \mathbf{G} & \mathbf{0} \\ \mathbf{0} & \mathbf{G} \end{bmatrix} \begin{Bmatrix} \dfrac{\partial \boldsymbol{V}}{\partial n} \\ \dfrac{\partial \boldsymbol{B}}{\partial n} \end{Bmatrix} = -Ha \begin{bmatrix} \mathbf{0} & \mathbf{M} \\ \mathbf{M} & \mathbf{0} \end{bmatrix} \begin{Bmatrix} \boldsymbol{V} \\ \boldsymbol{B} \end{Bmatrix} + \begin{bmatrix} \mathbf{D} & \mathbf{0} \\ \mathbf{0} & \mathbf{0} \end{bmatrix} \begin{Bmatrix} -1 \\ \mathbf{0} \end{Bmatrix}. \tag{3.9}$$

Rearranging the equation (3.9) results in the system

$$\left(\begin{bmatrix} \mathbf{H} & \mathbf{0} \\ \mathbf{0} & \mathbf{H} \end{bmatrix} + Ha \begin{bmatrix} \mathbf{0} & \mathbf{M} \\ \mathbf{M} & \mathbf{0} \end{bmatrix} \right) \begin{Bmatrix} \boldsymbol{V} \\ \boldsymbol{B} \end{Bmatrix} - \begin{bmatrix} \mathbf{G} & \mathbf{0} \\ \mathbf{0} & \mathbf{G} \end{bmatrix} \begin{Bmatrix} \dfrac{\partial \boldsymbol{V}}{\partial n} \\ \dfrac{\partial \boldsymbol{B}}{\partial n} \end{Bmatrix} = \begin{bmatrix} \mathbf{D} & \mathbf{0} \\ \mathbf{0} & \mathbf{0} \end{bmatrix} \begin{Bmatrix} -1 \\ \mathbf{0} \end{Bmatrix}. \tag{3.10}$$

For simplicity, the matrices can be defined as

$$\mathbf{H}' = \begin{bmatrix} \mathbf{H} & \mathbf{0} \\ \mathbf{0} & \mathbf{H} \end{bmatrix} + Ha \begin{bmatrix} \mathbf{0} & \mathbf{M} \\ \mathbf{M} & \mathbf{0} \end{bmatrix}, \qquad \mathbf{G}' = \begin{bmatrix} \mathbf{G} & \mathbf{0} \\ \mathbf{0} & \mathbf{G} \end{bmatrix}, \qquad \mathbf{D}' = \begin{bmatrix} \mathbf{D} & \mathbf{0} \\ \mathbf{0} & \mathbf{0} \end{bmatrix} \tag{3.11}$$

where $\mathbf{H}'$, $\mathbf{G}'$, $\mathbf{D}'$ are sizes of $2(N+L) \times 2(N+L)$. The enlarged system is obtained as

$$\mathbf{H}' \begin{Bmatrix} \mathbf{V} \\ \mathbf{B} \end{Bmatrix} = \mathbf{G}' \begin{Bmatrix} \dfrac{\partial \boldsymbol{V}}{\partial n} \\ \dfrac{\partial \boldsymbol{B}}{\partial n} \end{Bmatrix} + \mathbf{D}' \begin{Bmatrix} -\mathbf{1} \\ \mathbf{0} \end{Bmatrix}. \tag{3.12}$$

In this thesis, either velocity and the induced magnetic field or their normal derivative values are known on parts of the boundary, and also there is a slip velocity or variable conductivity condition on one part of the boundary. On the slipping or variably conducting wall, the velocity or the induced magnetic field is unknown, hence the normal derivatives of them are taken as $\dfrac{\partial V}{\partial n} = -\dfrac{1}{\alpha} V$ or $\dfrac{\partial B}{\partial n} = -\dfrac{1}{c} B$, respectively, where α is the slip length and c is the conductivity constant. If there is no slip velocity or no variable conducitvity on the boundary, then the velocity or the induced magnetic field is known and the uknowns are their normal derivatives. At the interior nodes, the velocity and the induced magnetic field are unknown and their normal derivatives are zero. After inserting all the boundary conditions into the matrix-vector equation

(3.12), the left hand side and the right hand side vectors contain some known and unknown values of the velocity and the induced magnetic field. The unknowns on the right hand side of the equation (3.12) are carried to the left hand side by swapping the corresponding columns of matrices $\mathbf{H}'$ and $\mathbf{G}'$ to obtain a linear system of equations. If there is a slip velocity or variable conductivity condition, i.e, the velocity or the induced magnetic field is unknown, the corresponding columns of the matrices $\mathbf{H}'$ and $\frac{1}{\alpha}\mathbf{G}'$ or $\frac{1}{c}\mathbf{G}'$ are added and carried to the left hand side, and the corresponding column on the right hand side is left as zero. After collecting all the unknowns on the left hand side, a linear system of equations in the form of

$$\boldsymbol{Ax} = \boldsymbol{d} \tag{3.13}$$

is obtained and it is solved. Then, one gets velocity V and the induced magnetic field B values on the boundary and in the interior of the domain as a whole.

3.3 DRBEM Solution of MHD Duct Flow Equations as an Inverse Problem

In this section, the DRBEM is explained for the inverse formulation of the MHD duct flow problem in a domain Ω

$$\begin{aligned} \nabla^2 V + Ha\frac{\partial B}{\partial x} &= -1 \\ \nabla^2 B + Ha\frac{\partial V}{\partial x} &= 0 \end{aligned} \tag{3.14}$$

with the Dirichlet and mixed boundary conditions

$$\begin{aligned} &V(x,y) = \bar{V}(x,y), && B(x,y) = \bar{B}(x,y) && (x,y) \in \Gamma_1 \\ &V(x,y) + \alpha\frac{\partial V}{\partial n}(x,y) = 0, && B(x,y) + c\frac{\partial B}{\partial n}(x,y) = 0 && (x,y) \in \Gamma_2 \end{aligned} \tag{3.15}$$

where $\bar{V}$ and $\bar{B}$ are prescribed functions, $\Gamma_1 + \Gamma_2 = \Gamma$ is the piecewisely smooth boundary of the problem region $\Omega \in R^2$, and α is the dimensionless slip length and c is the conductivity constant. When α is taken as $\alpha = 0$, then $V = 0$ and this part of the boundary is called as no-slip boundary. When $c = 0$, then $B = 0$ and the wall becomes insulated. In addition, if c approaches to the infinity, then $\frac{\partial B}{\partial n} = 0$ and the wall is called as perfectly conducting.

In some engineering applications one part of the boundary may allow both the velocity slip or conductivity change depending on the material which is made of. In addition, in some cases, the slip length and conductivity constant need to be determined that yields the inverse formulation of the MHD duct flow. An inverse formulation of MHD duct flow problem in a domain Ω can be defined as

$$\begin{aligned} \nabla^2 V + Ha\frac{\partial B}{\partial x} &= -1 \\ \nabla^2 B + Ha\frac{\partial V}{\partial x} &= 0 \end{aligned} \tag{3.16}$$

with the boundary conditions

$$\begin{aligned} &V(x,y) = \bar{V}(x,y), \quad \frac{\partial V}{\partial n}(x,y) = \frac{\partial \bar{V}}{\partial n}(x,y), && (x,y) \in \Gamma_1 \\ &B(x,y) = \bar{B}(x,y), \quad \frac{\partial B}{\partial n}(x,y) = \frac{\partial \bar{B}}{\partial n}(x,y), && (x,y) \in \Gamma_1 \\ &V(x,y) = ?, \qquad \frac{\partial V}{\partial n}(x,y) = ?, && (x,y) \in \Gamma_2 \\ &B(x,y) = ?, \qquad \frac{\partial B}{\partial n}(x,y) = ?, && (x,y) \in \Gamma_2 \end{aligned} \tag{3.17}$$

where $\bar{V}(x,y)$, $\bar{B}(x,y)$, $\dfrac{\partial \bar{V}}{\partial n}(x,y)$, $\dfrac{\partial \bar{B}}{\partial n}(x,y)$ are known on the boundary Γ_1. Since there are more than one boundary condition for V and B on that part of the boundary, Γ_1 is called as overspecified. Since there is no boundary information for V and B on Γ_2, Γ_2 is called as underspecified. The extra boundary information on the boundary Γ_1 is obtained from the direct problem which is given in the equation (3.14) with the boundary conditions (3.15) for specified values of the slip length α and the conductivity constant c.

The DRBEM procedure of the inverse formulation of MHD duct flow problem is the same as explained in Section 3.2. It differs only in inserting the overspecified boundary information. After inserting the boundary conditions into the system and swapping the columns of the **H** and **G** matrices, the system of linear algebraic equations is obtained as in the form of (3.13), but they are not same.

Due to the overspecified and underspecified boundary conditions on the parts of the boundary of the problem region, the DRBEM discretization yields an ill-posed system of equations. Therefore, the DRBEM application should be employed with a regularization technique.

3.4 Parameter Identification for the MHD Duct Flow

The inverse problem in terms of the parameter identification for the MHD duct flow in a domain Ω is given as

$$\begin{aligned} \nabla^2 V + Ha\frac{\partial B}{\partial x} &= -1 \\ \nabla^2 B + Ha\frac{\partial V}{\partial x} &= 0 \end{aligned} \tag{3.18}$$

with the Dirichlet and Neumann boundary conditions

$$\begin{aligned} V(x,y) &= \bar{V}_1(x,y), \quad \frac{\partial V}{\partial n}(x,y) = \frac{\partial \bar{V}_1}{\partial n}(x,y), \qquad (x,y) \in \Gamma_1 \\ B(x,y) &= \bar{B}_1(x,y), \quad \frac{\partial B}{\partial n}(x,y) = \frac{\partial \bar{B}_1}{\partial n}(x,y), \qquad (x,y) \in \Gamma_1 \\ V(x,y) &= \bar{V}_2(x,y), \quad \frac{\partial V}{\partial n}(x,y) = \frac{\partial \bar{V}_2}{\partial n}(x,y), \qquad (x,y) \in \Gamma_2 \\ B(x,y) &= \bar{B}_2(x,y), \quad \frac{\partial B}{\partial n}(x,y) = \frac{\partial \bar{B}_2}{\partial n}(x,y), \qquad (x,y) \in \Gamma_2 \end{aligned} \tag{3.19}$$

where $\bar{V}_1(x,y)$, $\bar{B}_1(x,y)$, $\bar{V}_2(x,y)$, $\bar{B}_2(x,y)$, $\frac{\partial \bar{V}_1}{\partial n}(x,y)$, $\frac{\partial \bar{B}_1}{\partial n}(x,y)$, $\frac{\partial \bar{V}_2}{\partial n}(x,y)$, $\frac{\partial \bar{B}_2}{\partial n}(x,y)$ are prescribed functions.

In addition, some internal values of V and B are also known. Here, the only parameter is Ha to be regained through inverse problem in the problem region.

The DRBEM discretization of the problem yields the following matrix-vector equation

$$\begin{bmatrix} \mathbf{H} & \mathbf{K} \\ \mathbf{K} & \mathbf{H} \end{bmatrix} \begin{Bmatrix} \boldsymbol{V} \\ \boldsymbol{B} \end{Bmatrix} = \begin{bmatrix} \mathbf{G} & \mathbf{0} \\ \mathbf{0} & \mathbf{G} \end{bmatrix} \begin{Bmatrix} \dfrac{\partial \boldsymbol{V}}{\partial n} \\ \dfrac{\partial \boldsymbol{B}}{\partial n} \end{Bmatrix} + \begin{Bmatrix} \mathbf{b} \\ \mathbf{0} \end{Bmatrix} \tag{3.20}$$

where **H**, **G** are BEM matrices with entries composed of boundary integrals of fundamental solution and its normal derivative, respectively. **K**=$(\mathbf{H}\hat{\boldsymbol{U}} - \mathbf{G}\hat{\boldsymbol{Q}})\mathbf{F}^{-1} Ha \dfrac{\partial \mathbf{F}}{\partial x}\mathbf{F}^{-1}$, **b**=$-(\mathbf{H}\hat{\boldsymbol{U}} - \mathbf{G}\hat{\boldsymbol{Q}})\mathbf{F}^{-1}(1,1,...,1)^T$.

The system (3.20) is rearranged as

$$\begin{bmatrix} \mathbf{H} & \mathbf{0} \\ \mathbf{0} & \mathbf{H} \end{bmatrix} \begin{Bmatrix} \boldsymbol{V} \\ \boldsymbol{B} \end{Bmatrix} = \begin{bmatrix} \mathbf{G} & \mathbf{0} \\ \mathbf{0} & \mathbf{G} \end{bmatrix} \begin{Bmatrix} \dfrac{\partial \boldsymbol{V}}{\partial n} \\ \dfrac{\partial \boldsymbol{B}}{\partial n} \end{Bmatrix} + \begin{bmatrix} \mathbf{K}' & \mathbf{0} \\ \mathbf{0} & \mathbf{K}'' \end{bmatrix} \begin{Bmatrix} \mathbf{Ha_1} \\ \mathbf{Ha_2} \end{Bmatrix} + \begin{Bmatrix} \mathbf{0} \\ \mathbf{b} \end{Bmatrix} \tag{3.21}$$

where $\mathbf{K}'$=$(\mathbf{H}\hat{\boldsymbol{U}} - \mathbf{G}\hat{\boldsymbol{Q}})\mathbf{F}^{-1}\dfrac{\partial \mathbf{F}}{\partial x}\mathbf{F}^{-1}diag(\boldsymbol{V})$, $\mathbf{K}''$=$(\mathbf{H}\hat{\boldsymbol{U}} - \mathbf{G}\hat{\boldsymbol{Q}})\mathbf{F}^{-1}\dfrac{\partial \mathbf{F}}{\partial x}\mathbf{F}^{-1}diag(\boldsymbol{B})$. The system (3.21) is solved for $(Ha_1, Ha_2)^T$ as an inverse problem with the overdetermined known solution obtained from the direct problem. Due the overspecified informations on each part of the boundary, the resulted system is ill-posed. Hence, to obtain the solution, the resulting DRBEM system should be supplied with a regularization technique.

3.5 Regularization Techniques for Cauchy MHD Duct Flow

In this thesis, Tikhonov regularization which is explained in Chapter 2, the direct-inverse iterations, and the well-posed iterations are used to solve the Cauchy MHD duct flow problems.

3.5.1 The Direct-Inverse Iterations for Cauchy MHD Duct Flow

Apart from classical regularization techniques such as Tikhonov regularization which is applied to solve an ill-posed problem, iterative methods can be developed to regularize some particular ill-posed problems.

In this section, the iterative procedure which includes the solution of direct and inverse problems is explained on the inverse formulation of the MHD duct flow problem in Ω [10]

$$\begin{aligned} \nabla^2 V + Ha\frac{\partial B}{\partial x} &= -1 \\ \nabla^2 B + Ha\frac{\partial V}{\partial x} &= 0 \end{aligned} \tag{3.22}$$

with the boundary conditions

$$\begin{aligned} &V(x,y) = \bar{V}(x,y), \quad \frac{\partial V}{\partial n}(x,y) = \frac{\partial \bar{V}}{\partial n}(x,y), && (x,y) \in \Gamma_1 \\ &B(x,y) = \bar{B}(x,y), \quad \frac{\partial B}{\partial n}(x,y) = \frac{\partial \bar{B}}{\partial n}(x,y), && (x,y) \in \Gamma_1 \\ &V(x,y) = ?, \qquad \frac{\partial V}{\partial n}(x,y) = ?, && (x,y) \in \Gamma_2 \\ &B(x,y) = ?, \qquad \frac{\partial B}{\partial n}(x,y) = ?, && (x,y) \in \Gamma_2. \end{aligned} \tag{3.23}$$

The iterative algorithm consisting of the solutions of direct and inverse formulations of MHD duct flow includes the following steps:

Step 1. The direct MHD duct flow problem in Ω

$$\begin{aligned} \nabla^2 V + Ha\frac{\partial B}{\partial x} &= -1 \\ \nabla^2 B + Ha\frac{\partial V}{\partial x} &= 0 \end{aligned} \tag{3.24}$$

with the Dirichlet and mixed boundary conditions

$$\begin{aligned} &V(x,y) = \bar{V}(x,y), && B(x,y) = \bar{B}(x,y) && (x,y) \in \Gamma_1 \\ &V(x,y) + \alpha\frac{\partial V}{\partial n}(x,y) = 0, && B(x,y) + c\frac{\partial B}{\partial n}(x,y) = 0 && (x,y) \in \Gamma_2 \end{aligned} \tag{3.25}$$

is solved to obtain the V and B values on Γ_2 corresponding to specified α and c.

Step 2. The direct MHD duct flow problem is solved with the Dirichlet type boundary conditions for V and B everywhere on the boundary to obtain the normal derivatives of V and B on Γ_1 as overspecified boundary conditions.

Step 3. The MHD duct flow problem in Ω as an inverse formulation given as

$$\begin{aligned} \nabla^2 V + Ha\frac{\partial B}{\partial x} &= -1 \\ \nabla^2 B + Ha\frac{\partial V}{\partial x} &= 0 \end{aligned} \tag{3.26}$$

with the boundary conditions

$$\begin{aligned} &V(x,y) = \bar{V}(x,y), && \frac{\partial V}{\partial n}(x,y) = \frac{\partial \bar{V}}{\partial n}(x,y), && (x,y) \in \Gamma_1 \\ &B(x,y) = \bar{B}(x,y), && \frac{\partial B}{\partial n}(x,y) = \frac{\partial \bar{B}}{\partial n}(x,y), && (x,y) \in \Gamma_1 \\ &V(x,y) = ?, && \frac{\partial V}{\partial n}(x,y) = ?, && (x,y) \in \Gamma_2 \\ &B(x,y) = ?, && \frac{\partial B}{\partial n}(x,y) = ?, && (x,y) \in \Gamma_2 \end{aligned} \tag{3.27}$$

where the normal derivavites of V and B on Γ_1 are obtained from step 2 is solved by using Tikhonov regularization.

Step 4. Replace V and B values on Γ_2 with the ones which are obtained from step 3.

Step 5. Repeat the steps 2-4 until V and B values converge to the solutions of the direct problem with corresponding slip length α and conductivity constant c.

3.5.2 The Well-posed Iterations for Cauchy MHD Duct Flow

In this section, an iterative algorithm which was advanced by Kozlov et al. [79] is explained for the Cauchy MHD duct flow problem. In this method, the main idea is alternating the given boundary informations on the overspecified boundary to reduce the ill-posed problem into a sequence of well-posed problems.

Step 1. The MHD duct flow equations (3.24) with the boundary conditions (3.25) is solved in one stroke as a direct problem with the specified α and c values to get the unknown values for V, B on Γ_2 and their normal derivatives on both Γ_1 and Γ_2. Now, the Cauchy MHD problem is constructed with the assumption that the underspecified conditions on Γ_2 (neither V, B nor $\dfrac{\partial V}{\partial n}$, $\dfrac{\partial B}{\partial n}$ are known) and overspecified conditions on Γ_1 (V, B and their normal derivatives are known).

Step 2. Solve the coupled MHD duct flow equations as a direct problem using the Dirichlet type boundary conditions for V and B on Γ_1 and Γ_2. The solution gives normal derivatives of V and B everywhere on the boundary.

Step 3. Use $\dfrac{\partial V}{\partial n}$ and $\dfrac{\partial B}{\partial n}$ on Γ_1 and Γ_2 obtained from *Step 2* for solving the direct problem to find the new V, B values.

Step 4. Update the values of V and B with the values obtained from step 3 on Γ_2.

Step 5. Repeat steps 2-4 until the velocity and the induced magentic field values converge to the solution of the direct problem corresponding to the specified slip length α and the conductivity constant c.

3.6 DRBEM Application to the Cauchy MHD Flow with a Slip Velocity Duct Wall

The two-dimensional, steady, and fully-developed MHD flow in a rectangular duct is considered under the effect of an external, horizontally applied magnetic field. It is assumed that the vertical walls have certain electrical conductivity. Furthermore, the left vertical and bottom horizontal walls which are perpendicular and parallel to the applied magnetic, respectively, allow the slip of the fluid, seperately. The non-

dimensional governing equations for the velocity $V(x, y)$ of the fluid and the induced magnetic field $B(x, y)$ are given in the domain Ω (3.3) as

$$\begin{aligned} \nabla^2 V + Ha\frac{\partial B}{\partial x} &= -1 \\ \nabla^2 B + Ha\frac{\partial V}{\partial x} &= 0 \end{aligned} \tag{3.28}$$

where $\Omega = \{(x, y) : -1 < x < 1, -1 < y < 1\}$ and $Ha = LB_0\sqrt{\sigma/\nu\rho}$ is the Hartmann number resulted during the non-dimensionalization of the equations, and L, B_0, σ, ν and ρ are the characteristic length, the external magnetic field intensity, electrical conductivity, kinematic viscosity, and the density of the fluid, respectively.

The purpose of this problem is to obtain the slip velocities with the reconstructed slip lengths on the left vertical and the bottom walls. Hence, the MHD duct flow problems are constructed as Cauchy problems in terms of the velocity $V(x, y)$ of the fluid and the induced magnetic field $B(x, y)$ as direct and inverse problems which are shown in Figure 3.2 and Figure 3.3, respectively.

Firstly, the MHD duct flow problem is studied when the velocity slip is on the left Hartmann wall placed perpendicular to the applied external magnetic field. All the other walls preassume no-slip velocity. Horizontal walls are electrically insulated and the Hartmann walls contain opposite constant value conductivity. Thus, the physical conformation of the channel walls leads the boundary conditions of the velocity and the induced magnetic field as

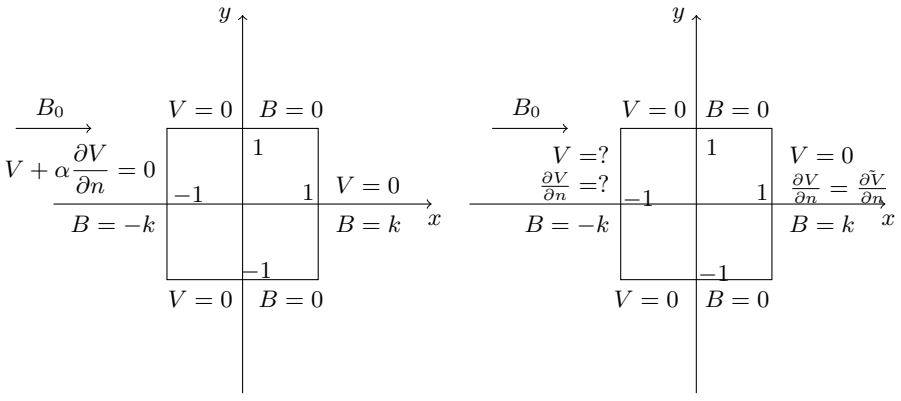


Figure 3.2: Problem 1. Left wall is slipping. Boundary conditions for the direct (left) and the Cauchy (right) problems.

$$
\begin{aligned}
&V = 0, && B = 0 && \text{on} \quad y = \mp 1, \quad -1 < x < 1 \\
&V = 0, && B = k && \text{on} \quad x = +1, \quad -1 < y < 1 \\
&V + \alpha \frac{\partial V}{\partial n} = 0, && B = -k && \text{on} \quad x = -1, \quad -1 < y < 1
\end{aligned}
\tag{3.29}
$$

where α is the dimensionless slip length which is going to be gained from the inverse formulation of the problem and k denotes the variable conductivity of the walls $x = \mp 1$. First, the MHD problem (3.28) with the boundary conditions (3.29) is going to be solved for a specific value of α. Then, with the obtained velocity value $V = v_l$ on the left wall, the direct problem, and with $V =?$ and $\dfrac{\partial V}{\partial n} =?$ on the left wall, the Cauchy problem are constructed, respectively, shown as Problem 1 on Figure 3.2 (left) and Figure 3.2 (right). The overspecified boundary conditions on the right wall are $V = 0$ and the obtained normal derivative value of V as $\dfrac{\partial \tilde{V}}{\partial n}$ from the direct problem solution which is considered as noisy data.

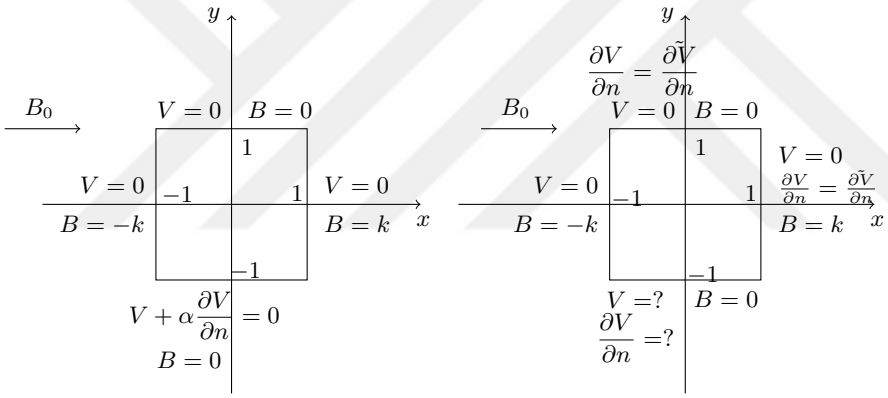


Figure 3.3: Problem 2. Bottom wall is slipping. Boundary conditions for the direct (left) and the Cauchy (right) problems.

Secondly, the MHD flow in a rectangular channel is considered with a slip velocity condition on the side bottom wall of the duct. The external magnetic field still applies horizontally. The problem is defined with the MHD flow equations (3.28) and the boundary conditions given as

$$
\begin{aligned}
&V + \alpha \frac{\partial V}{\partial n} = 0, && B = 0 && \text{on} \quad y = -1, \quad -1 < x < 1 \\
&V = 0, && B = 0 && \text{on} \quad y = +1, \quad -1 < x < 1 \\
&V = 0, && B = +k && \text{on} \quad x = +1, \quad -1 < y < 1 \\
&V = 0, && B = -k && \text{on} \quad x = -1, \quad -1 < y < 1.
\end{aligned}
\tag{3.30}
$$

Here, the dimensionless slip length α is going to be determined from the inverse formulation of the problem. In Figure 3.3 (left) and Figure 3.3 (right), the boundary conditions which are going to be used to obtain the overspecified boundary conditions on the opposite side of the slip wall, and then the boundary conditions for the inverse formulation to observe the slip length on the slip wall are shown, respectively.

Similar to Problem 1, the direct formulation of MHD flow is solved for a specified value of α. The overspecified boundary conditions on the top wall for the Cauchy problem are $V = 0$ and $\dfrac{\partial V}{\partial n} = \dfrac{\partial \tilde{V}}{\partial n}$ which are obtained from the direct solution. Since the resulted DRBEM discretized equations obtained from the inverse formulation of the MHD duct flow problem are ill-conditioned, the regularization techniques, namely, Tikhonov regularization, the direct-inverse and the well-posed iterations are employed during the solution procedure.

Tikhonov Regularization

Firstly, the direct problems are solved by using a specified value of the slip length α for Problem 1 and Problem 2. Then, with the obtained $\dfrac{\partial V}{\partial n}$ overspecified velocity values and $V = 0$ on the opposite walls and underspecified boundary conditions on the slip walls, the Cauchy problems will be solved as inverse problems using Tikhonov regularization. The ill-conditioned systems of equations in the form of $\boldsymbol{Ax} = \boldsymbol{b}$ resulted from the DRBEM discretized systems for the Cauchy problems, shown in Figure 3.2 and Figure 3.3, are solved by using Tikhonov regularization defined by

$$(\boldsymbol{A^T A} + \lambda \boldsymbol{I})\boldsymbol{x} = \boldsymbol{A^T b} \tag{3.31}$$

where λ is the regularization parameter obtained from the L-curve method.

The Direct-inverse Iterations

In this method, while the direct problems are solved with the Dirichlet type boundary conditions for V and B on each part of the boundary, but containing approximate velocities on the slipping walls, the inverse problems are solved with overspecified boundary conditions V, $\dfrac{\partial \tilde{V}}{\partial n}$ on the opposite walls. The iterations follow as;

Step 1. The direct problems are solved by using a specified value of the slip length α

for Problem 1 and Problem 2.

Step 2. With the obtained velocity values on the left wall or the bottom walls, the direct problems are again solved with Dirichlet type boundary conditions for V and B on each sides of the boundary.

Step 3. Solutions to the inverse problems are obtained by using $V = 0$ and $\frac{\partial \tilde{V}}{\partial n}$ values on the opposite walls to the slip walls obtained from the direct solution by using Tikhonov regularization.

Step 4. Update the values of V on the slip walls with the obtained ones from step 3, respectively.

Step 5. Repeat steps 2-4 until the velocity V on the slip walls converges to the velocity of the direct solution containing the approximation for the specified α value.

The Well-posed Iterations

This method converts the ill-posed problems to successive well-posed problems by alternating the given data on the overspecified part of the boundary. This iterative algorithm advanced by Kozlov et. al. [79] for Cauchy problems includes the following steps:

Step 1. The direct problems are solved by using a specified value of the slip length α for Problem 1 and Problem 2 to obtain the values of V on the slip walls.

Step 2. Solve the corresponding DRBEM discretized equations as a direct problem with the Dirichlet type boundary conditions for V and B.

Step 3. Solve the corresponding DRBEM discretized equations again as a direct problem with the normal derivative velocity values obtained from the direct solution in *Step 2* on the slipping and its opposite wall.

Step 4. Update the values of V in *Step 2* on the slip walls with the values obtained from *Step 3*, respectively.

Step 5. Repeat steps 2-4 until the velocity V on the slip wall converges to the velocity corresponding to the specified slip length α.

3.7 DRBEM Application to the Cauchy MHD Flow with a Slipping and Variably Conducting Duct Wall

An electrically conducting fluid is flowing in a long pipe of rectangular cross-section (duct) with a pressure gradient $\frac{\partial p}{\partial z}$, and an external uniform magnetic field is applied by forming an angle β with the y-axis. The flow becomes fully developed in the direction of pipe-axis and the problem reduces to two-dimension in the duct. Thus, the two-dimensional, steady and fully developed MHD flow in a rectangular duct under the effect of an externally applied oblique magnetic field is considered [41].

The left vertical wall allows the slip of the fluid and also variable conductivity. The non-dimensional governing equations for the velocity $V(x,y)$ of the fluid and the induced magnetic field $B(x,y)$ are given in the domain Ω as (3.1)

$$\begin{aligned} \nabla^2 V + Ha_x \frac{\partial B}{\partial x} + Ha_y \frac{\partial B}{\partial y} &= -1 \\ \nabla^2 B + Ha_x \frac{\partial V}{\partial x} + Ha_y \frac{\partial V}{\partial y} &= 0 \end{aligned} \tag{3.32}$$

where $\Omega = \{(x,y) : -1 < x,y < 1\}$ $Ha_x = Hasin(\beta)$, $Ha_y = Hacos(\beta)$ and $Ha = LB_0\sqrt{\sigma/\nu\rho} = \sqrt{(Ha_x)^2 + (Ha_y)^2}$ is the Hartmann number.

The physical configuration of the MHD duct flow problem with a slipping and variably conducting left wall, termed as Problem 3, leads to the boundary conditions (Figure 3.4)

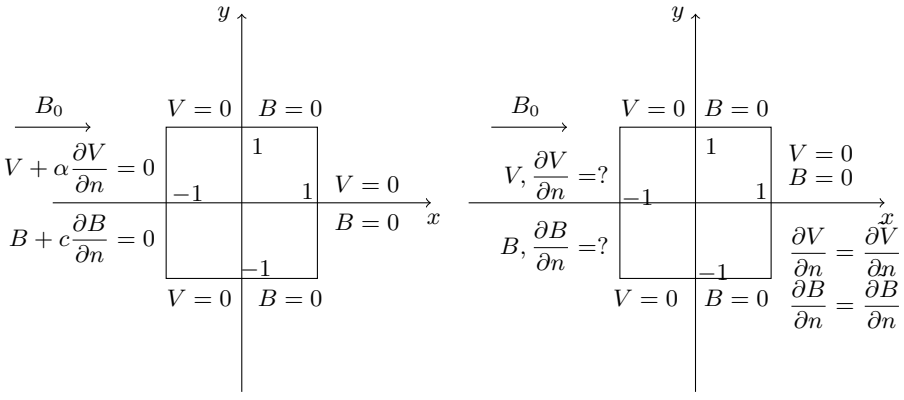


Figure 3.4: Problem 3. Left wall is both slipping and variably conducting. Boundary conditions for the direct (left) and the Cauchy (right) problems. $\tilde{V}$, $\tilde{B}$ denote direct problem solution.

$$
\begin{aligned}
&V = 0, B = 0 \quad \text{on} \quad y = \mp 1, \quad -1 < x < 1 \\
&V = 0, B = 0 \quad \text{on} \quad x = 1, \quad -1 < y < 1 \\
&V + \alpha \frac{\partial V}{\partial n} = 0 \ \text{on} \quad x = -1, \quad -1 < y < 1 \\
&B + c \frac{\partial B}{\partial n} = 0 \ \text{on} \quad x = -1, \quad -1 < y < 1.
\end{aligned}
\tag{3.33}
$$

where α is the dimensionless slip length and c is the conductivity constant which are going to be reconstructed through the inverse formulation of the MHD duct flow problem.

In the solution procedure, the MHD duct flow problem (3.32) with the boundary conditions (3.33) is solved as a direct problem for specific values of the slip length α and the conductivity constant c. Then, with the obtained normal derivative values of the velocity of the fluid and the induced magnetic field on the left wall, the Cauchy problem is constructed. The solution of the Cauchy problem are obtained through the DRBEM by using a regularization technique namely, the well-posed iterations.

The well-posed iterations

For the inverse MHD problem, the $\dfrac{\partial \tilde{V}}{\partial n}$ and $\dfrac{\partial \tilde{B}}{\partial n}$ values obtained from the direct formulation corresponding to a specified slip length and conductivity constant are taken as overspecified boundary conditions in addition to $V = 0$ and $B = 0$ on the right wall. The DRBEM discretization of the Cauchy MHD duct flow problem leads to an ill-conditioned system of equations in the form of $\boldsymbol{Ax} = \boldsymbol{b}$ due to overspecified conditions on the right wall and underspecified conditions on the left wall. The iterative algorithm developed by Kozlov et al. [79] is used to regularize the ill-posed Cauchy problem including the following steps

Step 1. Solve the matrix-vector equations obtained through the DRBEM in one stroke as a direct problem with the specified α and c values given as in Figure 3.4 to get the unknown values for V, B on $x = -1$ and their normal derivatives on $x = \mp 1$. Now, the Cauchy MHD problem is constructed with the assumption that the underspecified conditions on $x = -1$ (neither V, B nor $\dfrac{\partial V}{\partial n}$, $\dfrac{\partial B}{\partial n}$ are known) and overspecified conditions on $x = 1$ (V, B and their normal derivatives are known).

Step 2. Solve the coupled discretized equations resulted from the DRBEM as a direct problem using the Dirichlet type boundary conditions for V and B on $x = \mp 1$ part of the boundary. The solution gives normal derivatives of V and B everywhere on the boundary.

Step 3. Use $\dfrac{\partial V}{\partial n}$ and $\dfrac{\partial B}{\partial n}$ on $x = -1$ and $x = 1$ obtained from ***Step 2*** for solving the direct problem to find the new V, B values.

Step 4. Update the values of V and B with the values obtained from step 3 on $x = -1$.

Step 5. Repeat steps 2-4 until the velocity and the induced magentic field values converge to the solution of the direct problem corresponding to the specified slip length α and the conductivity constant c.

3.8 DRBEM Application to the Cauchy MHD Flow in a Duct with a Slipping Perturbed Upper Boundary

The two-dimensional, steady and fully developed MHD flow is considered in a rectangular duct with a small boundary perturbation on the upper wall. The magnetic field applies in the y-direction (the angle $\beta = 0$). The vertical walls are insulated and the bottom and upper walls are perfectly conducting. Furthermore, the upper Hartmann wall allows the slip of the fluid.

The non-dimensional governing equations for the velocity $V(x, y)$ of the fluid and the induced magnetic field $B(x, y)$ in Ω are [11]

$$\begin{aligned} \nabla^2 V + Ha \frac{\partial B}{\partial y} &= -1 \\ \nabla^2 B + Ha \frac{\partial V}{\partial y} &= 0 \end{aligned} \tag{3.34}$$

where $\Omega = \{(x, y) \in R^2 : -2 < x < 2, -1 < y < 1 - \epsilon f(x)\}$, $\epsilon << 1$, f is an arbitrary smooth function.

The aim is to obtain the slip velocity and recover the slip length on the upper perturbed curved wall. Thus, the MHD problem is reconstructed as a Cauchy problem in terms of the velocity $V(x, y)$ and the induced magnetic field $B(x, y)$ as direct and inverse

problems. Thus, the physical conformation of the channel walls leads the boundary conditions of the velocity and the induced magnetic field as (termed as Problem 4)

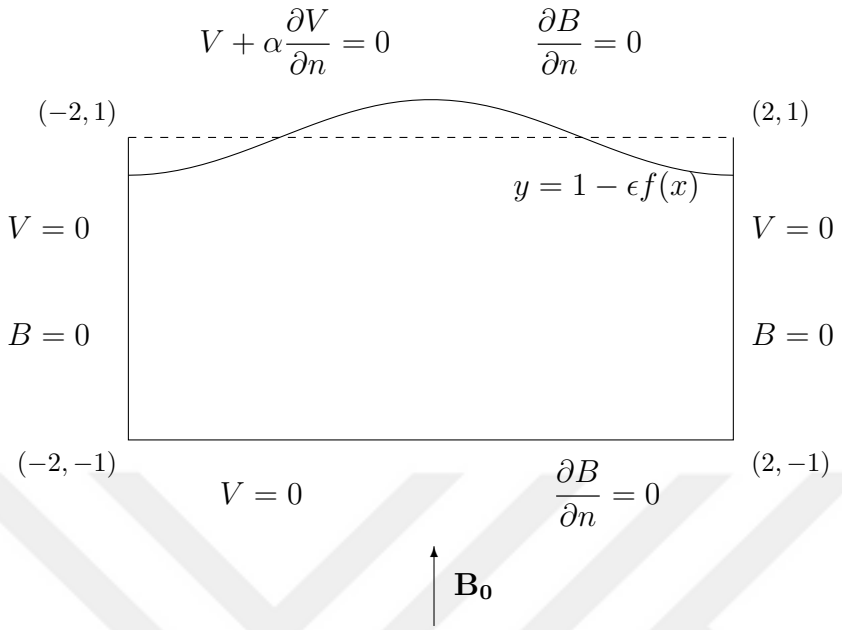


Figure 3.5: Problem 4. Upper wall is perturbed and slipping. Boundary conditions for the direct problem.

$$\begin{aligned} &V = 0, && \frac{\partial B}{\partial n} = 0 \quad \text{on} \quad y = -1, && -2 < x < 2 \\ &V + \alpha \frac{\partial V}{\partial n} = 0, && \frac{\partial B}{\partial n} = 0 \quad \text{on} \quad y = 1 - \epsilon f(x), && -2 < x < 2 \\ &V = 0, && B = 0 \quad \text{on} \quad x = \mp 2, && -1 < y < 1 - \epsilon f(x) \end{aligned} \tag{3.35}$$

where the domain of the problem is $\Omega^\epsilon = \{(x, y) \in R^2 : -2 < x < 2, -1 < y < 1 - \epsilon f(x)\}$ and α is the dimensionless slip length to be gained from the inverse formulation of the problem. The effects of both slipping and perturbed boundary on the MHD flow through a rectangular duct will be studied.

3.8.1 Asymptotic Analysis

We consider the domain $\Omega = \{(x, y) \in R^2 : -2 < x < 2, -1 < y < 1\} \subset \Omega^\epsilon$ so that the solution of (3.34)-(3.35) is defined on Ω. Therefore, the velocity and

induced magnetic field can be expanded in Taylor series with respect to y near the upper boundary [80].

They can be expanded as follows:

$$\begin{aligned} V(x,y) &= \sum_{k=0}^{\infty} \frac{1}{k!} \frac{\partial^k V}{\partial y^k}(x,1)(y-1)^k \\ B(x,y) &= \sum_{k=0}^{\infty} \frac{1}{k!} \frac{\partial^k B}{\partial y^k}(x,1)(y-1)^k \end{aligned} \tag{3.36}$$

In view of the boundary conditions (3.35) on the curved boundary, we derive

$$\begin{aligned} 0 &= V(x,1-\epsilon f(x)) + \alpha \frac{\partial V}{\partial y}(x,1-\epsilon f(x)) \\ &= V(x,1) - \epsilon f(x)\frac{\partial V}{\partial y}(x,1) + \frac{\epsilon^2}{2} f(x)^2 \frac{\partial^2 V}{\partial y^2}(x,1) \\ &\quad + \alpha \frac{\partial V}{\partial y}(x,1) - \alpha\epsilon f(x)\frac{\partial^2 V}{\partial y^2}(x,1) + \alpha \frac{\epsilon^2 f(x)^2}{2}\frac{\partial^3 V}{\partial y^3}(x,1) + \cdots \end{aligned} \tag{3.37}$$

$$\begin{aligned} 0 &= \frac{\partial B}{\partial y}(x,1-\epsilon f(x)) \\ &= \frac{\partial B}{\partial y}(x,1) - \epsilon f(x)\frac{\partial^2 B}{\partial y^2}(x,1) + \frac{\epsilon^2 f(x)^2}{2}\frac{\partial^3 B}{\partial y^3}(x,1) + \cdots \end{aligned} \tag{3.38}$$

We also write the asymptotic expansion of V and B in powers of ϵ,

$$V(x,y) = V^0(x,y) + \epsilon V^1(x,y) + \epsilon^2 V^2(x,y) + \cdots \tag{3.39}$$

$$B(x,y) = B^0(x,y) + \epsilon B^1(x,y) + \epsilon^2 B^2(x,y) + \cdots \tag{3.40}$$

Inserting the expansions (3.39) and (3.40) into (3.37) and (3.38), respectively, yields

$$\begin{aligned} 0 &= V^0(x,1) + \alpha \frac{\partial V^0}{\partial y}(x,1) \\ &\quad + \epsilon(V^1(x,1) - f(x)\frac{\partial V^0}{\partial y}(x,1) + \alpha \frac{\partial V^1}{\partial y}(x,1) - \alpha f(x)\frac{\partial^2 V^0}{\partial y^2}(x,1)) + \cdots \end{aligned} \tag{3.41}$$

$$0 = \frac{\partial B^0}{\partial y}(x,1) + \epsilon(\frac{\partial B^1}{\partial y}(x,1) - f(x)\frac{\partial^2 B^0}{\partial y^2}(x,1)) + \cdots \tag{3.42}$$

Now, we obtain the boundary conditions satisfied by the first two terms at the upper

boundary as

$$V^0(x,1) + \alpha \frac{\partial V^0}{\partial y}(x,1) = 0 \tag{3.43}$$

$$V^1(x,1) + \alpha \frac{\partial V^1}{\partial y}(x,1) = f(x)(\frac{\partial V^0}{\partial y}(x,1) + \alpha \frac{\partial^2 V^0}{\partial y^2}(x,1)) \tag{3.44}$$

$$\frac{\partial B^0}{\partial y}(x,1) = 0 \tag{3.45}$$

$$\frac{\partial B^1}{\partial y}(x,1) = f(x)\frac{\partial^2 B^0}{\partial y^2}(x,1). \tag{3.46}$$

Now, the two sets of MHD flow equations for (V^0, B^0) and (V^1, B^1) with the corresponding boundary conditions on the undisturbed boundary $\partial\Omega$ can be defined. The first-order approximation (V^0, B^0) satisfies the following MHD equations

$$\begin{aligned} \nabla^2 V^0 + Ha\frac{\partial B^0}{\partial y} &= -1 \qquad \text{in} \quad \Omega \\ \nabla^2 B^0 + Ha\frac{\partial V^0}{\partial y} &= 0 \qquad \text{in} \quad \Omega \end{aligned} \tag{3.47}$$

with the boundary conditions

$$\begin{aligned} &V^0(x,-1) = 0, \quad V^0(x,1) + \alpha\frac{\partial V^0}{\partial y}(x,1) = 0, \quad V^0(\mp 2, y) = 0 \\ &\frac{\partial B^0}{\partial y}(x,\mp 1) = 0 \qquad B^0(\mp 2, y) = 0. \end{aligned} \tag{3.48}$$

Since there is no effect of the boundary perturbation on the first order approximation, we continue with the next term (V^1, B^1), called as corrector, in the asymptotic expansions (3.39) and (3.40),

$$\begin{aligned} \nabla^2 V^1 + Ha\frac{\partial B^1}{\partial y} &= -1 \qquad \text{in} \quad \Omega \\ \nabla^2 B^1 + Ha\frac{\partial V^1}{\partial y} &= 0 \qquad \text{in} \quad \Omega \end{aligned} \tag{3.49}$$

with the boundary conditions

$$\begin{aligned} &V^1(\mp 2, y) = 0, \quad V^1(x,-1) = 0 \\ &V^1(x,1) + \alpha\frac{\partial V^1}{\partial y}(x,1) = f(x)\frac{\partial V^0}{\partial y}(x,1) + \alpha f(x)\frac{\partial^2 V^0}{\partial y^2}(x,1) \\ &B^1(\mp 2, y) = 0, \quad \frac{\partial B^1}{\partial y}(x,-1) = 0 \\ &\frac{\partial B^1}{\partial y}(x,1) = f(x)\frac{\partial^2 B^0}{\partial y^2}(x,1). \end{aligned} \tag{3.50}$$

3.8.2 The inverse formulations

The inverse formulation for the First Order Approximation: The Cauchy MHD problem is defined by the equation (3.47) with the boundary conditions

$$\begin{aligned} &V^0(x,-1)=0, \quad V^0(\mp 2,y)=0, \quad \frac{\partial V^0}{\partial y}(x,-1)=\frac{\partial \tilde{V}^0}{\partial y}(x,-1) \\ &\frac{\partial B^0}{\partial y}(x,\mp 1)=0 \qquad B^0(\mp 2,y)=0 \end{aligned} \tag{3.51}$$

where $\dfrac{\partial \tilde{V}^0}{\partial y}(x,-1)$ is obtained from the direct problem (3.47) with the boundary conditions (3.48).

Since there is no boundary condition on the upper straight wall $y=1$ and there are overspecified boundary conditions for $V^0(x,y)$ on $y=-1$, this problem is a Cauchy MHD flow problem in terms of the first order velocity $V^0(x,y)$.

The inverse formulation for the Corrector: The Cauchy MHD flow problem for the corrector (V^1,B^1) is defined by the equation (3.49) with the boundary conditions

$$\begin{aligned} &V^1(x,-1)=0, \quad V^1(\mp 2,y)=0, \quad \frac{\partial V^1}{\partial y}(x,-1)=\frac{\partial \tilde{V}^1}{\partial y}(x,-1) \\ &\frac{\partial B^1}{\partial y}(x,-1)=0, \qquad \frac{\partial B^1}{\partial y}(x,1)=f(x)\frac{\partial^2 B^0}{\partial y^2}(x,1) \\ &B^1(\mp 2,y)=0 \end{aligned} \tag{3.52}$$

where $\dfrac{\partial \tilde{V}^1}{\partial y}(x,-1)$ is obtained from the DRBEM solution of the direct formulation for the corrector (V^1,B^1) using the boundary conditions (3.50).

The solution of the Cauchy problems for (V^0,B^0) and (V^1,B^1) will provide both V^0 and $\dfrac{\partial V^0}{\partial y}$ and V^1 and $\dfrac{\partial V^1}{\partial y}$ on the straight boundary $y=1$ and then from equations (3.39), V and $\dfrac{\partial V}{\partial y}$. Thus, it is possible to recover the slip length α back from $V+\alpha\dfrac{\partial V}{\partial y}=0$ on the curved perturbed boundary.

3.9 Application of the DRBEM to Parameter Identification in MHD Duct Flow Cauchy Problem

The non-dimensional governing equations for the velocity $V(x,y)$ of the fluid and the induced magnetic field $B(x,y)$ are again given in the domain Ω as [11]

$$\begin{aligned} \nabla^2 V + Ha\frac{\partial B}{\partial y} &= -1 \\ \nabla^2 B + Ha\frac{\partial V}{\partial y} &= 0 \end{aligned} \tag{3.53}$$

where $\Omega = \{(x,y) \in R : -1 < x,y < 1\}$ and the magnetic field applies vertically. These equations are solved for various types of wall conditions and presented as Problems 1 and 2.

In this problem, the aim is to identify the Hartmann number Ha back contained in Equations (3.53) in the problem region. Hence, the MHD problem is considered as an inverse problem in terms of Ha with the knowledge of V, B and their normal derivatives on each part of the boundary, and also additional internal values for V and B. The overspecified boundary conditions and internal values for V, B to be used in the construction of the inverse problem are obtained from the direct formulation of the MHD duct flow problem through the DRBEM.

Since the inverse problem is ill-posed, the Tikhonov regularization method is used for solving the system of linear algebraic equations resulted from the DRBEM by utilizing the L-curve method to choose the optimal regularization parameter.

3.9.1 Parameter Identification - Problem 1

Firstly, the MHD duct flow problem is studied when each part of the duct boundary is no-slip and insulated wall. Thus, the physical conformation of the channel walls leads the boundary conditions of the velocity and the induced magnetic field as

$$\begin{aligned} V &= 0, \qquad B = 0 \quad \text{on} \quad y = \mp 1, \quad -1 < x < 1 \\ V &= 0, \qquad B = 0 \quad \text{on} \quad x = \mp 1, \quad -1 < y < 1 \end{aligned} \tag{3.54}$$

First, the MHD equations (3.53)-(3.54) are going to be solved for a specified value of Ha through the DRBEM which gives the normal derivative values for V and B

on each part of the boundary and the values for V and B at some selected interior nodes. Then, the inverse problem is constructed with V, B values and their normal derivatives on the boundary and V, B at the interior points to identify the Ha back in the problem domain since the walls are insulated. $\tilde{V}$ and $\tilde{B}$ denote the internal velocity of the fluid and induced magnetic field, respectively obtained from the direct formulation through the DRBEM.

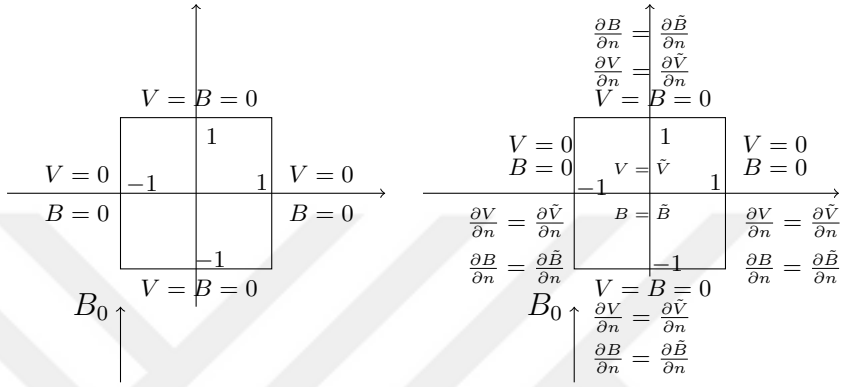


Figure 3.6: Problem 1. Boundary conditions for the direct (left) and the inverse (right) problems.

3.9.2 Parameter Identification - Problem 2

In this problem, the MHD flow in a rectangular channel is considered with no-slip walls but perfectly conducting top and bottom walls with the boundary conditions given below in (3.55). As it is configured in Problem 1, after obtaining all the necessary informations about V and B from the direct problem through the DRBEM, the Ha in the problem region is regained from the inverse problem.

$$\begin{aligned} V &= 0, & \frac{\partial B}{\partial n} &= 0 \quad \text{on} \quad y = \mp 1, \quad -1 < x < 1 \\ V &= 0, & B &= 0 \quad \text{on} \quad x = \mp 1, \quad -1 < y < 1. \end{aligned} \tag{3.55}$$

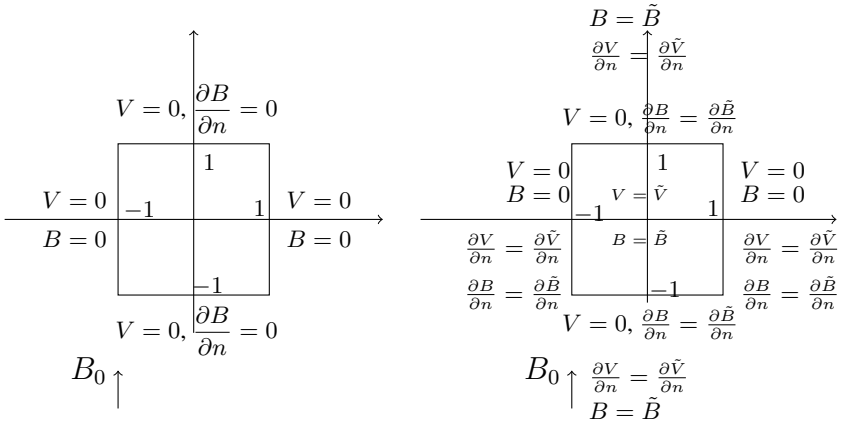


Figure 3.7: Problem 2. Boundary conditions for the direct (left) and the inverse (right) problems.

3.9.3 Parameter Identification - Problem 3

The MHD flow in a rectangular duct is considered where all the walls are variably conducting and they are no-slip walls. The problem is defined with the MHD flow equations (3.53) and the boundary conditions (3.56) given as

$$\begin{aligned} V = 0, \qquad & B + c\frac{\partial B}{\partial n} = 0 \qquad \text{on} \quad y = \mp 1, \quad -1 < x < 1 \\ V = 0, \qquad & B + c\frac{\partial B}{\partial n} = 0, \qquad \text{on} \quad x = \mp 1, \quad -1 < y < 1 \end{aligned} \tag{3.56}$$

where c is the conductivity constant.

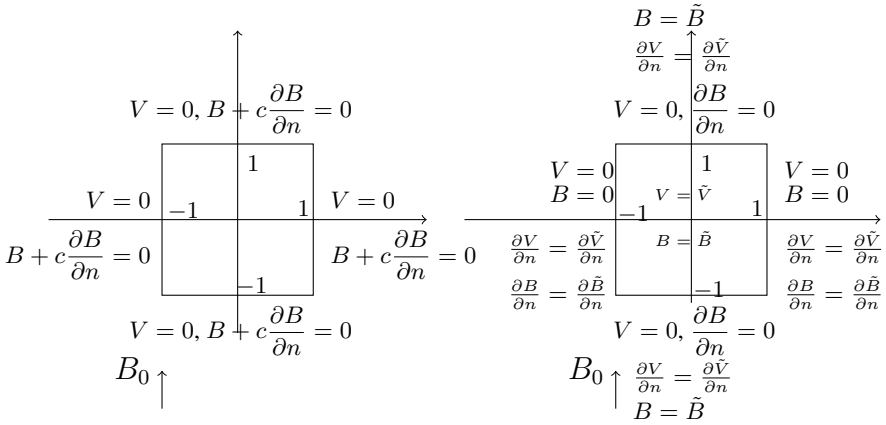


Figure 3.8: Problem 3. Boundary conditions for the direct (left) and the inverse (right) problems.

3.9.4 Parameter Identification - Problem 4

The MHD flow in a rectangular duct is considered where all the walls have slipping velocity and they are insulated. The problem is defined with the MHD flow equations (3.53) and the boundary conditions (3.57) given as

$$\begin{aligned} V + \alpha \frac{\partial V}{\partial n} = 0, \qquad & B = 0 \quad \text{on} \quad y = \mp 1, \quad -1 < x < 1 \\ V + \alpha \frac{\partial V}{\partial n} = 0, \qquad & B = 0 \quad \text{on} \quad x = \mp 1, \quad -1 < y < 1 \end{aligned} \tag{3.57}$$

where α is the slip length.

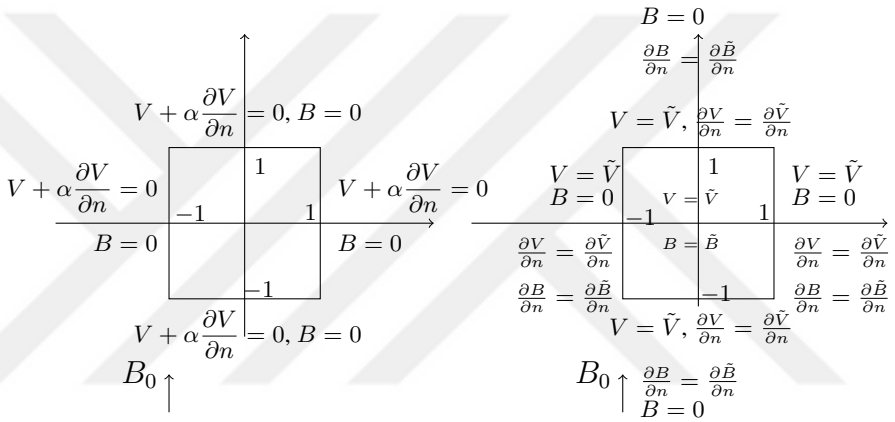


Figure 3.9: Problem 4. Boundary conditions for the direct (left) and the inverse (right) problems.

3.9.5 Parameter Identification - Problem 5

The MHD flow in a rectangular duct is considered where all the walls are slipping and variably conducting . The problem is defined with the MHD flow equations (3.53) and the boundary conditions (3.58) given below

$$\begin{aligned} V + \alpha \frac{\partial V}{\partial n} = 0, \qquad & B + c \frac{\partial B}{\partial n} = 0 \quad \text{on} \quad y = \mp 1, \quad -1 < x < 1 \\ V + \alpha \frac{\partial V}{\partial n} = 0, \qquad & B + c \frac{\partial B}{\partial n} = 0 \quad \text{on} \quad x = \mp 1, \quad -1 < y < 1 \end{aligned} \tag{3.58}$$

where α is the slip length and c is the conductivity constant.

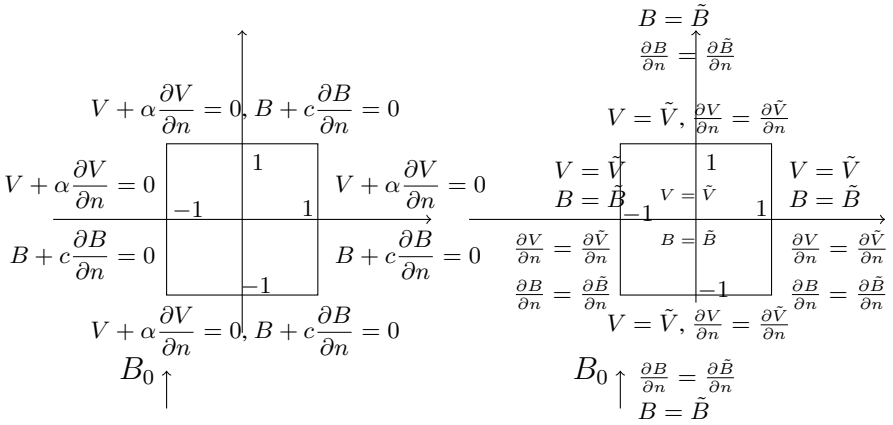


Figure 3.10: Problem 5. Boundary conditions for the direct (left) and the inverse (right) problems.

3.9.6 Solution Procedure

Firstly, the direct MHD flow problem is solved with the boundary condition given in Figure 3.4 (left) since we know the Dirichlet boundary conditions for V and B on the boundary, we need to get the Neumann boundary conditions for them, and the V and B values in the problem region through the direct solution using DRBEM. Then, we construct the inverse problem with those overdetermined V and B information on the boundary and interior V and B values shown in Figure 3.4(right) for identifying the Hartmann number Ha back in (3.53). Then, with all of these known information, the coupled DRBEM system can be reconstructed as

$$\begin{bmatrix} \mathbf{H} & \mathbf{0} \\ \mathbf{0} & \mathbf{H} \end{bmatrix} \begin{Bmatrix} \boldsymbol{V} \\ \boldsymbol{B} \end{Bmatrix} = \begin{bmatrix} \mathbf{G} & \mathbf{0} \\ \mathbf{0} & \mathbf{G} \end{bmatrix} \begin{Bmatrix} \dfrac{\partial \boldsymbol{V}}{\partial n} \\ \dfrac{\partial \boldsymbol{B}}{\partial n} \end{Bmatrix} + \begin{bmatrix} \mathbf{K}' & \mathbf{0} \\ \mathbf{0} & \mathbf{K}'' \end{bmatrix} \begin{Bmatrix} \mathbf{Ha_1} \\ \mathbf{Ha_2} \end{Bmatrix} + \begin{Bmatrix} \mathbf{0} \\ \mathbf{b} \end{Bmatrix} \tag{3.59}$$

where $\mathbf{K}' = (\mathbf{H}\hat{\boldsymbol{U}} - \mathbf{G}\hat{\boldsymbol{Q}})\mathbf{F}^{-1}\dfrac{\partial \mathbf{F}}{\partial y}\mathbf{F}^{-1} diag(\boldsymbol{V})$, $\mathbf{K}'' = (\mathbf{H}\hat{\boldsymbol{U}} - \mathbf{G}\hat{\boldsymbol{Q}})\mathbf{F}^{-1}\dfrac{\partial \mathbf{F}}{\partial y}\mathbf{F}^{-1} diag(\boldsymbol{B})$ and $\mathbf{b} = -(\mathbf{H}\hat{\boldsymbol{U}} - \mathbf{G}\hat{\boldsymbol{Q}})\mathbf{F}^{-1}(1, 1, ..., 1)^T$ are of sizes $(N+L)\times(N+L)$, $(N+L)\times(N+L)$, $(N+L)\times 1$, respectively. This system is transformed to the form $\boldsymbol{Ax} = \boldsymbol{b}$ with all the interior $\boldsymbol{V}$, $\boldsymbol{B}$ values and $\boldsymbol{V}$, $\boldsymbol{B}$, $\dfrac{\partial \boldsymbol{V}}{\partial n}$ and $\dfrac{\partial \boldsymbol{B}}{\partial n}$ boundary values obtained values from the direct formulation through the DRBEM. Hence, the only unknown

vector in the coupled system is [$\mathbf{Ha}_1$,$\mathbf{Ha}_2$]^T where $\mathbf{Ha}_1$ and $\mathbf{Ha}_2$ of sizes $(N+L)\times 1$ represent actually the same unknown vector for Hartmann number Ha values in the whole domain for the equation (3.53).

The MHD duct flow equations (3.53) for the inverse problem can also be solved by decoupling the equations as

$$\mathbf{H}\{\boldsymbol{V}\} - \mathbf{G}\{\frac{\partial \boldsymbol{V}}{\partial n}\} = -\mathbf{K}'\{\mathbf{Ha}_1\} \tag{3.60}$$

$$\mathbf{H}\{\boldsymbol{B}\} - \mathbf{G}\{\frac{\partial \boldsymbol{B}}{\partial n}\} = -\mathbf{K}''\{\mathbf{Ha}_2\} \tag{3.61}$$

with the known V, B and their normal derivatives on the boundary and also V, B values at some selected interior points in the problem region.

Since the problem is ill-posed due to the overspecified boundary conditions, a regularization technique must be employed to solve the coupled or decoupled systems of linear algebraic equations. In this part of the study, the Tikhonov regularization is used with the L-curve method.

In Chapter 3, the application of the DRBEM is given for the direct and inverse formulations (as boundary type inverse problems and as parameter identification problems) of the MHD duct flow problem with some boundary conditions from no-slip to slipping and from insulated to variably conducting. The application of the regularization techniques; Tikhonov regularization, the direct-inverse iterations, and the well-posed iterations are explained for the Cauchy MHD duct flow problem. In Chapter 4, the numerical procedures and the numerical results obtained from the DRBEM are going to be presented for the problems which are explained in Chapter 3 with specific boundary conditions and the problem parameters.

CHAPTER 4

NUMERICAL RESULTS OF THE DIRECT AND CAUCHY MHD DUCT FLOW WITH SLIP AND VARIABLE CONDUCTIVITY CONDITIONS

In this chapter, the DRBEM solutions of the direct and Cauchy MHD flow equations in a duct are presented with the most general form of wall conditions as slip velocity and variably conducting induced magnetic field. The Cauchy formulations of MHD flow problems are classified as two kinds of inverse problems, as the boundary type inverse problem and parameter identification. The obtained numerical results are simulated in terms of equivelocity and current lines for both the direct and inverse solutions.

In the MHD duct flow problems, the Hartmann layers of order $O(1/Ha)$ and the side layers of order $O(1/\sqrt{Ha})$ which are perpendicular and parallel to the externally applied magnetic field, respectively, are developed where Ha is the Hartmann number. Analytical solutions of MHD duct flow problems can be obtained for only some special geometry and boundary conditions such as insulated or perfectly conducting duct walls or two opposite insulated and the conducting other walls. In the general MHD flow problems, the velocity of the viscous fluid has usually no-slip boundary condition at solid duct walls under the assumption of enough wettability at the liquid-solid interface [11]. On the other hand, in some applications, such as nanofluidic and microfluidic devices whose surface are rough and the surface-to-volume ratio is large, the slip boundary condition is usually imposed [13]. The slip length is described as the distance from the fluid to the duct walls within the solid stage where the velocity of the fluid vanishes. Partly insulated, partly conducting or variably conducting whole walls are some important applications in nuclear reactors for MHD duct flows.

4.1 The Cauchy MHD Flow With Slipping and Variably Conducting Duct Walls

In this section, the two-dimensional, steady and fully-developed MHD flow is considered in a long channel with a rectangular cross-section.

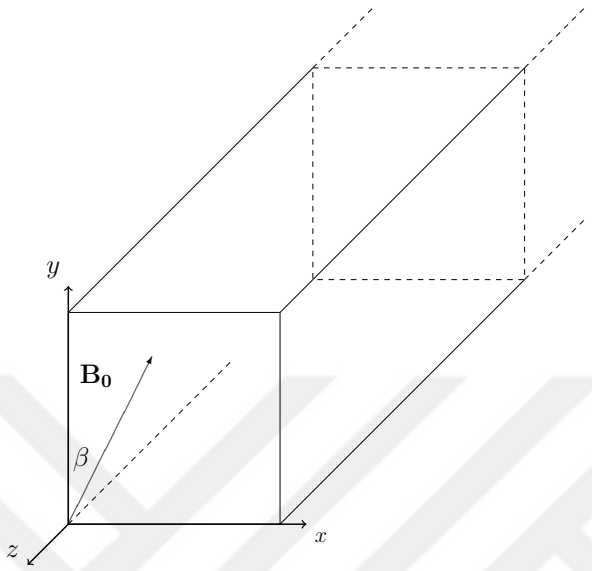


Figure 4.1: Fluid flow configuration under the applied uniform magnetic field.

The discretized matrix-vector equations (3.7) resulted from the DRBEM application and the solution procedure are given in Section 3.6 as (if the applied magnetic field is in the x-direction)

$$\begin{aligned} \mathbf{H}\boldsymbol{V} - \mathbf{G}\frac{\partial \boldsymbol{V}}{\partial n} &= -(\mathbf{H}\hat{\boldsymbol{U}} - \mathbf{G}\hat{\boldsymbol{Q}})\boldsymbol{F}^{-1}(Ha\frac{\partial \boldsymbol{B}}{\partial x} + 1) \\ \mathbf{H}\boldsymbol{B} - \mathbf{G}\frac{\partial \boldsymbol{B}}{\partial n} &= -(\mathbf{H}\hat{\boldsymbol{U}} - \mathbf{G}\hat{\boldsymbol{Q}})\boldsymbol{F}^{-1}(Ha\frac{\partial \boldsymbol{V}}{\partial x}) \end{aligned} \tag{4.1}$$

where $V(x, y)$ is the velocity of the fluid and $B(x, y)$ is the induced magnetic field in the rectangular cross-section of the long pipe $\Omega = \{(x, y) : -1 < x < 1, -1 < y < 1\}$. The slip $(V + \alpha\dfrac{\partial V}{\partial n} = 0)$ and variably conducting $(B + c\dfrac{\partial B}{\partial n} = 0)$ duct walls are considered.

In the application of the DRBEM, $N = 100, 120, 240$ constant boundary elements and $L = 625, 900, 3600$ interior nodes are taken for $Ha = 1, 10, 50$, respectively. Both

the insulated ($k = 0$) and conducting ($k = 1$) vertical walls cases are investigated. In the solution of direct formulations for MHD duct flow the specified slip length is taken as $\alpha = 0.2$.

4.1.1 MHD duct flow - Problem 1

The governing equations of MHD duct flow are given in the domain Ω as

$$\begin{aligned} \nabla^2 V + Ha\frac{\partial B}{\partial x} &= -1 \\ \nabla^2 B + Ha\frac{\partial V}{\partial x} &= 0 \end{aligned} \tag{4.2}$$

where $\Omega = \{(x, y) : -1 < x < 1, -1 < y < 1\}$ and $Ha = LB_0\sqrt{\sigma/\nu\rho}$ is the Hartmann number.

The side walls which are parallel to the applied magnetic field are electrically insulated and no-slip. The Hartmann walls which are perpendicular to the applied magnetic field are conducting and also the left Hartmann wall has a slip velocity condition while the right Hartmann wall is no-slip (Figure 4.2, Equation (4.3)).

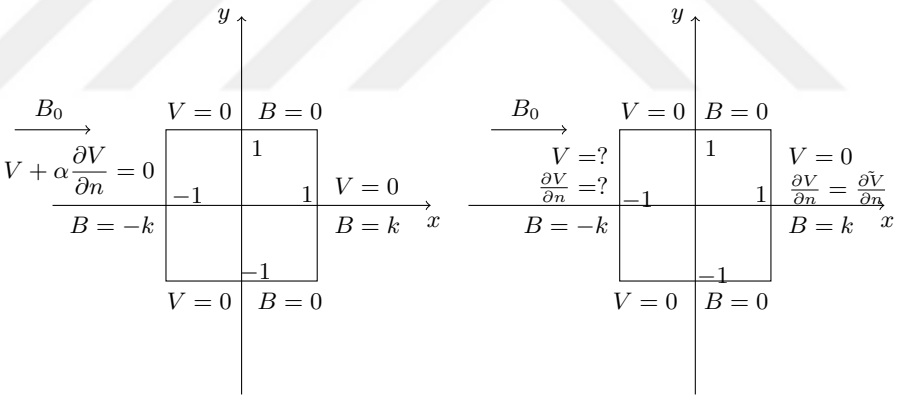


Figure 4.2: MHD duct flow - Problem 1: Boundary conditions for the direct (left) and the Cauchy (right) problems. Left wall is slipping.

The boundary conditions of the velocity and the induced magnetic field are given as

$$\begin{aligned} &V = 0, && B = 0 && \text{on} \quad y = \mp 1, \quad -1 < x < 1 \\ &V = 0, && B = k && \text{on} \quad x = +1, \quad -1 < y < 1 \\ &V + \alpha\frac{\partial V}{\partial n} = 0, && B = -k && \text{on} \quad x = -1, \quad -1 < y < 1 \end{aligned} \tag{4.3}$$

where α is the dimensionless slip length which is going to be recovered from the inverse formulation of the problem and k is the conductivity constant.

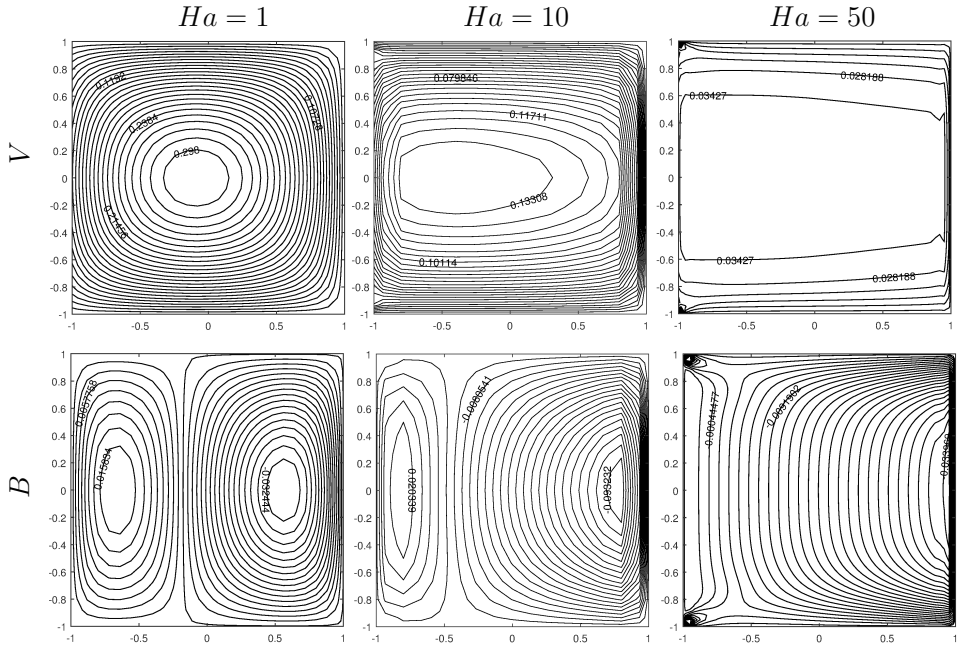


Figure 4.3: MHD duct flow - Problem 1: Velocity and induced magnetic field profiles from direct problem, $\alpha = 0.2$, $k = 0$

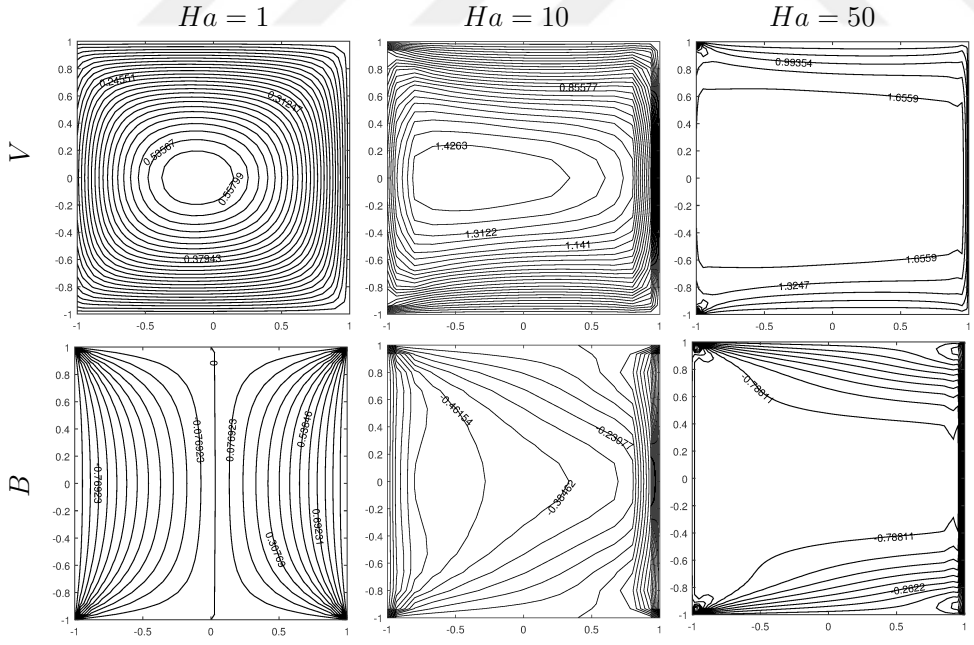


Figure 4.4: MHD duct flow - Problem 1: Velocity and induced magnetic field profiles from direct problem, $\alpha = 0.2$, $k = 1$.

The MHD duct flow equations (4.2) are solved numerically in terms of the velocity V of the fluid and the induced magnetic field B with the boundary conditions defined for the direct and inverse problems as given in Figure 4.2. The purpose is to regain the slip velocity and get the slip length on the left vertical wall through the inverse formulation.

Figure 4.3 and Figure 4.4 show the velocity and the induced magnetic field contours which are obtained from the direct problem solutions for insulated ($k = 0$) and conducting ($k = 1$) vertical walls with the specified slip length $\alpha = 0.2$ on the left vertical wall, respectively. It is observed that as Hartmann number Ha increases, Hartmann layers on the vertical walls and side layers on the horizontal walls are developed which is the well-known behaviour of the MHD duct flow. However, the slip on the left vertical wall weakens the Hartmann layer.

Figure 4.5 and Figure 4.6 show the velocity behaviours for the Cauchy MHD flow resulted from the Tikhonov regularization, the direct-inverse iterations, and the well-posed iterations, respectively for $k = 0$ and $k = 1$. They show that the slip velocity is regained and converged to the direct perturbed solution corresponding to the specified slip length value $\alpha = 0.2$. For all the Hartmann number values considered, the convergence to the velocity of the direct problem on the left slipping wall as well as the other parts is observed in all the three methods. When the Hartmann number is increased to $Ha = 50$, the slip of the velocity is located near the corners of the left wall due to the stagnant region developed at the centre of the duct. In all the methods, boundary layers (Hartmann layers of order $1/Ha$ on the walls perpendicular to the applied magnetic field and side layers of order $1/\sqrt{Ha}$ on the parallel walls) are observed when Hartmann number increases [11]. On the other hand, due to the velocity slip effect on the left wall, Hartmann layers are diminished as Hartmann number increases. When Hartmann number increases further to $Ha = 50$, the core region enlarges, fluid becomes stagnant there and the flow is flattened. The slip velocity is regained on the left wall with all the three regularization methods from the DRBEM solution of the Cauchy MHD duct flow problem.

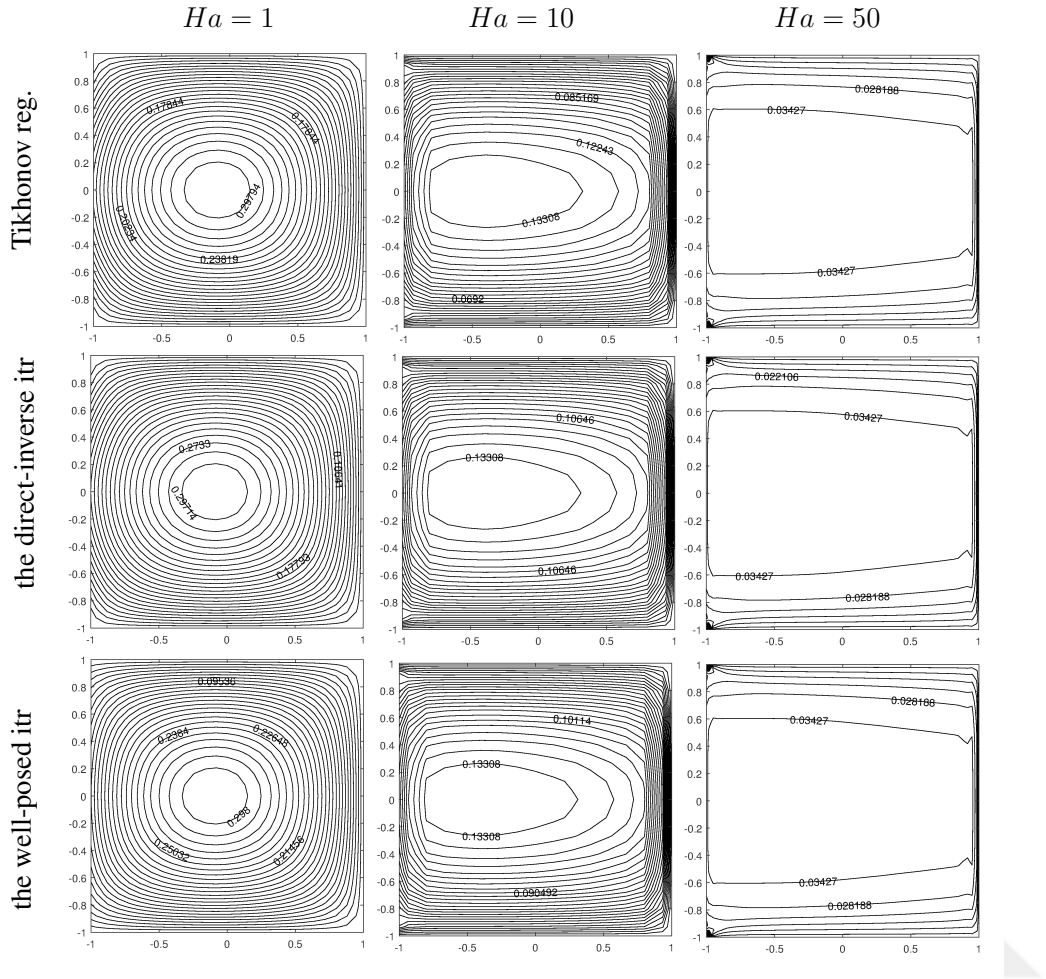


Figure 4.5: MHD duct flow - Problem 1: Velocity profiles from inverse solution, $k = 0$.

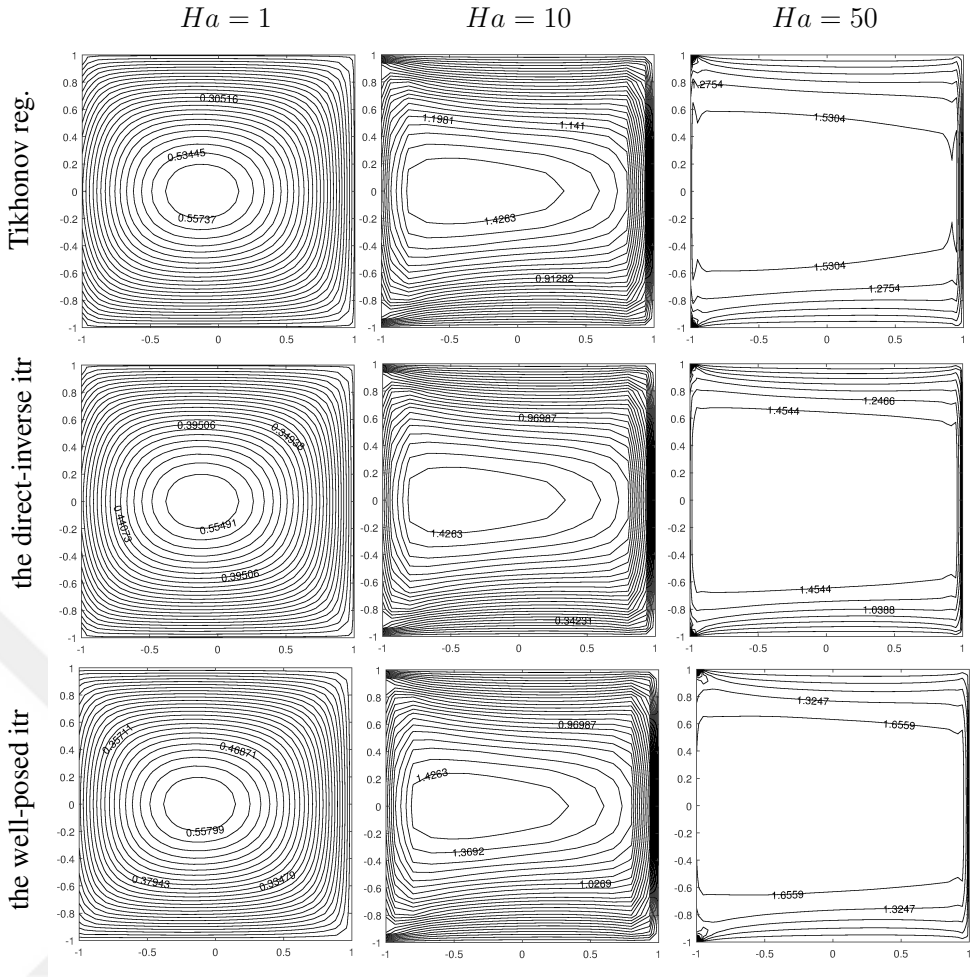


Figure 4.6: MHD duct flow - Problem 1: Velocity profiles from inverse solution, $k = 1$.

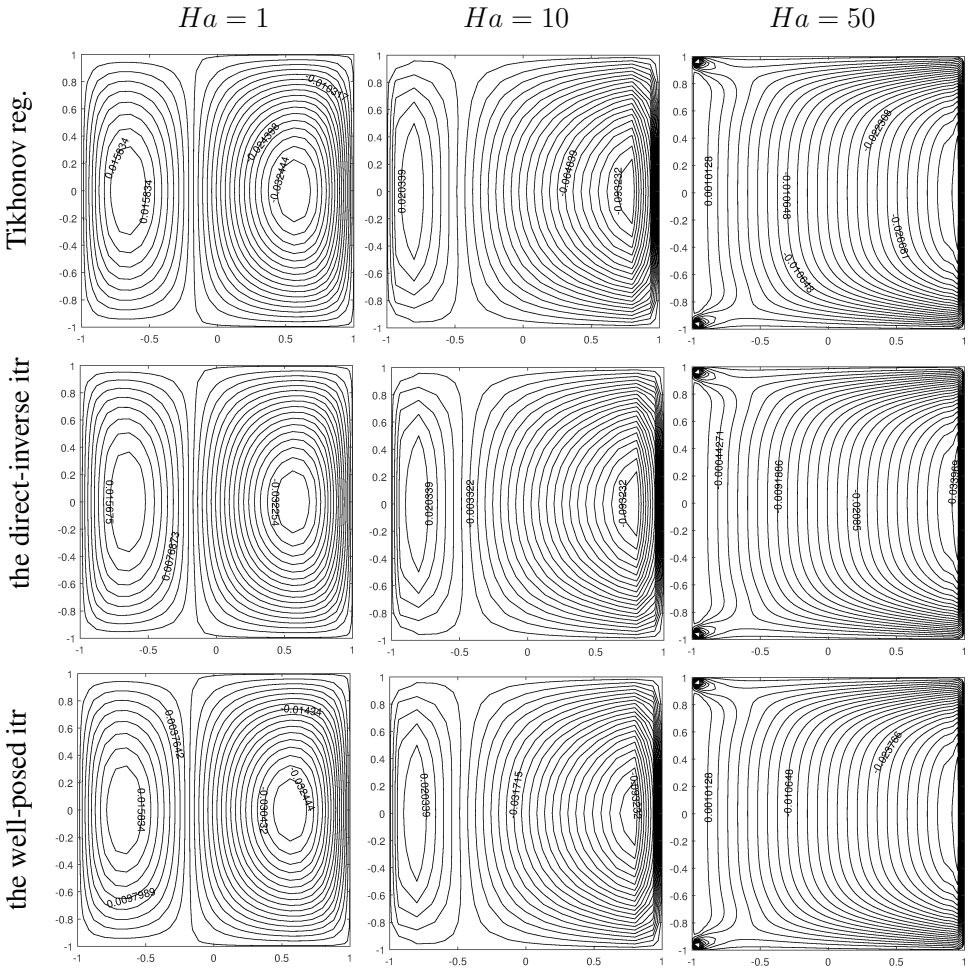


Figure 4.7: MHD duct flow - Problem 1: Induced magnetic field profiles from inverse solution, $k = 0$.

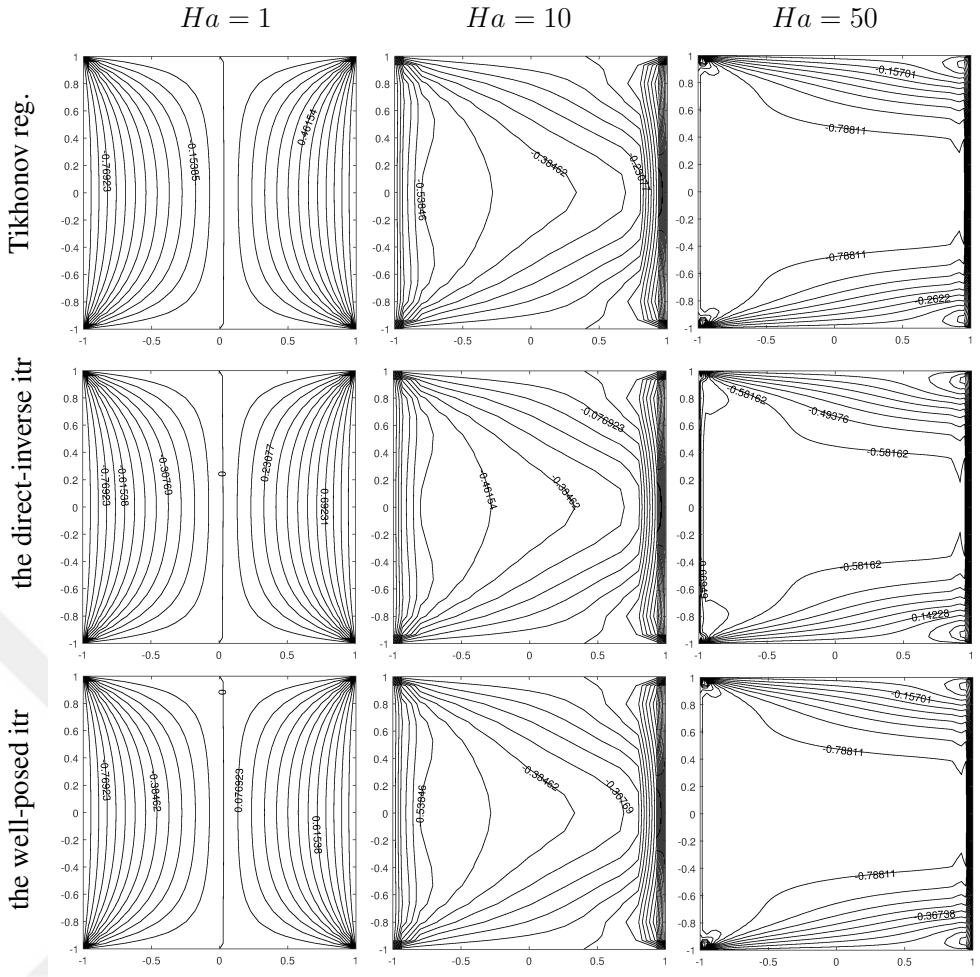


Figure 4.8: MHD duct flow - Problem 1: Induced magnetic field profiles from inverse solution, $k = 1$.

In Figures 4.7 and 4.8, we depict also induced magnetic field profiles obtained from the Cauchy problem using three regularization methods for insulated ($k = 0$) and conducting ($k = 1$) vertical walls, respectively. All of the three regularization techniques give exactly the same behaviour of the induced magnetic field converging to the direct solution which are given in Figures 4.3 and 4.4.

Resized slip length on the slipping wall from the inverse formulation is computed through the relation $\alpha = -V/\dfrac{\partial V}{\partial n}$ where V and $\dfrac{\partial V}{\partial n}$ are obtained from the DRBEM solution. These are represented in Figure 4.9, respectively for insulated ($k = 0$) and conducting ($k = 1$) vertical walls when $Ha = 10$. It can be seen that $\alpha = 0.2$ is

approached for all of the points on the slipping walls when the well-posed iterations technique is used. Variations at the centre points for the two other methods may be due to the inaccuracies in the numerical computations such as round off errors, the error propagations in the solution of final discretized system of equations. Figure 4.10 shows the error in the regained slip length for both the insulated and conducting vertical walls. It is seen that the accuracies are of order 10^{-6} and 10^{-5}, respectively.

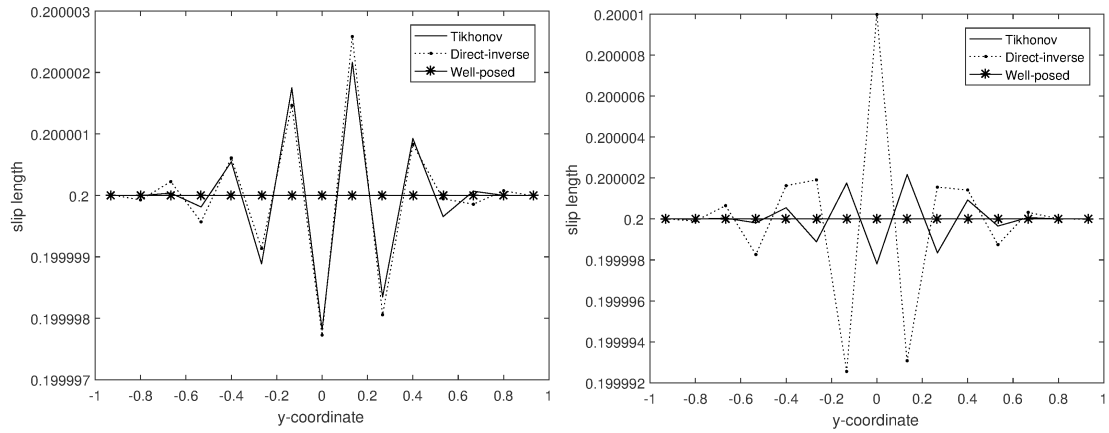


Figure 4.9: MHD duct flow - Problem 1: Slip lengths, Ha=10, $k = 0$, $k = 1$.

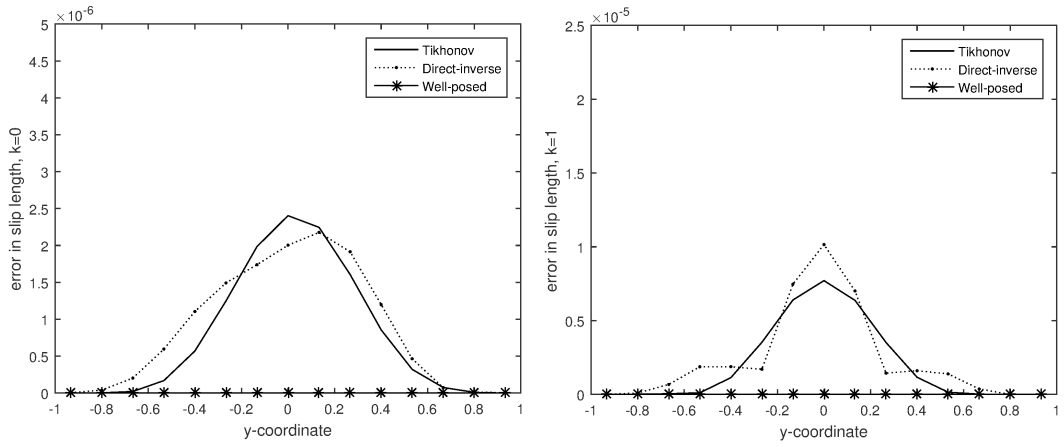


Figure 4.10: MHD duct flow - Problem 1: Error in slip length, Ha=10, $k = 0$, $k = 1$.

4.1.2 MHD duct flow - Problem 2

In Problem 2, the MHD flow in a rectangular channel is considered with a slip velocity condition on the side bottom wall of the duct. The external magnetic field still applies horizontally. The problem is defined with the MHD flow equations (4.2) and the boundary conditions (4.4) given as

$$\begin{aligned}
&V + \alpha \frac{\partial V}{\partial n} = 0, \quad B = 0 \qquad \text{on} \quad y = -1, \qquad -1 < x < 1 \\
&V = 0, \qquad\qquad B = 0 \qquad \text{on} \quad y = +1, \qquad -1 < x < 1 \\
&V = 0, \qquad\qquad B = +k \qquad \text{on} \quad x = +1, \qquad -1 < y < 1 \\
&V = 0, \qquad\qquad B = -k \qquad \text{on} \quad x = -1, \qquad -1 < y < 1.
\end{aligned} \tag{4.4}$$

The problem region and the boundary conditions for Problem 2 are shown in the Figure 4.11 as

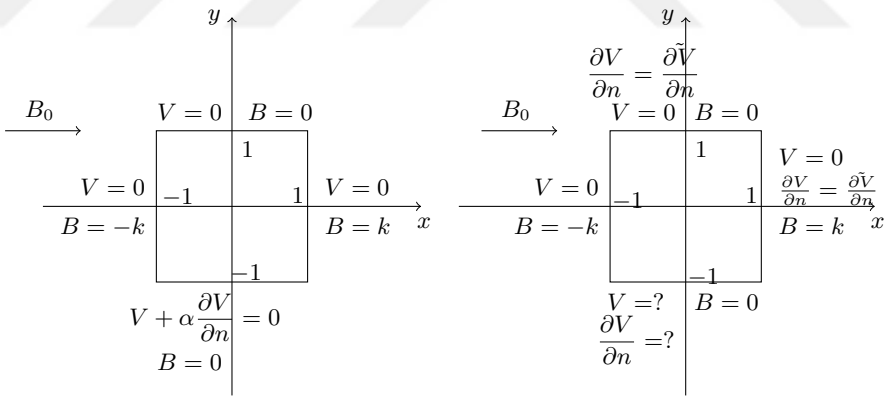


Figure 4.11: MHD duct flow - Problem 2: Boundary conditions for the direct (left) and the Cauchy (right) problems.

In Problem 2, the MHD duct flow equations (4.2) are solved by using the DRBEM in terms of direct and inverse problems for reconstructing the preassumed slip length $\alpha = 0.2$ on the bottom horizontal wall of the duct (Figure 4.11).

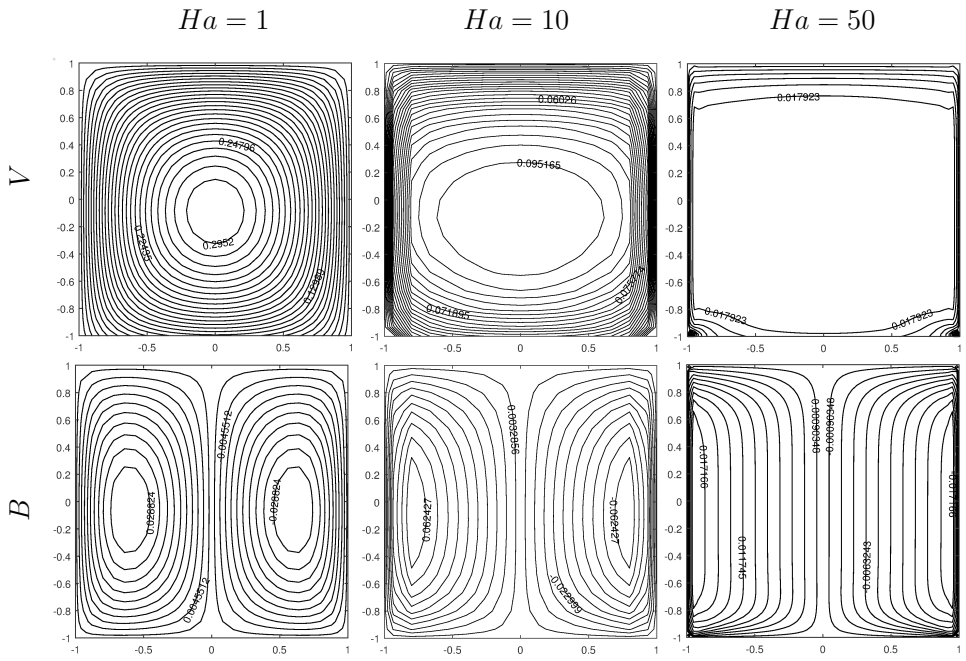


Figure 4.12: MHD duct flow - Problem 2: Velocity and induced magnetic field profiles from direct problem, $\alpha = 0.2$, $k = 0$.

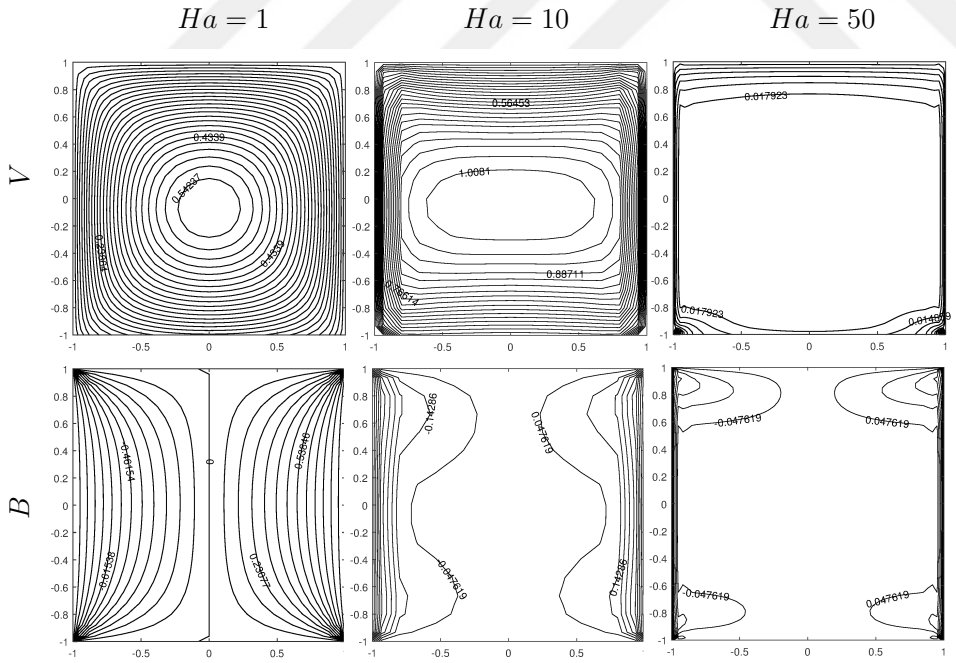


Figure 4.13: MHD duct flow - Problem 2: Velocity and induced magnetic field profiles from direct problem, $\alpha = 0.2$, $k = 1$.

In Figures 4.12 and 4.13, the velocity of the fluid $V(x, y)$ and induced magnetic field $B(x, y)$ profiles obtained from direct solutions of MHD flow equations (4.2) with the boundary conditions (4.4) and the slip length $\alpha = 0.2$ on the bottom wall are shown for Hartmann number values $Ha = 1, 10, 50$ with the insulated ($k = 0$) and conducting ($k = 1$) vertical walls, respectively.

Figures 4.14 and 4.15 show the velocity behaviours for the Cauchy MHD flow problem resulted from the three regularization methods, respectively for $k = 0$ and $k = 1$. It is observed that all the three methods seize the same velocity behaviour of the direct solutions for Hartmann number values $Ha = 1, 10, 50$ which are shown in Figure 4.12 and 4.13.

Similar to the Problem 1, an increase in the Hartmann number results in enlarging core region of the fluid. In addition, when Hartmann number is taken as $Ha = 50$, the fluid reaches to motionless flattened flow. Hartmann layers are formed as Ha increases. Side layers are also observed with Ha increase but the slip phenomenon is dominant on the bottom wall and it diminishes the side layer there showing the slip velocity especially near the bottom corners.

Figures 4.16 and 4.17 show the induced magnetic field behaviours obtained from the inverse problem employing the three regularization techniques for both insulated and conducting vertical duct walls, respectively. The same behaviour of the induced magnetic field as in the direct problem solution is obtained from all the three regularization methods.

Similar to Problem 1, Figure 4.18 shows that the well-posed iterations technique gives the exactly same value for the slip length α as $\alpha = 0.2$ which is used in the solution of the direct problem. On the other hand, the other two methods lead to some innaccuries which is of order 10^{-4} due to the round off errors in the solution of the DRBEM discretized system of equations.

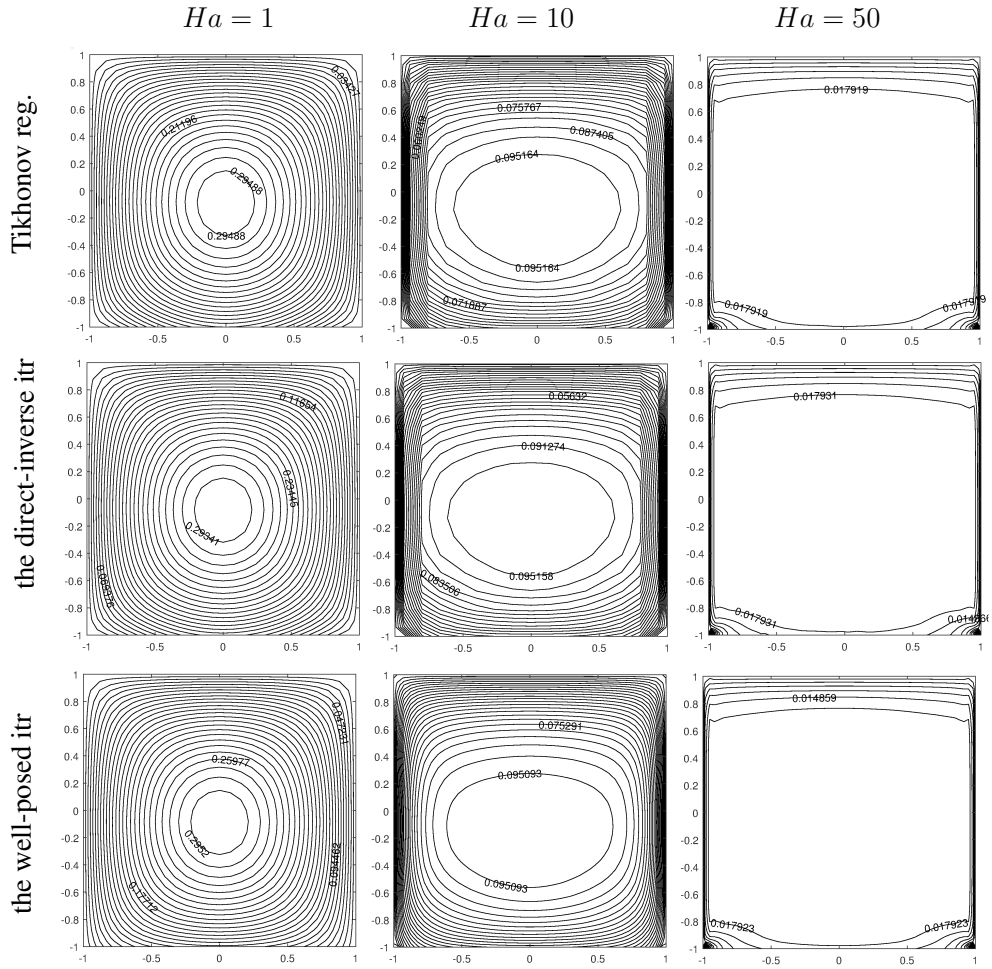


Figure 4.14: MHD duct flow - Problem 2: Velocity profiles from inverse solution, $k = 0$.

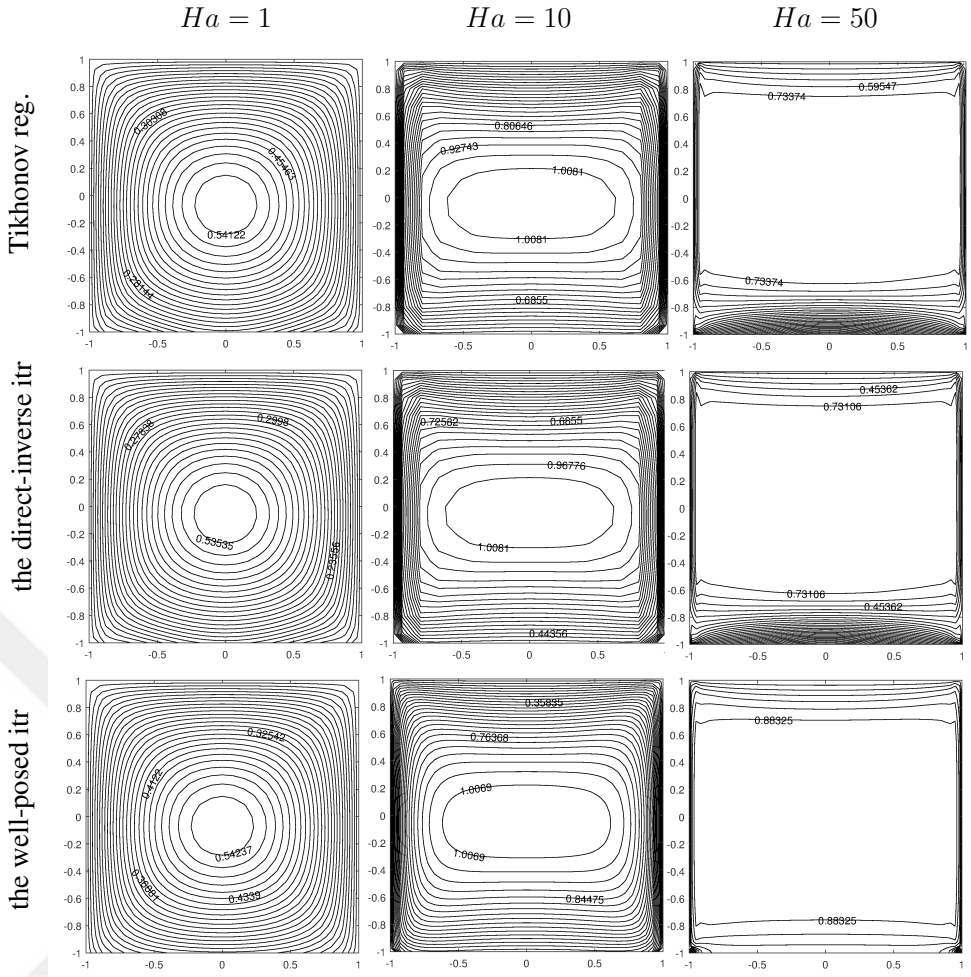


Figure 4.15: MHD duct flow - Problem 2: Velocity profiles from inverse solution, $k = 1$.

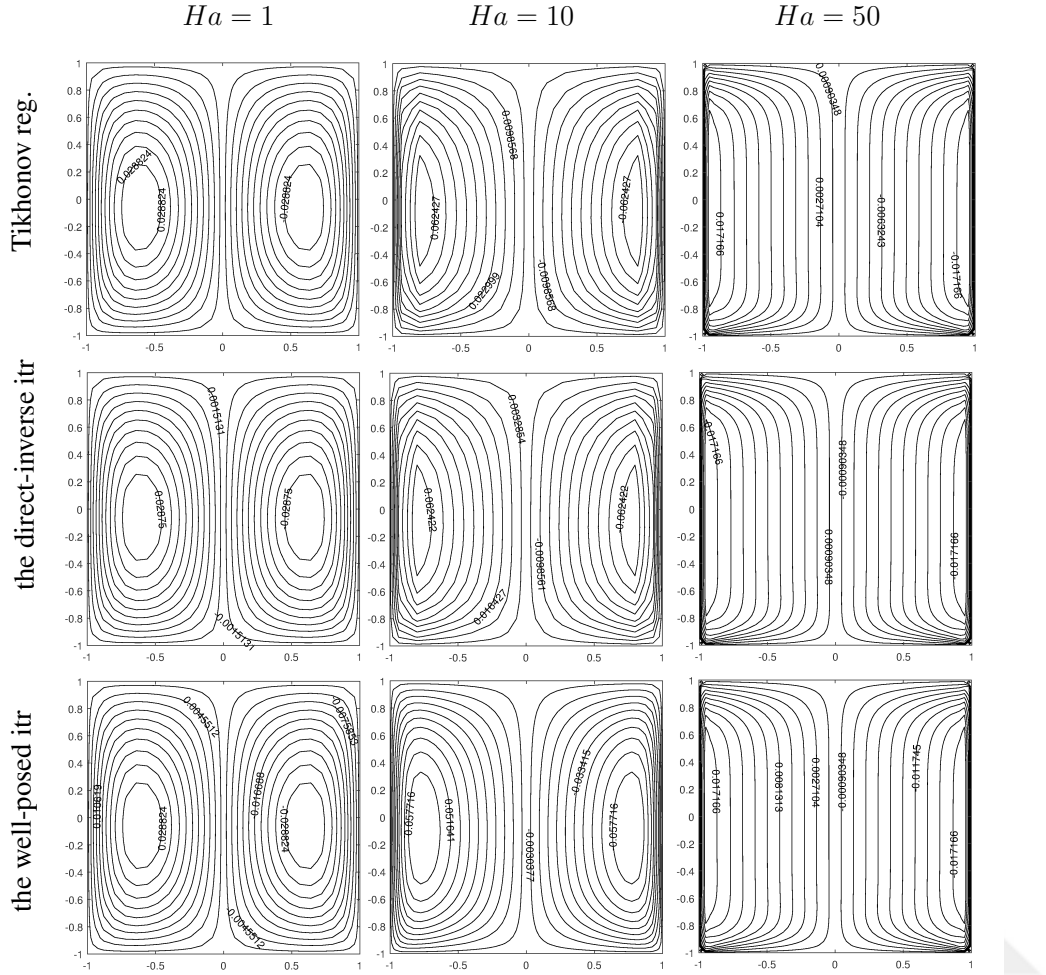


Figure 4.16: MHD duct flow - Problem 2: Induced magnetic field profiles from inverse solution, $k = 0$.

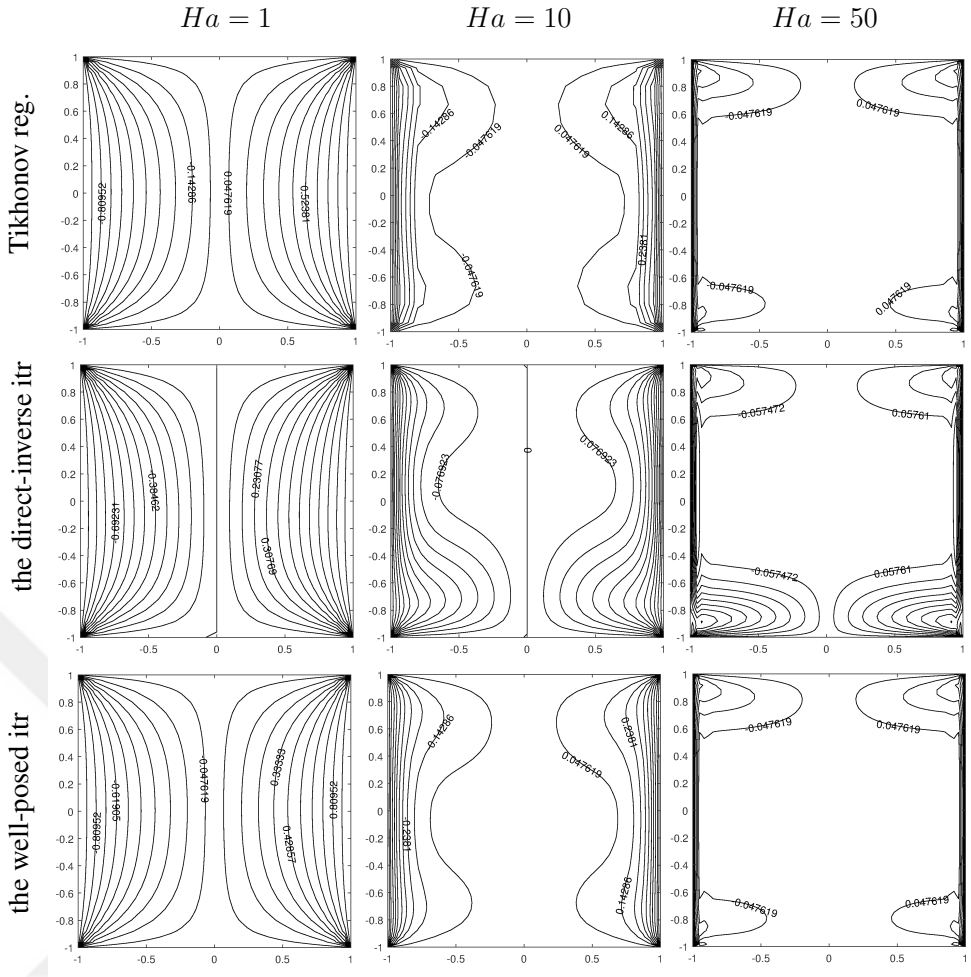
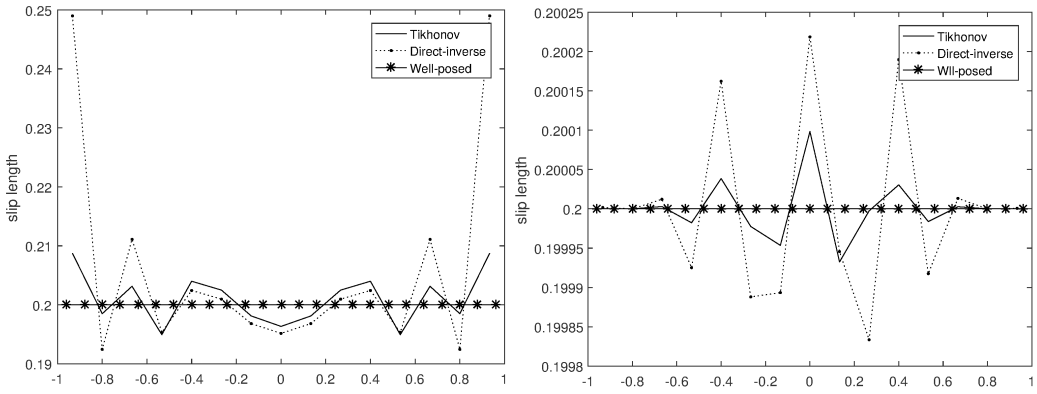


Figure 4.17: MHD duct flow - Problem 2: Induced magnetic field profiles from inverse solution, $k = 1$.



y-coordinate y-coordinate

Figure 4.18: MHD duct flow - Problem 2: Slip lengths, Ha=10, $k = 0$, $k = 1$.

4.1.3 MHD duct flow - Problem 3

In Problem 3, the two-dimensional, steady and fully-developed MHD flow in a rectangular duct under the effect of an externally applied oblique magnetic field is considered. The non-dimensional governing equations for the velocity $V(x, y)$ of the fluid and the induced magnetic field $B(x, y)$ in the domain Ω are

$$\begin{aligned} \nabla^2 V + Ha_x \frac{\partial B}{\partial x} + Ha_y \frac{\partial B}{\partial y} &= -1 \\ \nabla^2 B + Ha_x \frac{\partial V}{\partial x} + Ha_y \frac{\partial V}{\partial y} &= 0 \end{aligned} \tag{4.5}$$

where $\Omega = \{(x, y) \in R : -1 < x, y < 1\}$, $Ha_x = Hasin(\beta)$, $Ha_y = Hacos(\beta)$ and $Ha = LB_0\sqrt{\sigma/\nu\rho} = \sqrt{(Ha_x)^2 + (Ha_y)^2}$ is the Hartmann number. The magnetic field applies in the direction obtained with an angle β from the y-axis.

In Problem 3, the left vertical wall allows the slip of the fluid and also variable conductivity at the same time.

The boundary conditions of the MHD duct flow with slipping and variably conducting

left wall are given as

$$\begin{aligned} &V = 0, B = 0 \quad \text{on} \quad y = \mp 1, \quad -1 < x < 1 \\ &V = 0, B = 0 \quad \text{on} \quad x = 1, \quad -1 < y < 1 \\ &V + \alpha \frac{\partial V}{\partial n} = 0 \ \text{on} \quad x = -1, \quad -1 < y < 1 \\ &B + c \frac{\partial B}{\partial n} = 0 \ \text{on} \quad x = -1, \quad -1 < y < 1. \end{aligned} \tag{4.6}$$

where α is the dimensionless slip length and c is the conductivity constant.

Similar to Problem 1 and Problem 2, the MHD duct flow problem is formulated as a Cauchy problem so that the slip length and the conductivity constant on the left vertical wall are regained. The physical configuration of the boundary conditions for both the direct and inverse formulations of MHD duct flow is given in Figure 4.19

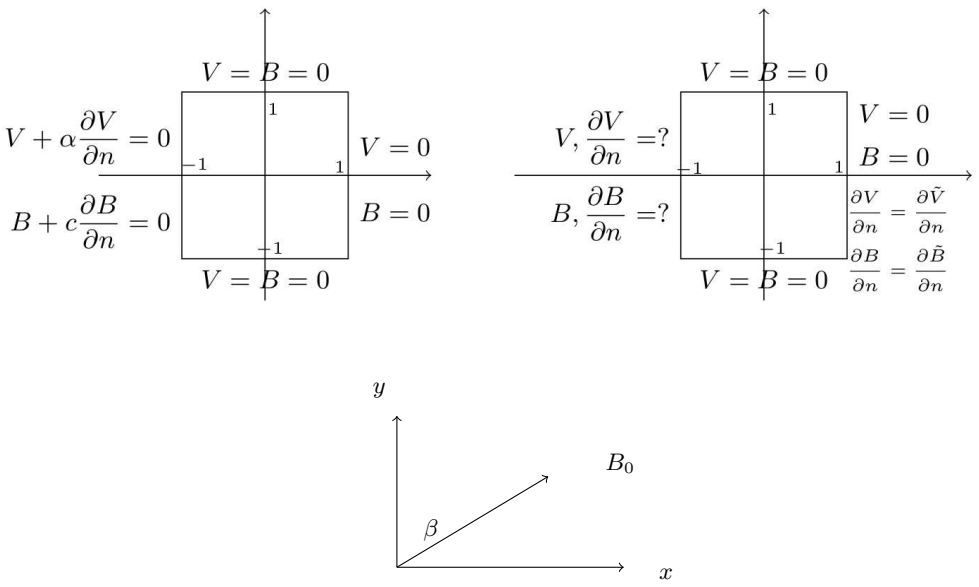


Figure 4.19: MHD duct flow - Problem 3: Boundary conditions for the direct (left) and the Cauchy (right) problems. $\tilde{V}$, $\tilde{B}$ denote direct problem solution.

In Problem 3, for the solution of inverse formulation, the well-posed iterations technique is used to solve the ill-posed problem due to the overspecified and underspecified boundary conditions of Cauchy MHD duct flow.

In the application of the DRBEM, $N = 80, 100, 160$ constant boundary elements and

$L = 400, 625, 1600$ interior nodes are taken for $Ha = 5, 10, 50$, respectively. In the well-posed iterations, the convergence criteria is taken as 10^{-4} as the maximum absolute error in the values of V and B, seperately, between the consecutive iterations.

The direct problem is solved when the left wall is taken as slipping and variably conducting by taking the slip length $\alpha = 0.2$ and the conductivity constant $c = 0.3$. In addition, the external magnetic field is applied with an angle $\beta = 0, \frac{\pi}{4}, \frac{\pi}{3}, \frac{\pi}{2}$ formed with the y-axis.

The direct solutions for V and B are obtained by using the radial basis functions as $f = 1 + r$, $f = 1 + r + r^2$, $f = r^2 lnr$ for the angle $\beta = \frac{\pi}{2}$ and the Hartmann number $Ha = 10$. The Figure 4.20 indicates that there is no significant difference between the solutions, hence because of the simplicity and computational effort, the rest of the calculations are carried by using $f = 1 + r$.

The direct solutions of MHD flow equations (4.5) for V and B with the boundary conditions (4.6) and the slip length $\alpha = 0.2$, conductivity constant $c = 0.3$ on the left wall are presented for Hartmann number values $Ha = 5, 10, 50$ for the angle $\beta = 0$ in Figure 4.21. It is noted that when $\beta = 0$, the external magnetic field B_0 applies in the y-direction. It is observed that as Ha number increases, Hartmann layers near the top and bottom walls are developed for both V and B which is the well-known behaviour of the MHD duct flow. Also, on the left wall the slip effect is observed which is weakened when Ha increases. In addition, as Ha increases, the core region of the fluid enlarges and flow becomes flattened. The induced current seperates into two bunches. Due to the variable conductivity, current lines cross the left walls.

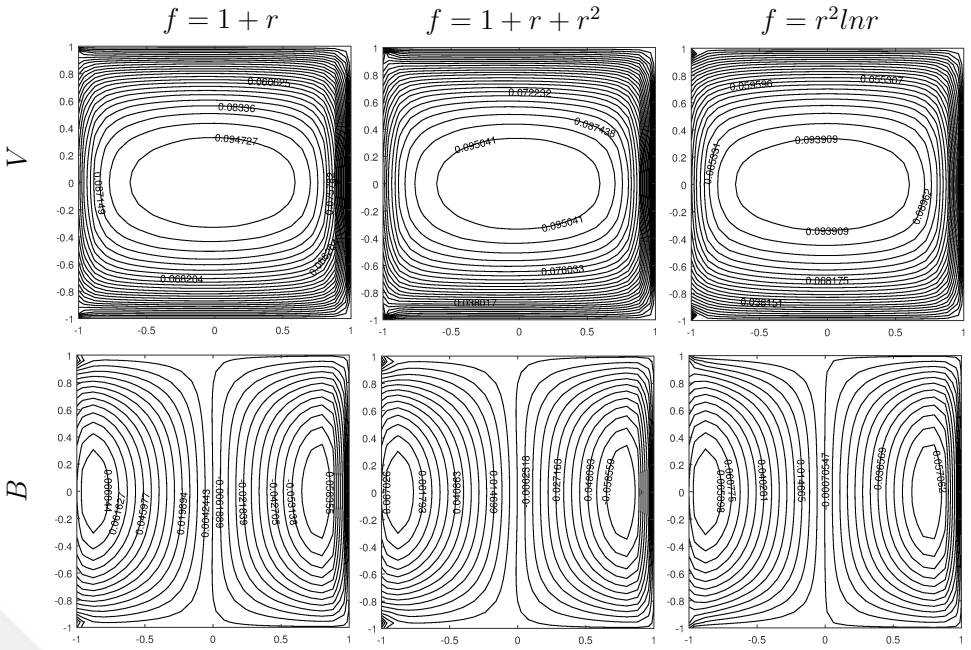


Figure 4.20: MHD duct flow - Problem 3: Velocity and induced magnetic field from direct solution, $\beta = \dfrac{\pi}{2}, \alpha = 0.2, c = 0.3, Ha = 10$.

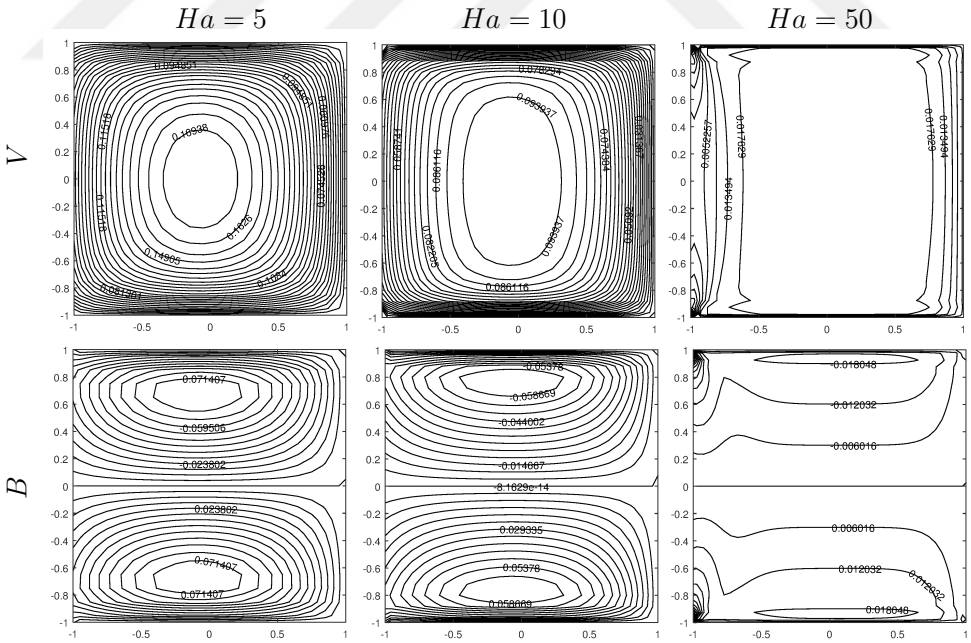


Figure 4.21: MHD duct flow - Problem 3: Velocity and induced magnetic field from direct problem, $\beta = 0, \alpha = 0.2, c = 0.3$.

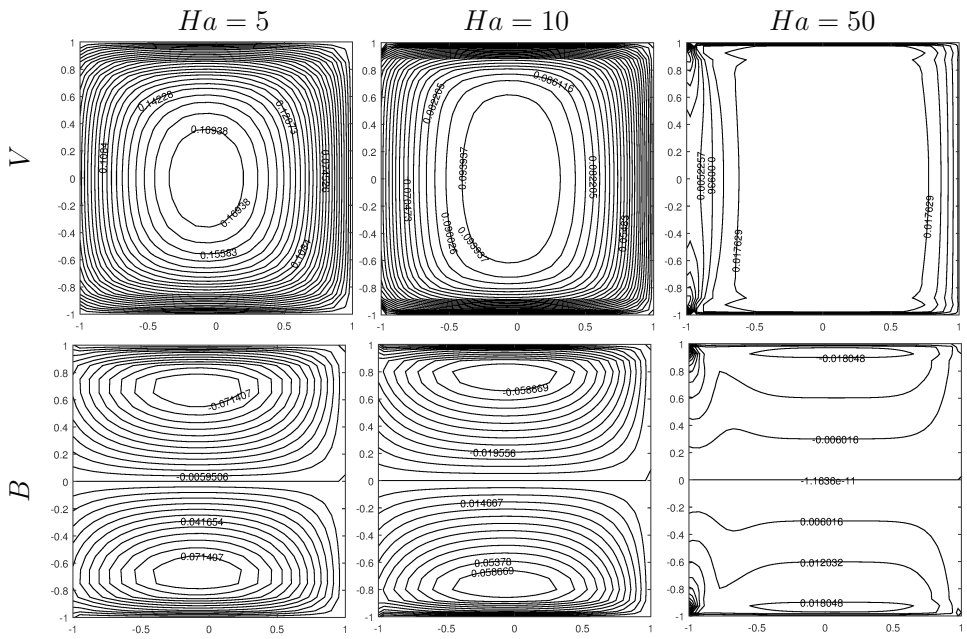


Figure 4.22: MHD duct flow - Problem 3: Velocity and induced magnetic field from inverse solution, $\beta = 0$

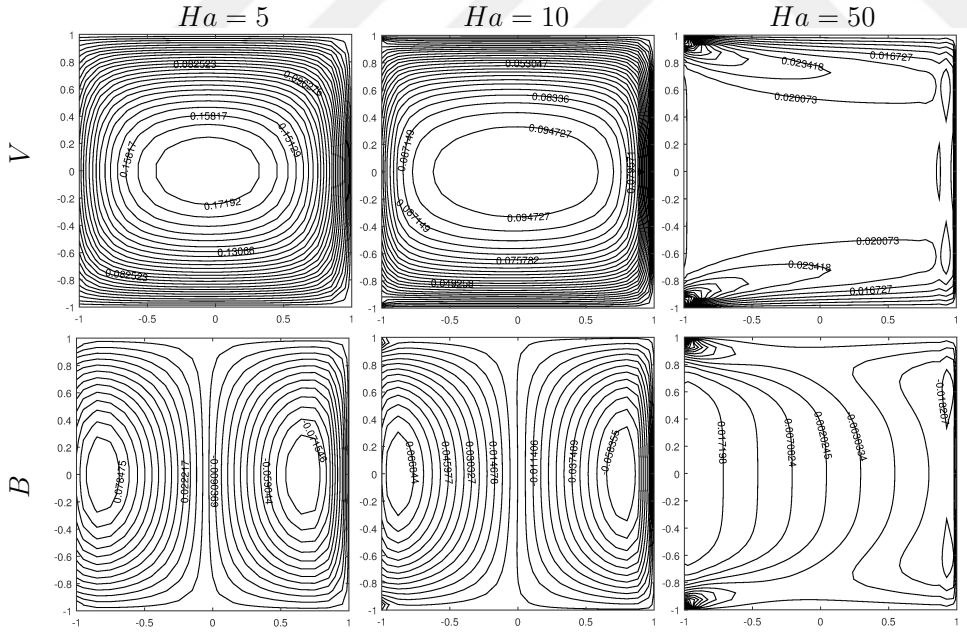


Figure 4.23: MHD duct flow - Problem 3: Velocity and induced magnetic field from direct problem, $\beta = \dfrac{\pi}{2}, \alpha = 0.2, c = 0.3$.

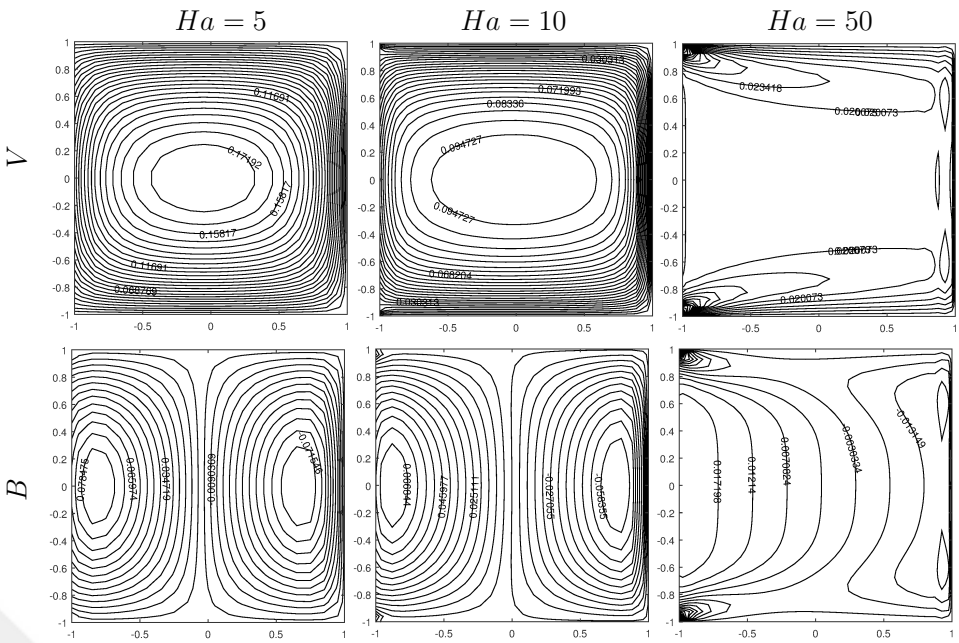


Figure 4.24: MHD duct flow - Problem 3: Velocity and induced magnetic field from inverse solution, $\beta = \dfrac{\pi}{2}$

Figure 4.22 shows the velocity and the induced magnetic field behaviours for the Cauchy MHD flow problem resulted from the well-posed iterations for $Ha = 5, 10, 50$ and $\beta = 0$. It can be seen that the velocity contours obtained from the inverse formulation are in a very well agreement with the ones in the direct problem obtained for $\alpha = 0.2$ and $c = 0.3$.

In Figures 4.23-4.24, the angle β is taken as $\beta = \dfrac{\pi}{2}$, i.e, the external magnetic field applies in the x-direction. It is clearly seen that the slip and variable conductivity effect weakens the Hartmann layer near the left wall. A further increase in Hartmann number separates the flow through the top and bottom walls and diminishes the slip phenomenon on the left wall. In addition, the solutions of the direct and inverse problems (converged to the direct solution) are in a very well agreement in the sense of fluid movement and the induced current behavior.

Due to the variable conductivity, current lines cross the left walls. An increase in Ha results in squeezing the right bunch of the induced current through the right wall.

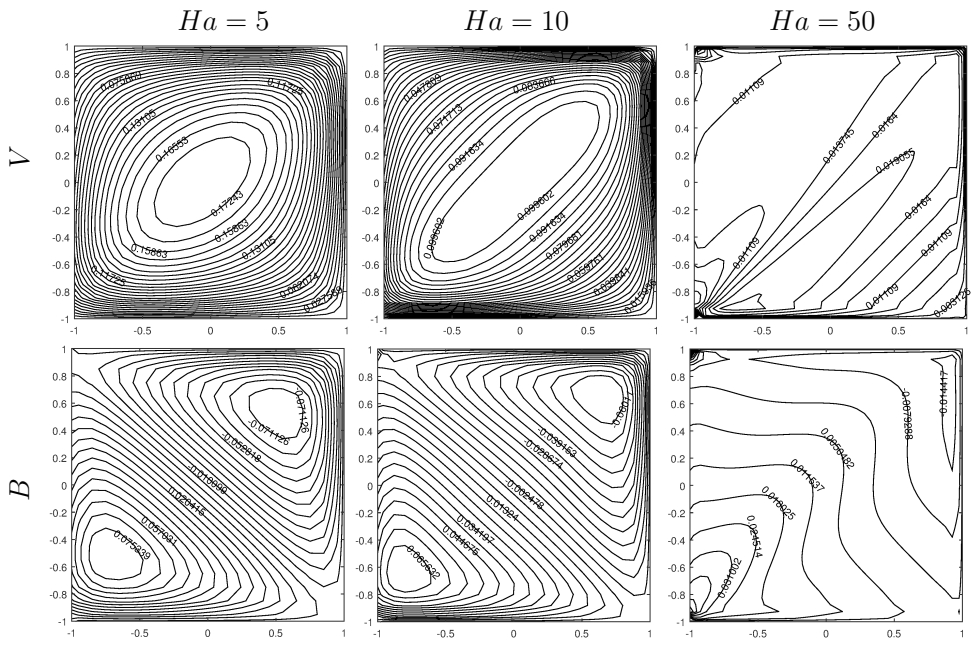


Figure 4.25: MHD duct flow - Problem 3: Velocity and induced magnetic field from direct problem, $\beta = \dfrac{\pi}{4}, \alpha = 0.2, c = 0.3$.

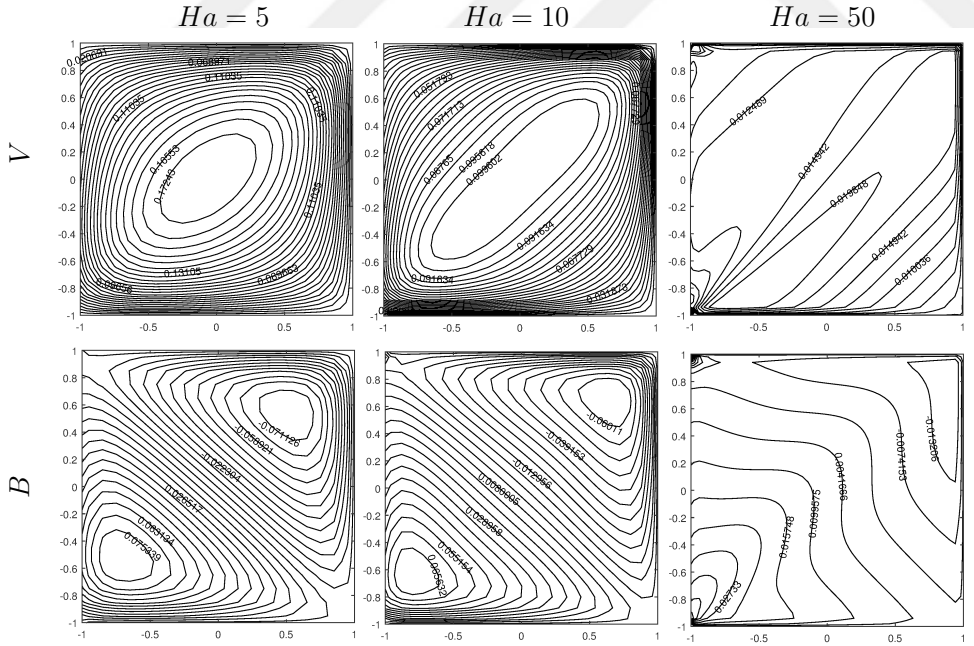


Figure 4.26: MHD duct flow - Problem 3: Velocity and induced magnetic field from inverse solution, $\beta = \dfrac{\pi}{4}$

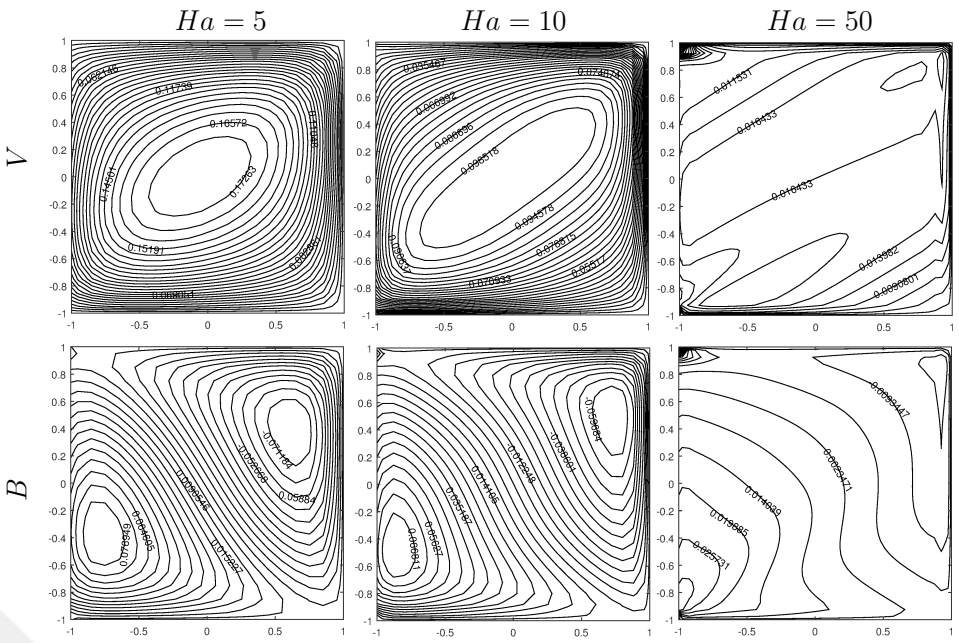


Figure 4.27: MHD duct flow - Problem 3: Velocity and induced magnetic field from direct problem, $\beta = \dfrac{\pi}{3}, \alpha = 0.2, c = 0.3$.

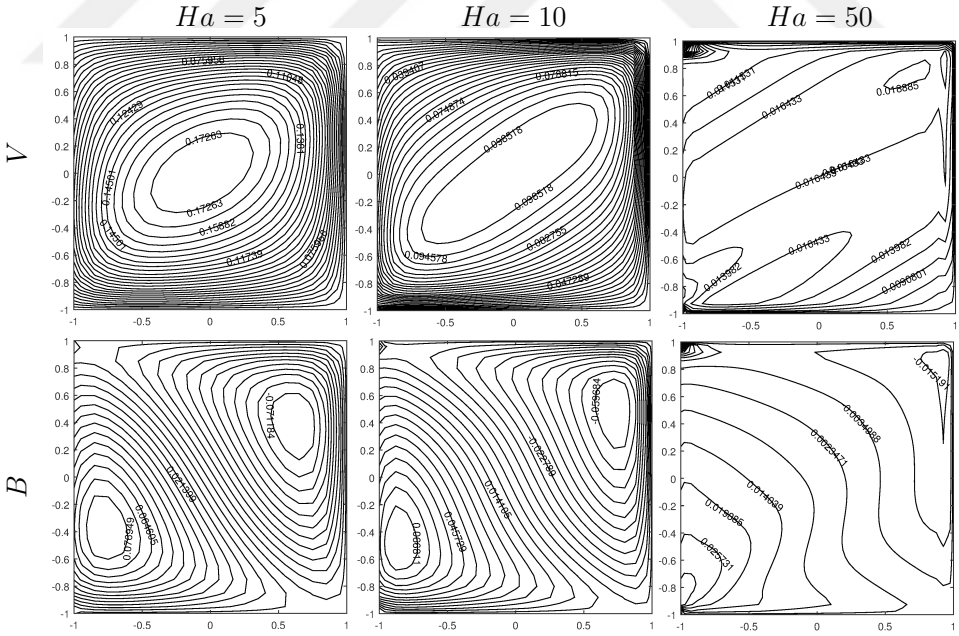


Figure 4.28: MHD duct flow - Problem 3: Velocity and induced magnetic field from inverse solution, $\beta = \dfrac{\pi}{3}$

When the angle $\beta = \frac{\pi}{4}, \frac{\pi}{3}$ are taken, the direct and inverse solutions for the velocity V and the induced magnetic field B are given in the Figures 4.25 - 4.28. It is depicted that the core region of the fluid rotates in accordance with the angle β with the y-axis showing the slip near the left wall. The boundary layers are directed near the corners of the duct in the external applied magnetic field direction showing the well-known behavior of the MHD duct flow. It is observed that the Cauchy MHD flow problem solutions through the well-posed iterations show the very well agreement with the ones in the direct problem solutions for each angle considered.

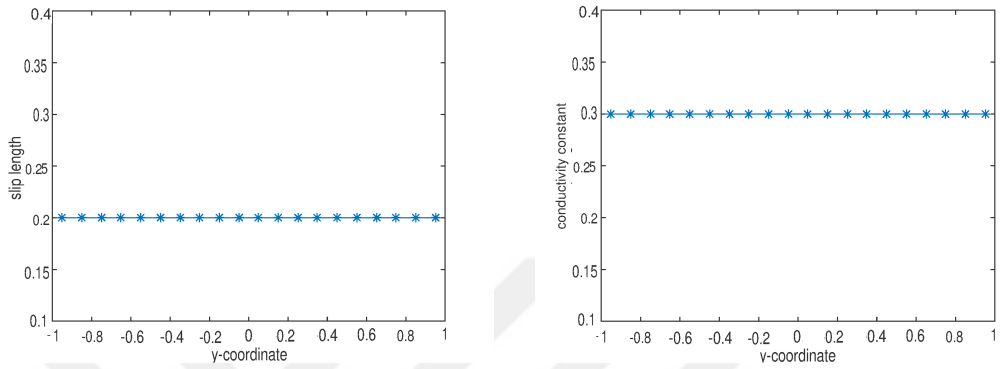
The mesh independence is shown in Table 4.1 for Hartmann number $Ha = 10$. The velocity and induced magnetic field values at the point $x = -1, y = 0$ which is on the slipping and variably conducting part of the duct are given for several numbers of constant boundary elements. It is seen that when N is taken as larger than $N = 100$, the values of V and B are the same up to the order 10^{-4}. Hence, $N = 100$ can be taken as the optimal number of boundary elements for that Hartmann number.

N	44	60	68	76	84	92	100	108	116
V	0.0630	0.0623	0.0621	0.0620	0.0619	0.0619	0.0618	0.0618	0.0618
B	0.0618	0.0616	0.0616	0.0616	0.0616	0.0616	0.0616	0.0616	0.0616

Table 4.1: MHD duct flow - Problem 3: Velocity and induced magnetic field values from the inverse solution at the point $(-1, 0)$, $Ha = 10, \beta = \frac{\pi}{2}, \alpha = 0.2, c = 0.3$.

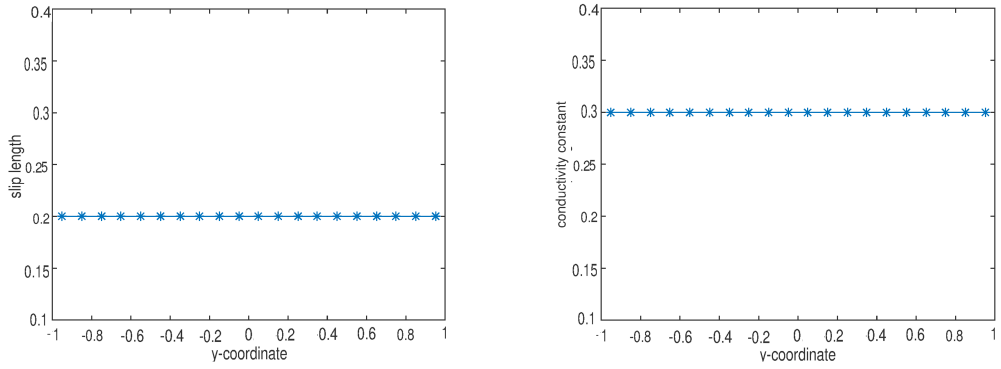
The slip condition and variable conductivity condition contain both the velocity, the induced magnetic field and their normal derivative values on the left part of the boundary, one need both of these computed values to extract α from the equation $V + \alpha\frac{\partial V}{\partial n} = 0$ and also c from $B + c\frac{\partial B}{\partial n} = 0$. Resized slip length α and the conductivity constant c on the left wall from the inverse formulations are computed through the relation
$\alpha = -V/\frac{\partial V}{\partial n}$ and $c = -B/\frac{\partial B}{\partial n}$ where V, B and their normal derivatives are obtained from the DRBEM application.

Figures 4.29 - 4.32 show that the slip length $\alpha = 0.2$ and the conductivity constant $c = 0.3$ are very well approached from the Cauchy MHD flow problem for all of the points on the slipping and variably conducting left wall for $\beta = 0, \frac{\pi}{4}, \frac{\pi}{3}, \frac{\pi}{2}$, and $M = 5, 10, 50$ when the well-posed iterations technique is used.



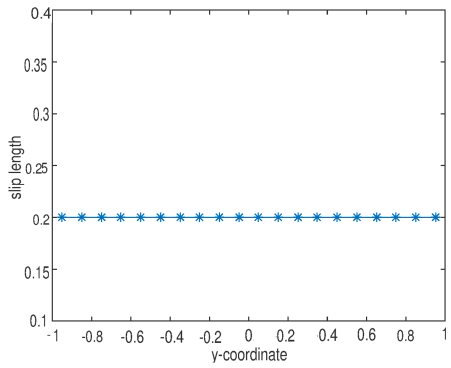
(a) slip length, α (b) coductivity constant, c

Figure 4.29: MHD duct flow - Problem 3: $\beta = 0$, $x = -1$.

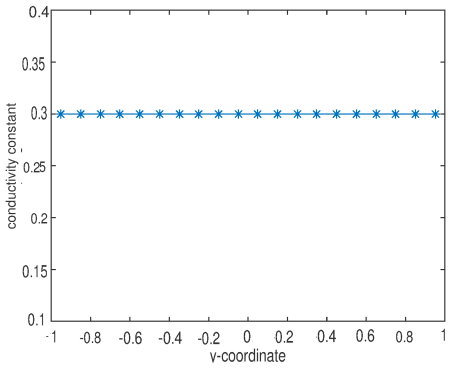


(a) slip length, α (b) coductivity constant, c

Figure 4.30: MHD duct flow - Problem 3: $\beta = \frac{\pi}{4}$, $x = -1$.

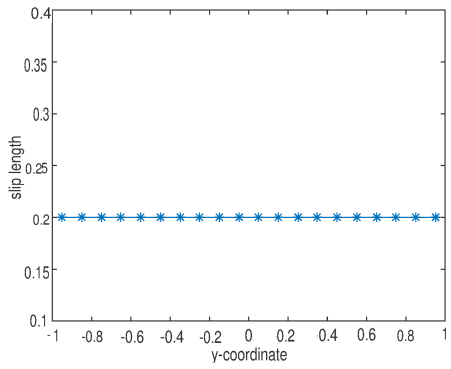


(a) slip length, α

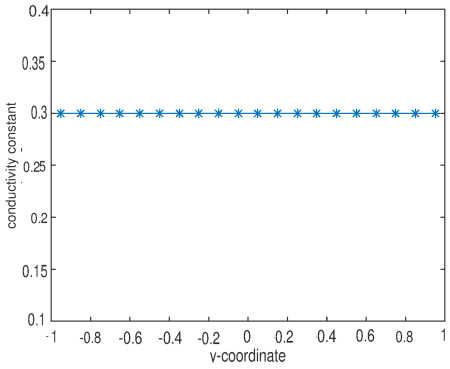


(b) coductivity constant, c

Figure 4.31: MHD duct flow - Problem 3: $\beta = \dfrac{\pi}{3}$, $x = -1$.



(a) slip length, α



(b) coductivity constant, c

Figure 4.32: MHD duct flow - Problem 3: $\beta = \dfrac{\pi}{2}$, $x = -1$.

4.2 The Cauchy MHD Duct Flow with a Slipping Perturbed Upper Boundary, Problem 4

In this section, we consider the two-dimensional, steady and fully developed MHD flow in a rectangular duct with a small boundary perturbation on the upper wall under an applied magnetic field in the $y-$ direction. The non-dimensional governing equations for the velocity $V(x, y)$ of the fluid and the induced magnetic field $B(x, y)$ in Ω

are the same as (3.34)

$$\begin{aligned} \nabla^2 V + Ha\frac{\partial B}{\partial y} &= -1 \\ \nabla^2 B + Ha\frac{\partial V}{\partial y} &= 0 \end{aligned} \tag{4.7}$$

where $\Omega = \{(x, y) \in R^2 : -2 < x < 2, -1 < y < 1 - \epsilon f(x)\}$, $\epsilon << 1$, f is an arbitrary smooth function.

The insulated vertical walls and the perfectly conducting bottom and upper walls with the slipping upper Hartmann wall gives the boundary conditions of the velocity of the fluid and the induced magnetic field as (3.35)

$$\begin{aligned} &V = 0, && \frac{\partial B}{\partial n} = 0 \quad \text{on} \quad y = -1, && -2 < x < 2 \\ &V + \alpha\frac{\partial V}{\partial n} = 0, && \frac{\partial B}{\partial n} = 0 \quad \text{on} \quad y = 1 - \epsilon f(x), && -2 < x < 2 \\ &V = 0, && B = 0 \quad \text{on} \quad x = \mp 2, && -1 < y < 1 - \epsilon f(x) \end{aligned} \tag{4.8}$$

where the domain of the problem is $\Omega^\epsilon = \{(x, y) \in R^2 : -2 < x < 2, -1 < y < 1 - \epsilon f(x)\}$ and α is the dimensionless slip length which is to be gained from the inverse configuration of the problem (Problem 4). The effects of both slipping and perturbed boundary on the MHD flow through a rectangular duct will be studied.

The MHD problem is reconstructed as a Cauchy problem in terms of the velocity $V(x, y)$ and the induced magnetic field $B(x, y)$ so that the slip length on the upper perturbed curved boundary is recovered.

The problem region and the boundary conditions of the MHD duct flow with a slipping perturbed upper boundary are given for the direct problem in Figure 4.33 and and for the inverse problem in Figure 4.34.

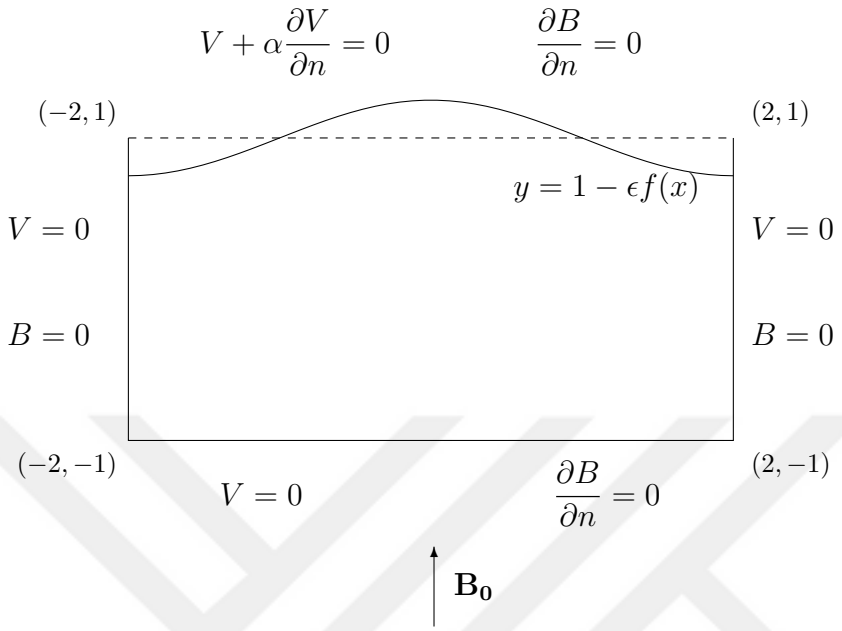


Figure 4.33: MHD Duct Flow-Problem 4, Boundary conditions for the direct problem. Upper wall is perturbed and slipping.

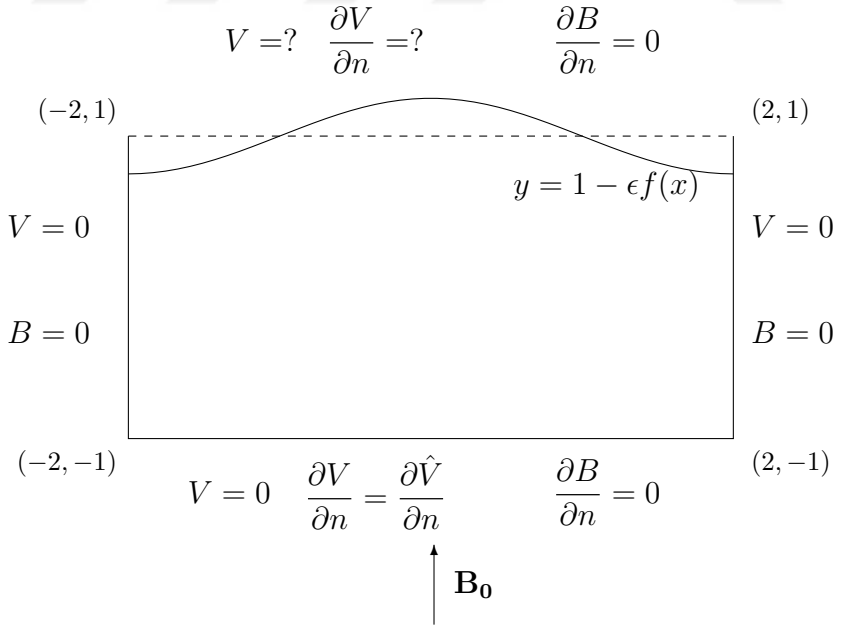


Figure 4.34: MHD Duct Flow-Problem 4, Boundary conditions for the inverse problem. Upper wall is perturbed and slipping.

The MHD duct flow equations (4.7) with the boundary conditions (4.8) involving perturbed upper boundary are solved with the DRBEM through the asymptotic analysis given in Section 3.8.1 for the first order approximation and the corrector. In the application of the DRBEM, $N = 120$ constant boundary elements and $L = 900$ interior nodes are taken for the considered $Ha = 5$ and 10 values. The direct and inverse solutions for the velocity and the induced magnetic field are simulated in a rectangular duct with a small boundary perturbation on the upper wall using the functions $f(x) = -cos(\frac{2\pi x}{3})$, $f(x) = -(1-x^2)cos(2\pi x)$, and $f(x) = -cos(\frac{\pi x}{4})$. The velocity and induced magnetic field contours are obtained for the perturbation parameter $\epsilon = 0.1, 0.2$ and 0.3. The regularization parameter λ is taken as 10^{-5} to perform the Tikhonov regularization.

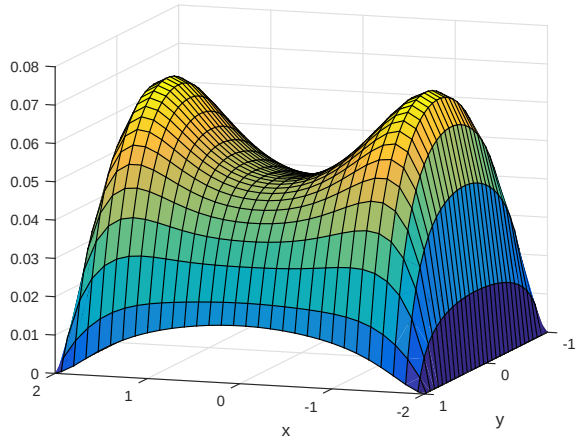


Figure 4.35: Problem 4. Velocity , $Ha = 5$, $\alpha = 0$, $\epsilon = 0.1$, $f(x) = -cos(\frac{\pi x}{4})$, $f(r) = 1 + r$.

In the literature, MHD duct flow solution with a perturbed slipping boundary is not avaliable. Thus, we compare (validate) our present algorithm results with the ones in reference [80] which provides explicit asymptotic solution to the same MHD flow problem with $f(x) = -cos(\frac{\pi x}{4})$ and no-slip perturbed upper wall. In Figure 4.35, we present velocity level curve obtained from the direct solution for Ha=5, $\epsilon = 0.1$ using $f(x) = -cos(\frac{\pi x}{4})$ in the absence of slip ($\alpha = 0$). The agreement is very well with the velocity level curve given in Figure 14 in [80].

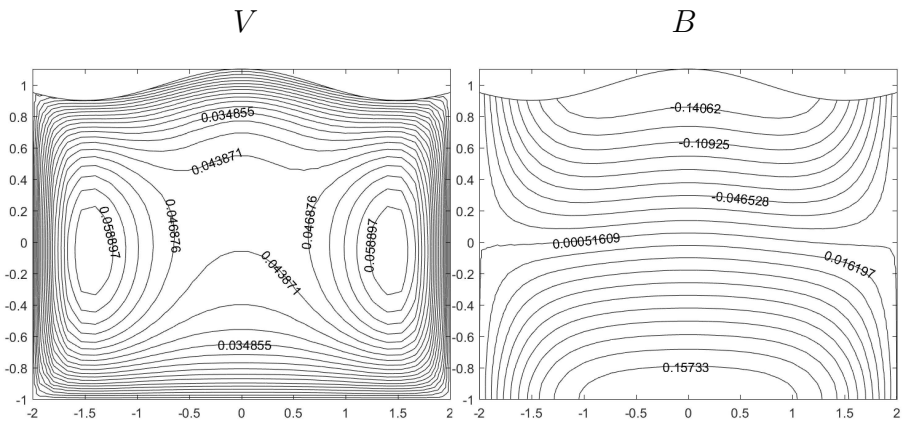


Figure 4.36: Problem 4. Velocity and induced magnetic field from direct problem, $Ha = 5$, $\alpha = 0$, $f(x) = -cos(\frac{2\pi x}{3})$, $\epsilon = 0.1$, $f(r) = 1 + r$.

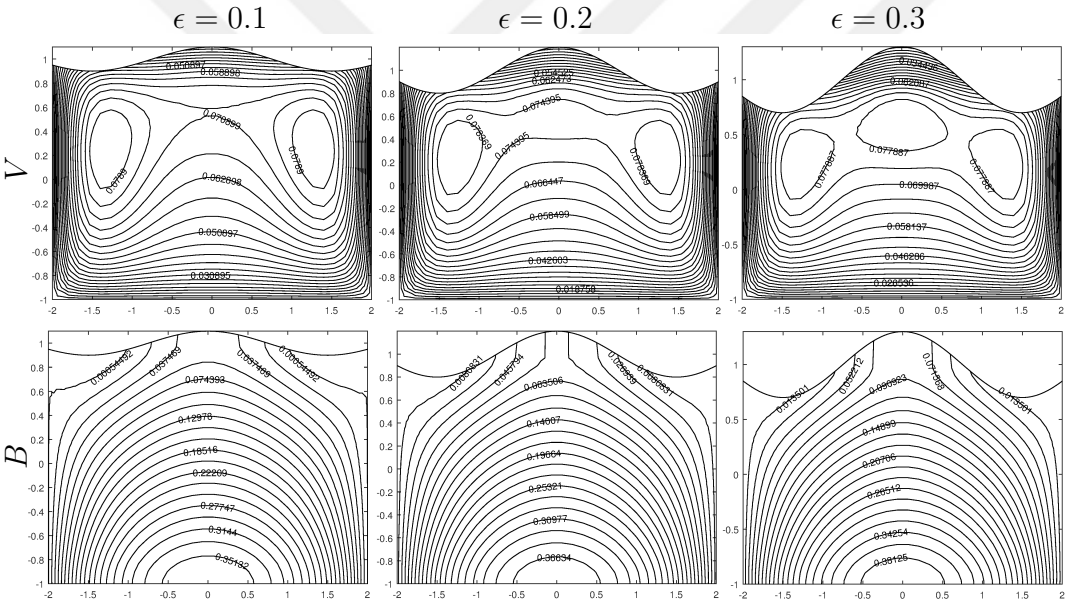


Figure 4.37: Problem 4. Velocity and induced magnetic field from direct problem, $Ha = 5$, $\alpha = 0.2$, $f(x) = -cos(\frac{2\pi x}{3})$, $f(r) = 1 + r$.

In Figure 4.36, the slip length α is taken as 0, and hence $V = 0$ (no-slip) on the upper wall when $f(x) = -cos(\frac{2\pi x}{3})$ is used. Although there is no-slip on the upper boundary, because of the curved boundary, velocity contours seem to be crossing the boundary in the regions of the curve which are concave up. When there is no-slip

on the upper boundary, the induced magnetic field forms two antisymmetric current bunches obeying to the perfectly conducting condition both on the bottom straight and upper curved boundary.

When the slip is imposed on the curved boundary by inserting $\alpha = 0.2$, it is seen from the direct solutions in Figure 4.37 that, the velocity contours clearly indicate the velocity slips everywhere on the boundary. As it is expected, an increase in the slip length α increases the magnitude of the velocity as in the case of a rectangular duct. The slipping curved boundary has a strong effect on the induced magnetic field in the sense that current lines are completely destroyed, they leave the antisymmetry, but still they obey perfectly conducting conditions on the Hartmann walls. In addition, the magnitude of the induced magnetic field is considerably increases. When the perturbation parameter ϵ increases, there is a slight decrease in the velocity magnitude, but the current intensity increases. The behavior of the flow is affected when the perturbation parameter increases in the sense that fluid tends to move through the curved boundary and becomes sligthly stagnant at the center of the duct. In Figure 4.38, the MHD duct flow inverse solutions for the velocity and the induced magnetic field are shown, and they capture the same profiles of those in the direct formulations with $\alpha = 0.2$ (Figure 4.37) as it is expected. In Figure 4.39, the inverse velocity and induced magnetic field solutions are shown when the quadratic radial basis function $f(r) = 1 + r + r^2$ is used instead of the linear radial basis function $f(r) = 1 + r$ in the DRBEM formulation. The behaviors and the magnitudes are the same in using quadratic radial basis functions when Figure 4.38 is compared with Figure 4.39. Figure 4.40 shows the V, B behaviors of the inverse solution obtained by using $f(r) = 1 + r$, $f(r) = 1 + r + r^2$ and $f(r) = r^2 lnr$. One can notice that there is no significant difference in behaviors and magnitudes of the flow and induced magnetic field in using these different radial basis functions. Hence, the rest of the computations are carried with $f(r) = 1 + r$ due to the easy implementation.

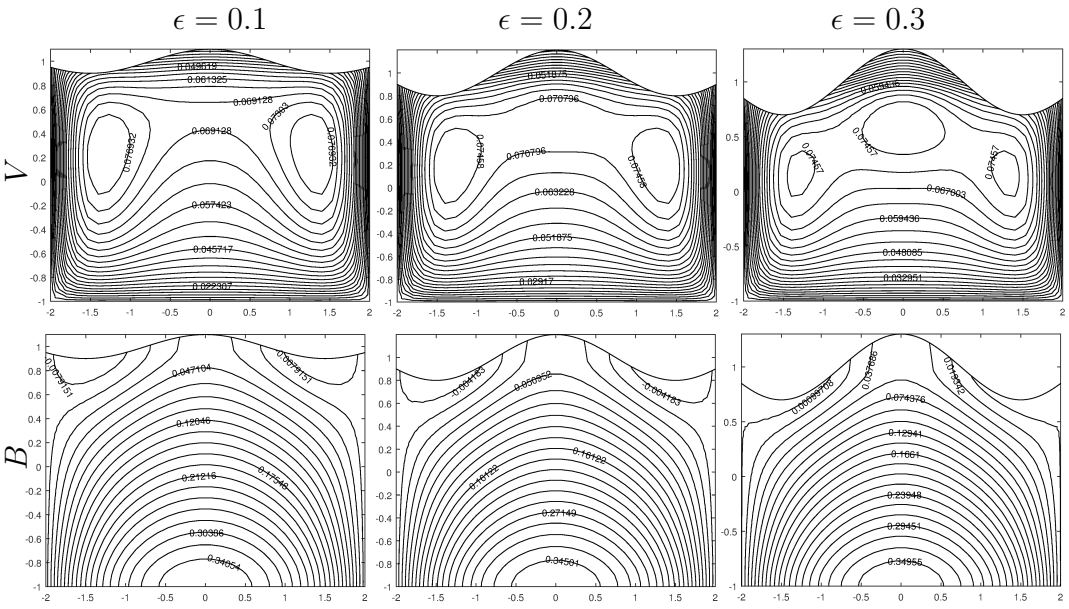


Figure 4.38: Problem 4. Velocity and induced magnetic field from inverse formulation, $Ha = 5$, $f(x) = -cos(\frac{2\pi x}{3})$, $f(r) = 1 + r$.

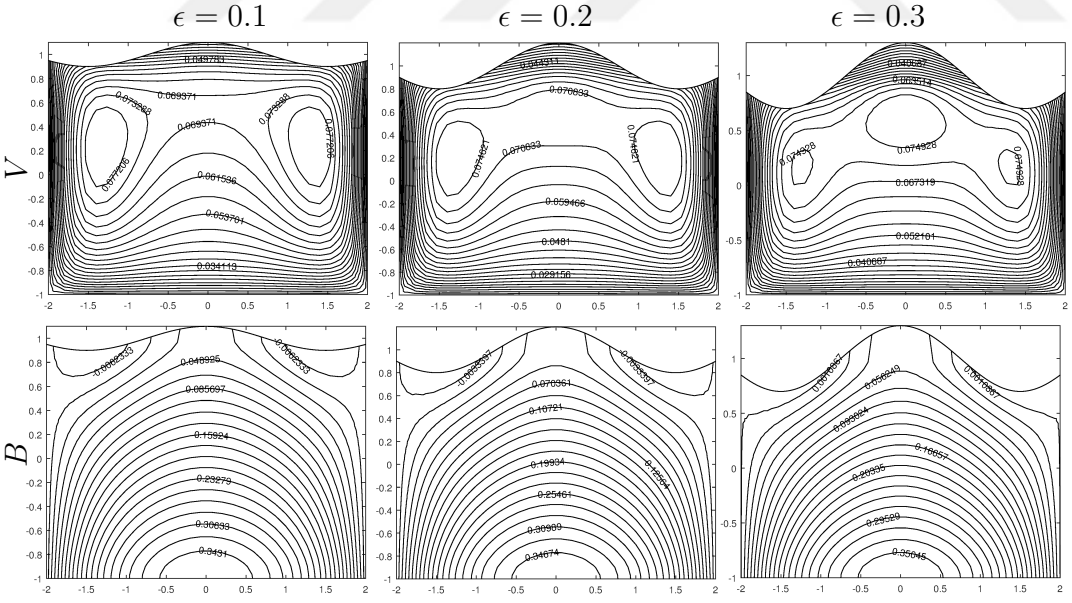


Figure 4.39: Problem 4. Velocity and induced magnetic field from inverse formulation, $Ha = 5$, $\alpha = 0.2$, $f(x) = -cos(\frac{2\pi x}{3})$, $f(r) = 1 + r + r^2$.

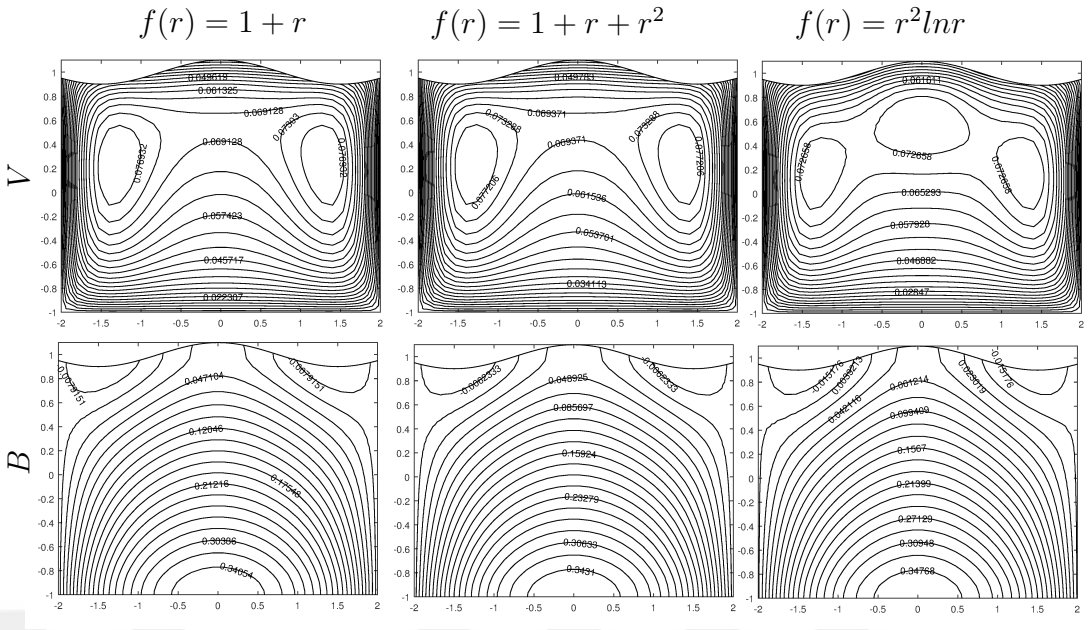


Figure 4.40: Problem 4. Velocity and induced magnetic field from inverse formulation, $Ha = 5$, $\alpha = 0.2$, $\epsilon = 0.1$, $f(x) = -cos(\frac{2\pi x}{3})$.

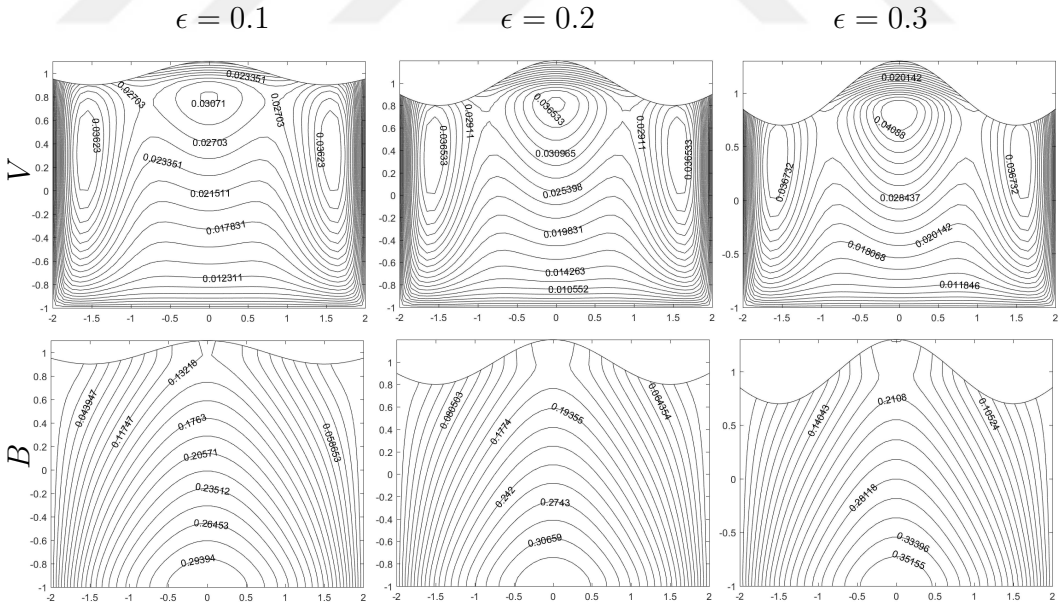


Figure 4.41: Problem 4. Velocity and induced magnetic field from direct problem, $Ha = 10$, $\alpha = 0.2$, $f(x) = -cos(\frac{2\pi x}{3})$, $f(r) = 1 + r$.

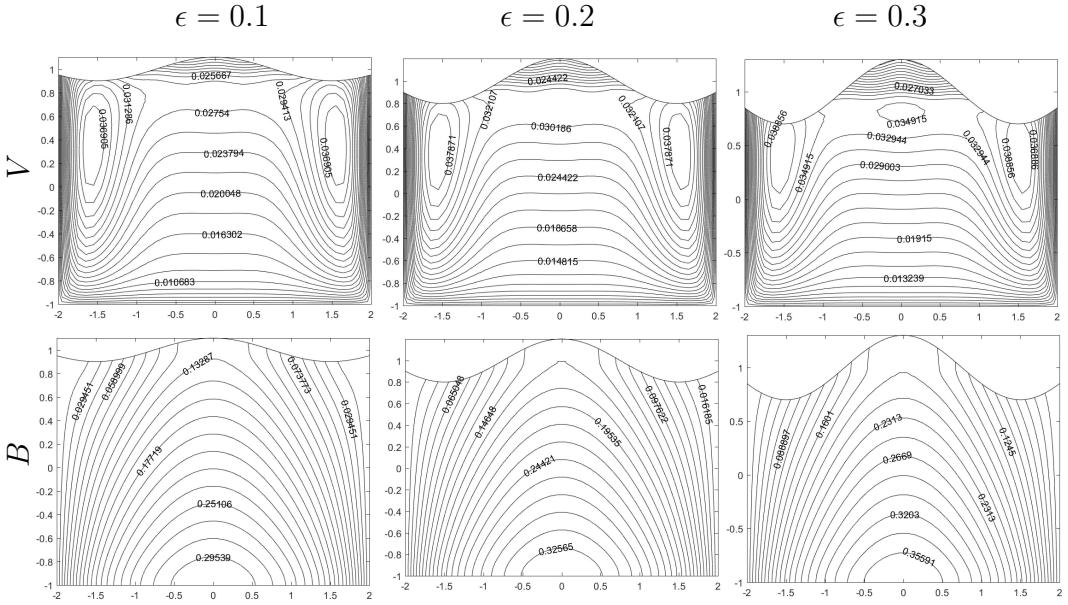


Figure 4.42: Problem 4. Velocity and induced magnetic field from inverse formulation, $Ha = 10$, $f(x) = -cos(\frac{2\pi x}{3})$, $f(r) = 1 + r$.

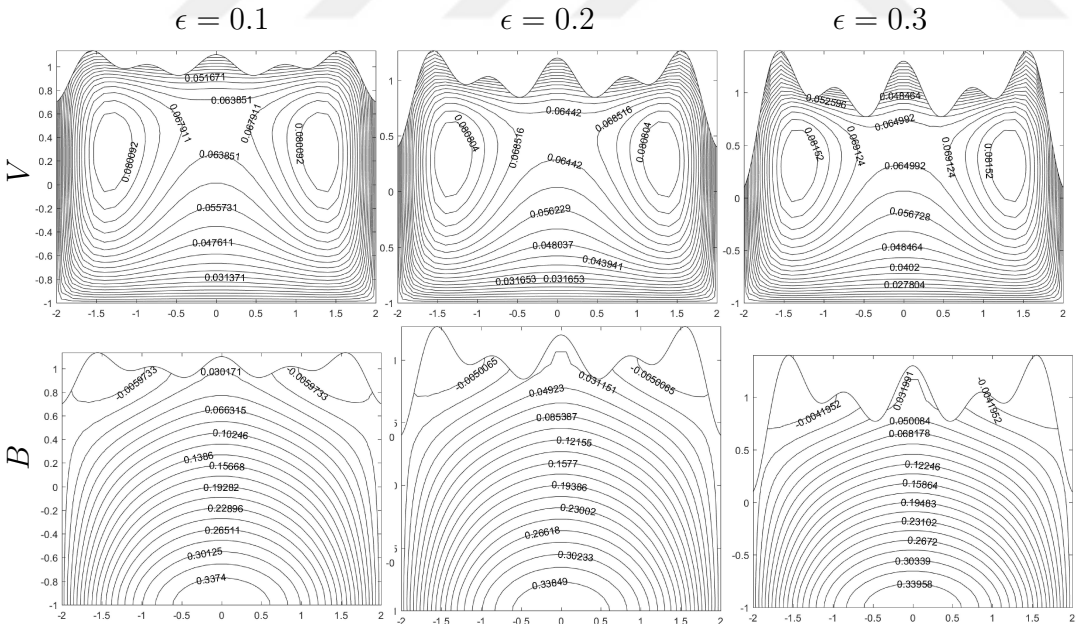


Figure 4.43: Problem 4. Velocity and induced magnetic field from direct problem, $Ha = 5$, $\alpha = 0.2$, $f(x) = -(1 - x^2)cos(2\pi x)$, $f(r) = 1 + r$.

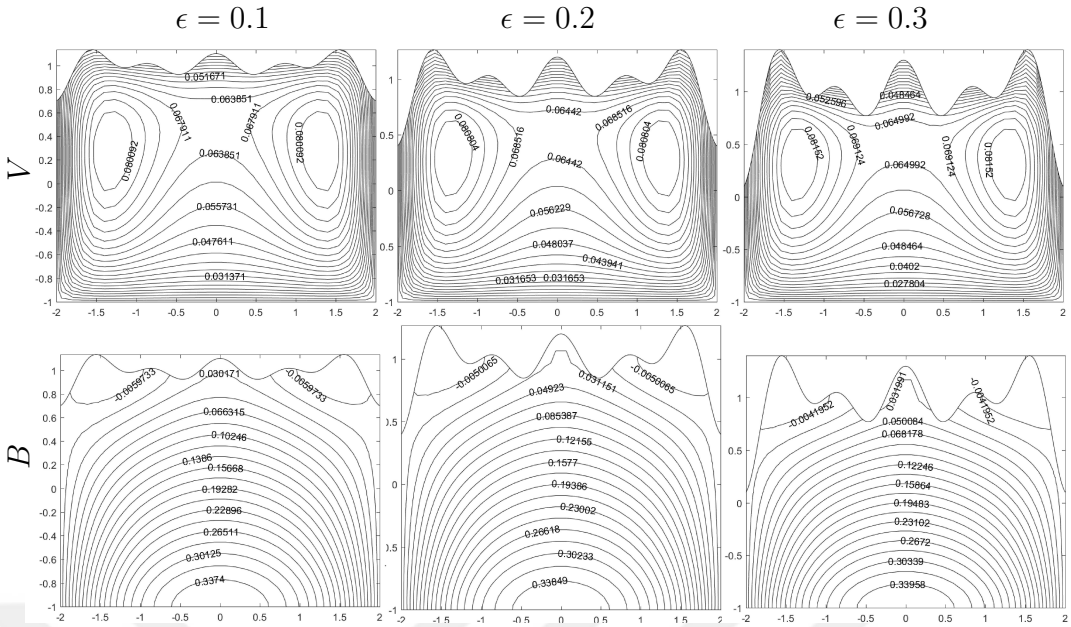


Figure 4.44: Problem 4. Velocity and induced magnetic field from inverse formulation, $Ha = 5$, $f(x) = -(1-x^2)cos(2\pi x)$, $f(r) = 1 + r$.

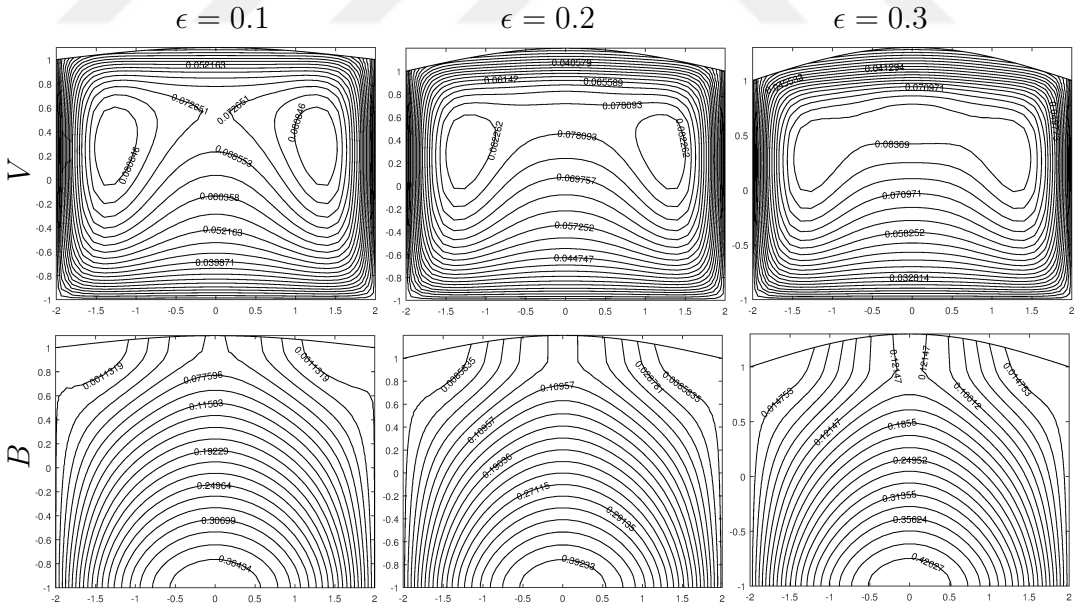


Figure 4.45: Problem 4. Velocity and induced magnetic field from direct problem, $Ha = 5$, $\alpha = 0.2$, $f(x) = -cos(\frac{\pi x}{4})$, $f(r) = 1 + r$.

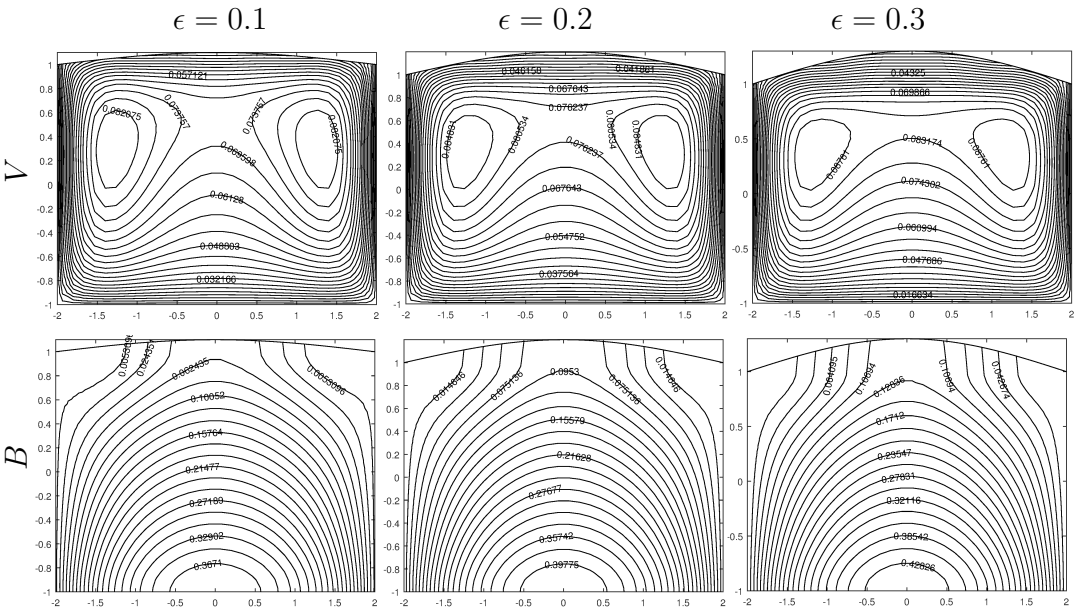


Figure 4.46: Velocity and induced magnetic field from inverse formulation, $Ha = 5$, $\alpha = 0.2$, $f(x) = -cos(\frac{\pi x}{4})$, $f(r) = 1 + r$.

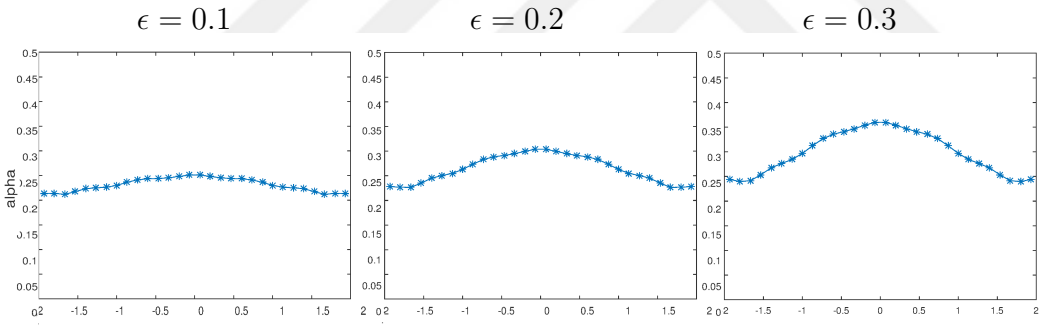


Figure 4.47: Reseized slip lengths, $Ha = 5$, $f(x) = -cos(\frac{2\pi x}{3})$

As Ha increases the flow is flattened as in the case of rectangular duct. Hartmann and side layers are formed on the horizontal and vertical sides, respectively. As ϵ increases, Hartmann layer on the upper curved boundary is completely squeezed to the region where the curve has its maximum. The increase in the perturbation parameter ϵ causes circulations of the flow close to the upper wall and in front of the side layers instead of the Hartmann layers as it is shown in Figures 4.41 and 4.42 for Ha=10. Figures 4.43 and 4.44 show the velocity and induced magnetic field obtained from

the direct and inverse formulations for $f(x) = -(1-x^2)cos(2\pi x)$ as a function in the perturbation on upperwall. It is seen that the behaviors are almost the same in the direct and inverse problem solutions. Similarly, in Figures 4.45 and 4.46, the similar behaviour of V and B in the direct and inverse solutions are obtained when $f(x)$ is taken as $f(x) = -cos(\frac{\pi x}{4})$.

Resized slip length on the slipping wall from the inverse formulations for Cauchy MHD duct flow can be computed through the relation $\alpha = -V/\frac{\partial V}{\partial n}$ where V and $\frac{\partial V}{\partial n}$ are obtained by employing both the DRBEM and asymptotic expansions technique. These are represented in Figure 4.47 in the case of $f(x) = -cos(\frac{2\pi x}{3})$.

It can be seen that despite of the variations at the centre points, $\alpha = 0.2$ is approached on the slipping and curved boundary when the Cauchy MHD flow problem is solved through the DRBEM and the asymptotic expansions technique where $\epsilon = 0.1$. When the perturbation parameter is increased to $\epsilon = 0.2$ and 0.3, the round off errors increase due to the interpolation in the region near the curved boundary.

4.3 Parameter Identification in MHD Duct Flow Cauchy Problem

In this section, the important parameter Hartmann number in the problem region is regained from the construction of the inverse MHD duct flow problem by employing the DRBEM for no-slip to slip and insulated to perfectly conducting duct walls in terms of five problems. The inverse problem for the MHD duct flow is formulated with the overspecified velocity values of the fluid and the induced magnetic field and their normal derivatives on each part of the boundary and some internal values of them obtained from the direct MHD duct flow problem through the DRBEM for a specified Ha value. Since the resulting DRBEM equations for the inverse MHD duct flow are ill-conditioned, the Tikhonov regularization is employed to solve the systems. The numerical results for the direct and inverse MHD duct flow are generally shown for Ha=5, 10 and 50. The regained Ha values are examined in terms of the convergence to the pre-defined Hartmann numbers.

We consider the two-dimensional, steady and fully developed MHD flow in a rectangular duct under the effect of an external, vertically applied magnetic field (Equations

(3.53)). The governing equations are solved for various types of wall conditions and presented as Problems 1, 2, 3, 4, and 5. The non-dimensional governing equations for the velocity $V(x, y)$ of the fluid and the induced magnetic field $B(x, y)$ in the domain Ω are [11]

$$\begin{aligned} \nabla^2 V + Ha\frac{\partial B}{\partial y} &= -1 \\ \nabla^2 B + Ha\frac{\partial V}{\partial y} &= 0 \end{aligned} \tag{4.9}$$

where $\Omega = \{(x, y) \in R : -1 < x, y < 1\}$ and Ha is the Hartmann number.

In the application of the DRBEM, $N = 100, 120, 160, 240$ constant boundary elements are taken for $Ha = 5, 10, 30, 50$ and as the interior nodes, the mesh from the intersection of boundary nodes is taken for both the direct and inverse problems for the solution of the MHD duct flow. For the inverse problem, to regain the Ha in the problem region, the equations (4.9) are solved in both the coupled and decoupled forms for each problem cases and the results are compared with each other. The regularization parameter λ is mostly found from the L-curve method (which are of order 10^{-7} or 10^{-8}), however, in the Problems 4 and 5, $\lambda = 0$ is taken since in this case, the L-curve gives very small value of order less than 10^{-10} in both solving the system in coupled or decoupled forms. The velocity and induced magnetic field profiles from the direct solution are presented for each boundary condition cases (Prob.1- Prob.5) for several values of problem parameters.

4.3.1 Parameter Identification - Problem 1

Firstly, the MHD duct flow problem is studied when each part of the duct wall is no-slip and insulated. Thus, the physical conformation of the channel walls leads the boundary conditions of the velocity and the induced magnetic field as

$$\begin{aligned} V &= 0, \qquad B = 0 \quad \text{on} \quad y = \mp 1, \quad -1 < x < 1 \\ V &= 0, \qquad B = 0 \quad \text{on} \quad x = \mp 1, \quad -1 < y < 1 \end{aligned} \tag{4.10}$$

First, the MHD problem (4.9)-(4.10) is going to be solved for a specified value of Ha through the DRBEM which gives the normal derivative values for V and B on each part of the boundary and the values for V and B at some selected interior nodes. Then, the inverse problem is constructed with V, B and their normal derivatives on the boundary and V, B at the interior points in the problem region to identify the Ha in the equation itself in the domain of the problem.

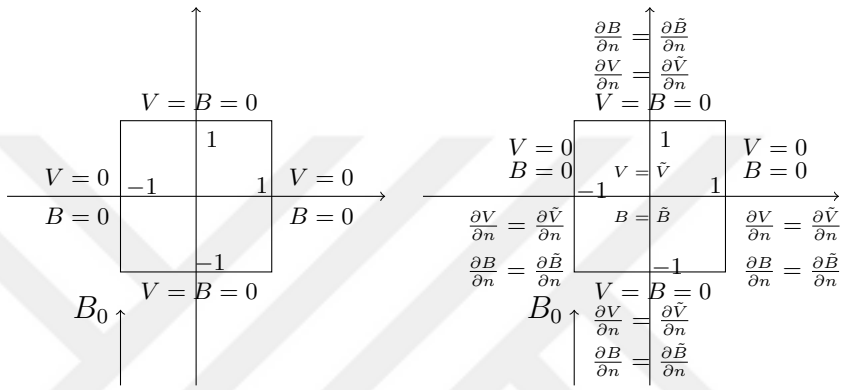


Figure 4.48: Parameter Identification - Problem 1: Boundary conditions for the direct (left) and the inverse (right) problems.

Here, $\tilde{V}$ and $\tilde{B}$ denote the velocity of the fluid and induced magnetic field obtained from the direct formulation through the DRBEM.

The velocity and induced magnetic field contours for Ha=5, 10, and 50 are given in Figure 4.49 obtained from the direct problem solution when all parts of the duct boundary are no-slip and insulated walls. As it is seen from this figure, an increase in the Hartmann number leads to Hartmann layers on the horizontal walls and side layers on the vertical walls. When Hartmann number increases to Ha=50, the fluid becomes stagnant, the core region enlarges and the flow is flattened (velocity magnitude drops). Induced magnetic field seperates into two antisymmetric loops with respect to the x-axis and develops also boundary layers on the Hartmann walls as Ha increases.

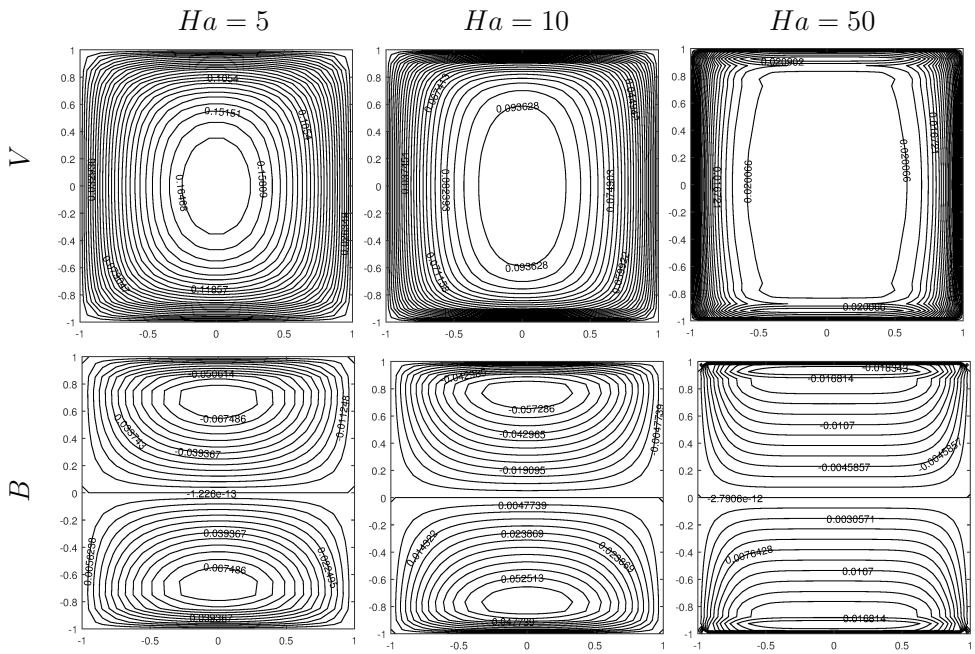


Figure 4.49: Parameter Identification - Problem 1: Velocity and induced magnetic fiel, $\alpha = c = 0$ (direct solution).

Table 4.2: Parameter Identification - Problem 1: The maximum errors in Ha, $\alpha = c = 0$.

	Coupled		Decoupled	
Ha	e_1	e_2	e_1	e_2
5	6.2×10^{-5}	2.3×10^{-7}	4.1×10^{-5}	3.4×10^{-5}
10	1.3×10^{-2}	3.5×10^{-6}	2.1×10^{-4}	0.7×10^{-4}
30	2.2×10^{-2}	2.6×10^{-6}	7.8×10^{-4}	1.5×10^{-4}
50	2.4×10^{-2}	5.4×10^{-6}	0.1×10^{-2}	1.1×10^{-4}

In Table 4.2, the maximum errors in Hartmann number identified from the inverse problem are given. The maximum error is defined as $e_1 = \max_i |Ha_i - Ha_{1_i}|$ and $e_2 = \max_i |Ha_i - Ha_{2_i}|$ where $N+1 \leq i \leq N+L$ and Ha is the specified Hartmann number which is used in the direct formulation of the MHD duct flow problem.

As Ha increases, the inverse problem regains the Hartmann number with almost the same accuracy when the system is solved in coupled or decoupled form. Interior Ha values obtained from the second half of the unknown vector $[Ha_2]$ show better accuracy.

4.3.2 Parameter Identification - Problem 2

Here, the top and bottom walls are perfectly conducting while other parts are insulated and no-slip walls as given in (4.11) and Figure 4.49.

$$\begin{aligned} &V = 0, && \frac{\partial B}{\partial n} = 0 \quad \text{on} \quad y = \mp 1, \quad -1 < x < 1 \\ &V = 0, && B = 0 \quad \text{on} \quad x = \mp 1, \quad -1 < y < 1. \end{aligned} \tag{4.11}$$

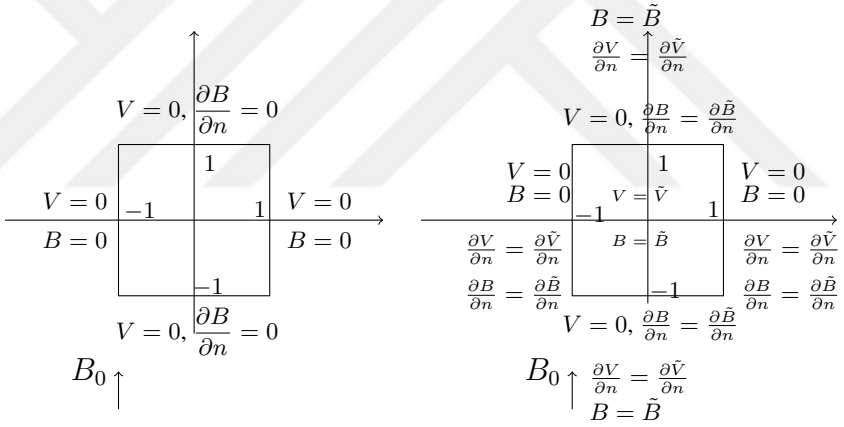


Figure 4.50: Problem 2: Boundary conditions for the direct (left) and the inverse (right) problems.

In Figure 4.51 below, the behaviours of V and B are investigated for increasing values of Ha. As in the Problem 1, the Hartmann layers and side layers occur on the horizontal and vertical walls, respectively when Ha increases. In addition, the fluid tends to be divided into two symmetric parts towards to the side layers with the effect of perfecly conducting top and bottom walls when Ha=10 or 50 is taken.

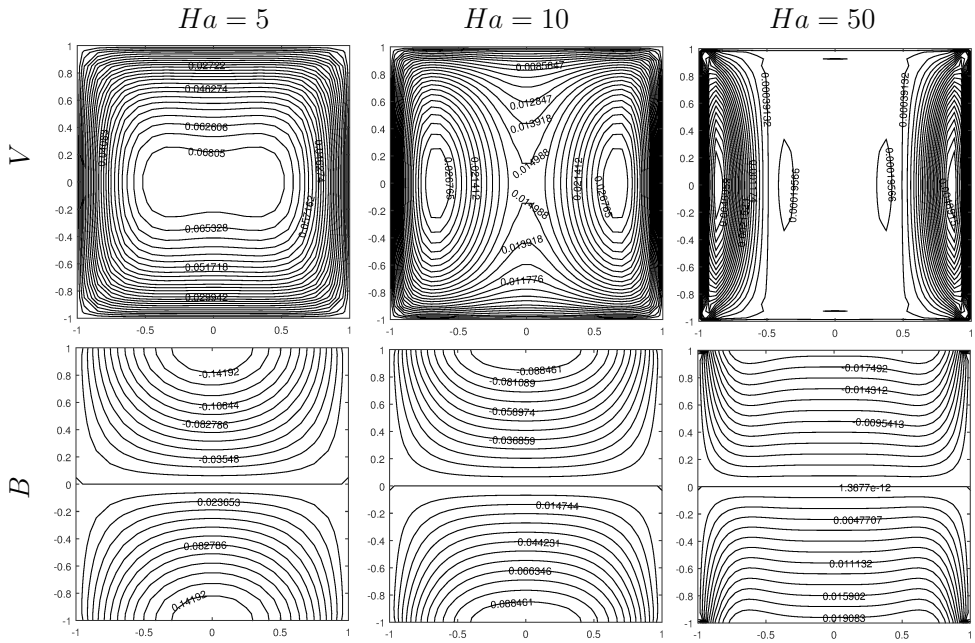


Figure 4.51: Parameter Identification - Problem 2: Velocity and induced magnetic field, $\alpha = 0$, c is large on the Hartmann walls(direct solution).

The maximum errors in Ha values obtained from the inverse problem are given in the Table 4.3.

Table 4.3: Parameter Identification - Problem 2: The maximum errors in Ha, $\alpha = 0$, c is large on Hartmann walls.

	Coupled		Decoupled	
Ha	e_1	e_2	e_1	e_2
5	4.3×10^{-4}	1.6×10^{-4}	1.1×10^{-4}	3.3×10^{-5}
10	5.1×10^{-5}	1.9×10^{-7}	2.1×10^{-4}	4×10^{-5}
30	5×10^{-4}	1.7×10^{-6}	3.34	1.5×10^{-6}
50	3.61	9×10^{-1}	1.1×10^{-2}	1.6×10^{-5}

In this case of boundary conditions, Ha is still obtained back with almost the same accuracy from the second parts of the solution vectors of the coupled and decoupled DRBEM systems. However, in the coupled form of the inverse DRBEM system, the

accuracy drops when $Ha = 50$.

4.3.3 Parameter Identification - Problem 3

In this problem, all parts of the duct boundary are no-slip and variably conducting as given in (4.12) and Figure 4.51

$$\begin{aligned} &V = 0, && B + c\frac{\partial B}{\partial n} = 0 && \text{on} \quad y = \mp 1, \quad -1 < x < 1 \\ &V = 0, && B + c\frac{\partial B}{\partial n} = 0, && \text{on} \quad x = \mp 1, \quad -1 < y < 1 \end{aligned} \tag{4.12}$$

where c is the conductivity constant.

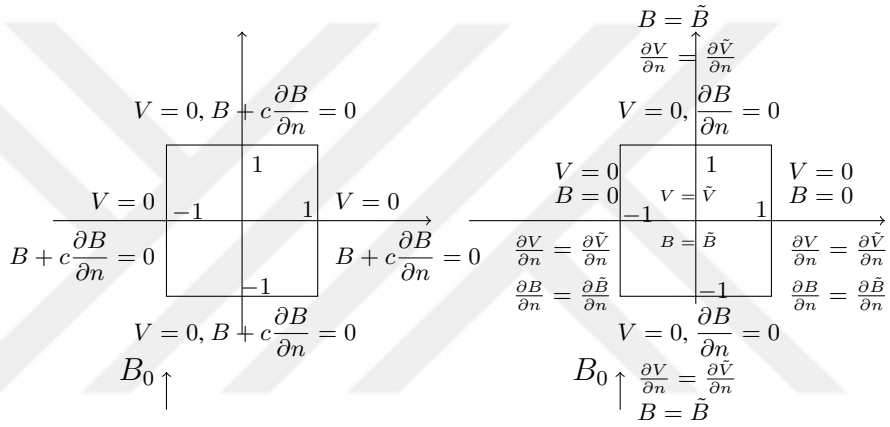


Figure 4.52: Problem 3: Boundary conditions for the direct (left) and the inverse (right) problems.

In Figure 4.53, the velocity V of the fluid and the induced magnetic field B are shown for increasing values of conductivity constant c by keeping Hartmann number $Ha = 10$ fixed for no-slip but variably conducting duct walls. It is observed that the fluid tends to be divided into two bunches at the center of the duct and its velocity magnitude drops when the conductivity parameter c increases. Induced current still develops two antisymmetric loops with respect to the x-axis but its contours are forced to become orthogonal to the walls due to the variably conducting boundary conditions. When c is increasing, the two current loops are connected at the center as straight lines directly orthogonal to the side walls. A slight magnitude increase is observed in the induced current as c increases. The maximum errors between the

regained Ha from the inverse problem and the actual Ha used in the direct problem are given in the tables, Table 4.4 - Table 4.7 for $c = 0.3, c = 1, 2$ and 5, respectively.

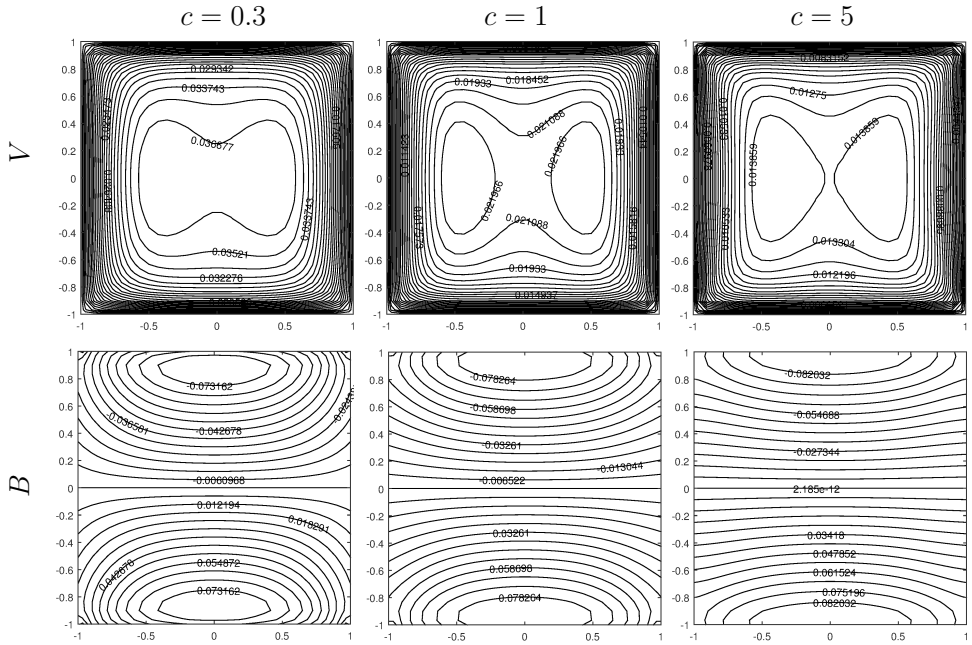


Figure 4.53: Parameter Identification - Problem 3: Velocity and induced magnetic field for $Ha = 10$, $\alpha = 0$ (direct solution).

Table 4.4: The maximum errors in Ha, $\alpha = 0$, $c = 0.3$ Prob. 3

	Coupled		Decoupled	
Ha	e_1	e_2	e_1	e_2
5	5.4×10^{-6}	3.8×10^{-8}	9.8×10^{-2}	2.6×10^{-5}
10	9.9×10^{-2}	1.5×10^{-4}	1×10^{-1}	3.1×10^{-5}
30	8×10^{-1}	6×10^{-2}	6×10^{-1}	5.6×10^{-5}
50	1.22	1×10^{-1}	9.2×10^{-5}	5.5×10^{-5}

Table 4.5: Parameter Identification - Problem 3: The maximum errors in Ha, $\alpha = 0$, $c = 1$.

	Coupled		Decoupled	
Ha	e_1	e_2	e_1	e_2
5	0.1319	0.0117	9.5×10^{-2}	2.9×10^{-5}
10	0.2263	0.1211	0.1398	5.2×10^{-5}
30	0.6723	0.9582	0.5251	5.2×10^{-5}
50	0.0303	0.0089	4.9×10^{-5}	0.6396

Table 4.6: Parameter Identification - Problem 3: The maximum errors in Ha, $\alpha = 0$, $c = 2$.

	Coupled		Decoupled	
Ha	e_1	e_2	e_1	e_2
5	0.0072	7.3×10^{-4}	9.1×10^{-2}	2.2×10^{-5}
10	0.0199	0.0060	0.1206	3.9×10^{-5}
30	0.1622	0.11	0.5368	6.1×10^{-5}
50	0.3947	0.2894	5.1×10^{-5}	0.9074

Table 4.7: Parameter Identification - Problem 3: The maximum errors in Ha, $\alpha = 0$, $c = 5$.

	Coupled		Decoupled	
Ha	e_1	e_2	e_1	e_2
5	0.0072	7.3×10^{-4}	9.1×10^{-2}	2.2×10^{-5}
10	3.1×10^{-5}	1.9×10^{-5}	8.8×10^{-6}	4.3×10^{-5}
30	0.3386	0.6406	0.5038	8×10^{-5}
50	0.2397	0.5360	0.8206	8.4×10^{-5}

For all the variably conducting walls, the accuracy in obtaining the Ha back is better when the system is solved in the decoupled form compared to the solution accuracy obtained from coupled form.

4.3.4 Parameter Identification - Problem 4

In this problem, all the walls are assumed to be slip and insulated as shown in (4.13) and Figure 4.53.

$$\begin{aligned} V + \alpha \frac{\partial V}{\partial n} = 0, \qquad & B = 0 \quad \text{on} \quad y = \mp 1, \quad -1 < x < 1 \\ V + \alpha \frac{\partial V}{\partial n} = 0, \qquad & B = 0 \quad \text{on} \quad x = \mp 1, \quad -1 < y < 1 \end{aligned} \tag{4.13}$$

where α is the slip length.

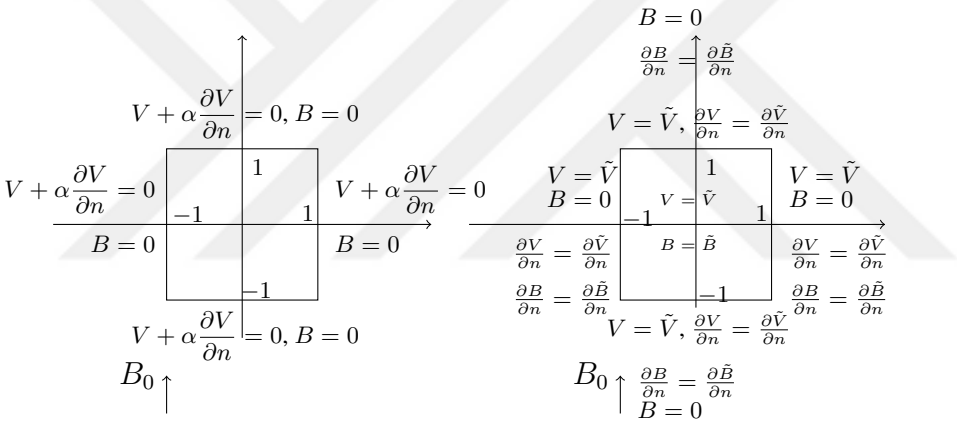


Figure 4.54: Problem 4: Boundary conditions for the direct (left) and the inverse (right) problems.

In the Figure 4.55, the velocity and induced magnetic field behaviors are shown for the slipping and insulated duct walls for $\alpha = 0.1, 0.2$, and 0.3 for a fixed value of $Ha = 10$. It is observed that when the slip length α increases, the magnitude of V increases.

When all the walls are slipping but insulated, we need to give $\lambda = 0$ instead of finding it from the L-curve method in both solving the system in coupled or decoupled forms. However, the accuracy is of order at least 10^{-6} which is better than the accuracies

obtained in problems 1,2 and 3. The accuracies for regained Ha are given in Table 4.8. Also, the first and the second halves of the unknown vector provide Ha with the same accuracy about 10^{-6}.

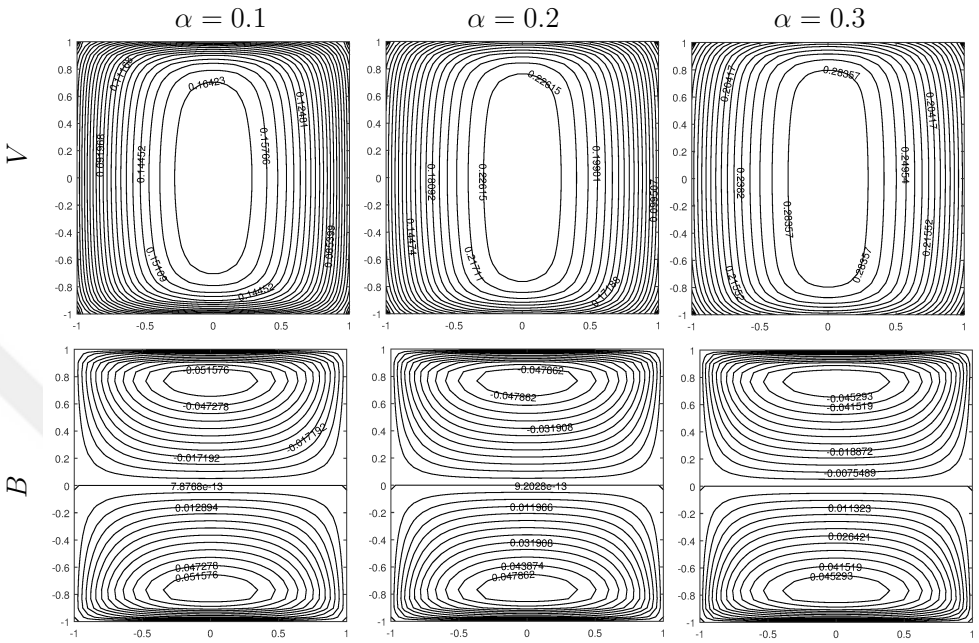


Figure 4.55: Parameter Identification - Problem 4: Velocity and induced magnetic field for $Ha = 10$, $c = 0$ (direct solution).

Table 4.8: Parameter Identification - Problem 4: The maximum errors in Ha, $\alpha = 0.2$, $c = 0$.

	Coupled		Decoupled	
Ha	e_1	e_2	e_1	e_2
5	1×10^{-7}	3.3×10^{-7}	1.2×10^{-7}	3.3×10^{-7}
10	4.4×10^{-8}	2×10^{-7}	4.4×10^{-8}	2×10^{-7}
30	9.1×10^{-7}	1.5×10^{-6}	7.9×10^{-7}	1.5×10^{-6}
50	1.2×10^{-7}	5.4×10^{-7}	1.2×10^{-7}	5.4×10^{-7}

4.3.5 Parameter Identification - Problem 5

Here, all the walls are both slipping and variably conducting as given in (4.14) and Figure 4.55

$$\begin{aligned} V+\alpha\frac{\partial V}{\partial n}=0, \qquad & B+c\frac{\partial B}{\partial n}=0 \quad \text{on} \quad y=\mp 1, \quad -1<x<1 \\ V+\alpha\frac{\partial V}{\partial n}=0, \qquad & B+c\frac{\partial B}{\partial n}=0 \quad \text{on} \quad x=\mp 1, \quad -1<y<1 \end{aligned} \tag{4.14}$$

where α is the slip length and c is the conductivity constant.

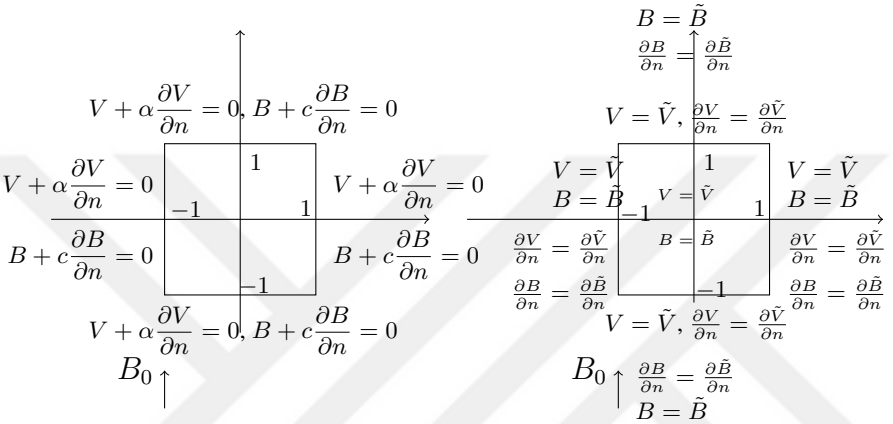


Figure 4.56: Problem 5: Boundary conditions for the direct (left) and the inverse (right) problems.

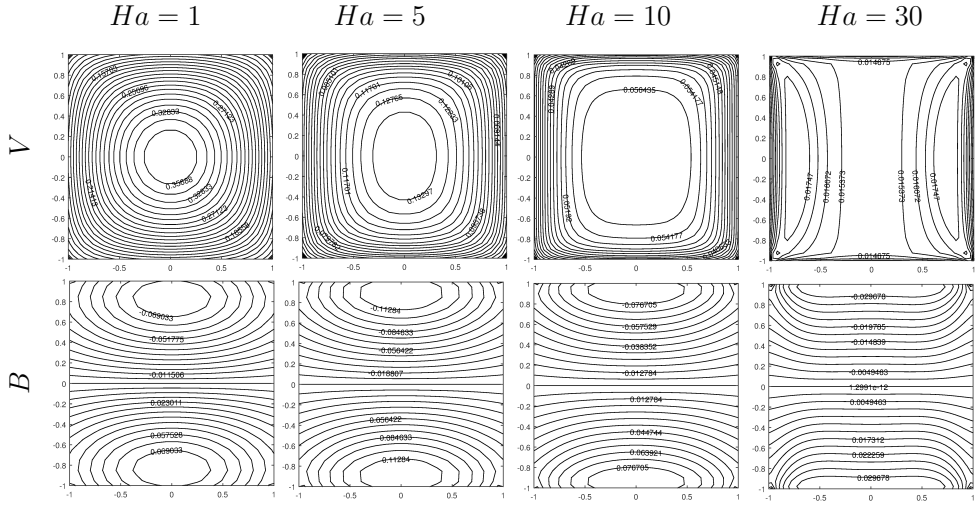


Figure 4.57: Parameter Identification - Problem 5: Velocity and induced magnetic field profiles, $\alpha=0.2$, $c=1$.

The velocity and induced magnetic field contours are shown in Figure 4.57 for increasing number of Ha and for the slip length $\alpha = 0.2$ and conductivity constant $c = 1$.

Table 4.9: Parameter Identification - Problem 5: The maximum errors in Ha, $\alpha = 0.2$, $c = 5$.

	Coupled		Decoupled	
Ha	e_1	e_2	e_1	e_2
5	1.01×10^{-7}	2.42×10^{-8}	9.97×10^{-8}	2.4×10^{-8}
10	8.8×10^{-7}	4.9×10^{-7}	9.54×10^{-7}	4.97×10^{-7}
30	1.52×10^{-5}	2.5×10^{-6}	1.48×10^{-5}	2.5×10^{-6}
50	3.82×10^{-6}	5.88×10^{-6}	3.73×10^{-6}	5.8×10^{-6}

In Table 4.9, the maximum errors are shown in the Ha values regained from the inverse MHD duct flow problem. When both the slip and conductivity conditions are in the most general form, Ha is obtained back with an accuracy of at least 10^{-5} from the coupled system and from the both half of the unknown vector when the regularization parameter λ is taken as $\lambda = 0$ instead of finding it from the L-curve method.

In Chapter 4, the numerical results of the direct and Cauchy MHD flow equations in a duct are presented for slip velocity and variably conducting induced magnetic field through the DRBEM. The numerical results are obtained for the two kinds of inverse problems namely, the boundary type inverse problem in Section 4.1 including externally applied oblique magnetic field, in Section 4.2 for a perturbed upper wall duct, and parameter identification MHD flow problems in Section 4.3 for obtaining Ha back. The obtained numerical results are represented in terms of equivelocity and current lines, and regained Hartmann number values are tabulated for slipping and variably conducting duct walls.

CHAPTER 5

CONCLUSION

This thesis provides the Dual Reciprocity Boundary Element Method solution of the direct and inverse formulations of the MHD duct flow problems. The two-dimensional, steady flow of a viscous, incompressible, and electrically conducting fluid is considered under the effect of an externally applied magnetic field for all the problems in the thesis. The MHD duct flow equations are accompanied by the duct wall conditions ranging from the no-slip to slip and insulated to perfectly conducting. Two types of inverse problems which are boundary inverse problems and parameter identification are considered in the construction of Cauchy MHD duct flow. While the boundary inverse problems are constructed to regain the slip length on the slipping part of the boundary, in the parameter identification, the aim is to recompute the Hartmann number in the problem region. Due to the ill-posedness of the Cauchy problems resulting from the incomplete boundary informations, three regularization techniques, namely Tikhonov regularization, the direct-inverse iterations, and the well-posed iterations are used with the DRBEM for obtaining the solution of the Cauchy MHD flow in a duct.

The DRBEM is carried for the MHD rectangular duct flow equations by using the fundamental solution of Laplace equation. The inhomogeneities are generally approximated by using the polynomial basis function as $f = 1 + r$. On the other hand, in some problems considered in the thesis, $f = 1 + r + r^2$ and $f = r^2 lnr$ are also used. However, since there is no significant difference between the solutions obtained from the DRBEM by using these three types radial basis functions and due to the less computational cost, most of the computations are carried with $f = 1 + r$.

The DRBEM solutions of the direct and inverse formulations of the MHD flow with

slipping and variably conducting duct walls (which are explained as Problems 1-3) are obtained first for Hartmann number values up to 50 for both insulated and conducting duct walls by taking the conductivities as $k = 0$ and $k = 1$ for vertical walls. Then, the Cauchy MHD flow problem is considered in a duct with a perturbed slipping upper boundary (Problem 4) for $Ha \leq 50$ and the upper boundary is defined as $1 - \epsilon f(x)$ where ϵ is the perturbation parameter and $f(x)$ is an arbitrary function. In this problem, the asymptotic expansions are used to get the solution instead of discretizing the curved part of the boundary. This technique provides elimination of the difficulties in discretization of the curved boundary. In these problems, an increase in the Hartmann number value leads to Hartmann layers on the Hartmann walls and side layers on the side walls. However, the slip effect weakens the formation of boundary layers. When the three regularization techniques used in the solution of inverse problems are compared, it is observed that the velocity and induced magnetic field magnitudes are in a very well accordance. Also, the regained slip length and conductivity constant values are almost the same with the values used in the preassigned velocity and induced magnetic field with an accuracy of order 10^{-5} to 10^{-6}.

Lastly, the important MHD problem parameter, Hartmann number, is regained in the problem region by constructing the inverse MHD duct flow in terms of parameter identification problem for no-slip to slip and insulated to perfectly conducting duct walls (Problems 1-5). In the solution of inverse problems, the Tikhonov regularization is used to solve the resulting DRBEM discretized system. The numerical results are mostly given for $Ha = 5, 10, 30, 50$ by taking the number of constant boundary elements as $N = 100, 120, 160, 240$. The regained Hartmann number values are examined in terms of the convergence to the pre-defined Hartmann numbers, and it is observed that they are obtained with an accuracy of order 10^{-4} to 10^{-7}. In future studies, for both the boundary inverse and parameter identification inverse problems, noise should be added to the overspecified boundary conditions obtained from the direct problem solutions in the construction of inverse formulations.

The DRBEM is a suitable numerical method for the Cauchy MHD flow problems, since it gives both the unknown itself and its normal derivative at the same time on the duct walls. In addition, the DRBEM enables us to discretize only the boundary of the domain giving the solution of the problem with a low computational cost.

REFERENCES

[1] C. A. Brebbia, *The Boundary Element Method for Engineers*. WIT Press, 1980.

[2] C. A. Brebbia and J. Dominguez, *Boundary Elements: An Introductory Course*. WIT press, 1994.

[3] C. A. Brebbia, J. C. F. Telles, and L. C. Wrobel, *Boundary Element Techniques: Theory and Applications in Engineering*. Springer Science & Business Media, 2012.

[4] P. K. Banerjee and R. Butterfield, *Boundary Element Methods in Engineering Science*, vol. 17. McGraw-Hill London, 1981.

[5] P. W. Patridge, C. A. Brebbia, and L. C. Wrobel, *The Dual Reciprocity Boundary Element Method*. Computational Mechanics Publications, Elsevier Science, 1992.

[6] D. Nardini and C. Brebbia, "A new approach to free vibration analysis using boundary elements," *Applied Mathematical Modelling*, vol. 7, no. 3, pp. 157–162, 1983.

[7] P. Partridge and C. Brebbia, "Computer implementation of the bem dual reciprocity method for the solution of general field equations," *Communications in Applied Numerical Methods*, vol. 6, no. 2, pp. 83–92, 1990.

[8] P. W. Partridge and L. C. Wrobel, "The dual reciprocity boundary element method for spontaneous ignition," *International Journal for Numerical Methods in Engineering*, vol. 30, no. 5, pp. 953–963, 1990.

[9] M. Tezer-Sezgin, "Boundary element method solution of mhd flow in a rectangular duct," *International Journal for Numerical Methods in Fluids*, vol. 18, no. 10, pp. 937–952, 1994.

[10] N. Alsoy-Akgun, "The dual reciprocity boundary element solution of helmholtz-type equations in fluid dynamics," *Ph.D. Thesis, METU*, 2013.

[11] L. Dragos, *Magnetofluid Dynamics*. 1975.

[12] J. Shercliff, "Steady motion of conducting fluids in pipes under transverse magnetic fields," in *Mathematical Proceedings of the Cambridge Philosophical Society*, vol. 49, pp. 136–144, Cambridge University Press, 1953.

[13] S. Smolentsev, "Mhd duct flows under hydrodynamic "slip" condition," *Theoretical and Computational Fluid Dynamics*, vol. 23, no. 6, p. 557, 2009.

[14] J. Liģere, I. Dzenīte, and A. Matvejevs, "Analytical solution to a problem on mhd flow in a rectangular duct under slip condition on its side walls," *20th International Conference on Mathematical Modelling and Analysis*, pp. 44–44, 2015.

[15] H. Alfvén, "Existence of electromagnetic-hydrodynamic waves," *Nature*, vol. 150, no. 3805, p. 405, 1942.

[16] U. Müller and L. Bühler, *Magnetofluiddynamics in Channels and Containers*. Springer Science & Business Media, 2013.

[17] C. C. Chang and T. S. Lundgren, "Duct flow in magnetohydrodynamics," *Zeitschrift für Angewandte Mathematik und Physik ZAMP*, vol. 12, no. 2, pp. 100–114, 1961.

[18] R. R. Gold, "Magnetohydrodynamic pipe flow. part 1," *Journal of Fluid Mechanics*, vol. 13, no. 4, pp. 505–512, 1962.

[19] J. Hunt, "Magnetohydrodynamic flow in rectangular ducts," *Journal of Fluid Mechanics*, vol. 21, no. 4, pp. 577–590, 1965.

[20] B. Singh and J. Lal, "Magnetohydrodynamic axial flow in a triangular pipe under transverse magnetic field," *Indian J. Pure Appl. Math*, vol. 9, pp. 101–115, 1978.

[21] B. Singh and J. Lal, "Mhd axial-flow in a triangular pipe under transverse magnetic-field parallel to a side of the triangle," *Indian Journal of Technology*, vol. 17, no. 5, pp. 184–189, 1979.

[22] B. Singh and J. Lal, "Finite element method in magnetohydrodynamic channel flow problems," *International Journal for Numerical Methods in Engineering*, vol. 18, no. 7, pp. 1104–1111, 1982.

[23] B. Singh and J. Lal, "Heat transfer for mhd flow through a rectangular pipe with discontinuity in wall temperatures," *International Journal of Heat and Mass Transfer*, vol. 25, no. 10, pp. 1523–1529, 1982.

[24] B. Singh and J. Lal, "Finite element method for unsteady mhd flow through pipes with arbitrary wall conductivity," *International Journal for Numerical Methods in Fluids*, vol. 4, no. 3, pp. 291–302, 1984.

[25] G. Yagawa and M. Masuda, "Finite element analysis of magnetohydrodynamics and its application to lithium blanket design of a fusion reactor," *Nuclear Engineering and Design*, vol. 71, no. 1, pp. 121–136, 1982.

[26] J. Ramos and N. Winowich, "Finite difference and finite element methods for mhd channel flows," *International Journal for Numerical Methods in Fluids*, vol. 11, no. 6, pp. 907–934, 1990.

[27] T. Hua and J. Walker, "Three-dimensional mhd flow in insulating circular ducts in non-uniform transverse magnetic fields," *International Journal of Engineering Science*, vol. 27, no. 9, pp. 1079–1091, 1989.

[28] A. Sterl, "Numerical simulation of liquid-metal mhd flows in rectangular ducts," *Journal of Fluid Mechanics*, vol. 216, pp. 161–191, 1990.

[29] L. Gardner and G. Gardner, "A two dimensional bi-cubic b-spline finite element: used in a study of mhd-duct flow," *Computer Methods in Applied Mechanics and Engineering*, vol. 124, no. 4, pp. 365–375, 1995.

[30] M. Tezer-Sezgin and S. Köksal, "Finite element method for solving mhd flow in a rectangular duct," *International Journal for Numerical Methods in Engineering*, vol. 28, no. 2, pp. 445–459, 1989.

[31] Z. Demendy and T. Nagy, "A new algorithm for solution of equations of mhd channel flows at moderate hartmann numbers," *Acta Mechanica*, vol. 123, no. 1-4, pp. 135–149, 1997.

[32] A. Meir, "Finite element analysis of magnetohydrodynamic pipe flow," *Applied Mathematics and Computation*, vol. 57, no. 2-3, pp. 177–196, 1993.

[33] K. Barrett, "Duct flow with a transverse magnetic field at high hartmann numbers," *International Journal for Numerical Methods in Engineering*, vol. 50, no. 8, pp. 1893–1906, 2001.

[34] F. Shakeri and M. Dehghan, "A finite volume spectral element method for solving magnetohydrodynamic (mhd) equations," *Applied Numerical Mathematics*, vol. 61, no. 1, pp. 1–23, 2011.

[35] A. I. Nesliturk and M. Tezer-Sezgin, "The finite element method for mhd flow at high hartmann numbers," *Computer Methods in Applied Mechanics and Engineering*, vol. 194, no. 9-11, pp. 1201–1224, 2005.

[36] A. Nesliturk and M. Tezer-Sezgin, "Finite element method solution of electrically driven magnetohydrodynamic flow," *Journal of Computational and Applied Mathematics*, vol. 192, no. 2, pp. 339–352, 2006.

[37] M. Sezgin, "Magnetohydrodynamic flow in a rectangular duct," *International Journal for Numerical Methods in Fluids*, vol. 7, no. 7, pp. 697–718, 1987.

[38] B. Singh and P. Agarwal, "Numerical solution of a singular integral equation appearing in magnetohydrodynamics," *Zeitschrift für Angewandte Mathematik und Physik ZAMP*, vol. 35, no. 6, pp. 760–770, 1984.

[39] A. Carabineanu, A. Dinu, and I. Oprea, "The application of the boundary element method to the magnetohydrodynamic duct flow," *Zeitschrift für Angewandte Mathematik und Physik ZAMP*, vol. 46, no. 6, pp. 971–981, 1995.

[40] M. Tezer-Sezgin and S. H. Aydın, "Solution of magnetohydrodynamic flow problems using the boundary element method," *Engineering Analysis with Boundary Elements*, vol. 30, no. 5, pp. 411–418, 2006.

[41] C. Bozkaya and M. Tezer-Sezgin, "Fundamental solution for coupled magnetohydrodynamic flow equations," *Journal of Computational and Applied Mathematics*, vol. 203, no. 1, pp. 125–144, 2007.

[42] M. Tezer-Sezgin and C. Bozkaya, "Boundary element method solution of magnetohydrodynamic flow in a rectangular duct with conducting walls parallel to applied magnetic field," *Computational Mechanics*, vol. 41, no. 6, pp. 769–775, 2008.

[43] M. Tezer-Sezgin and S. H. Aydin, "Dual reciprocity boundary element method for magnetohydrodynamic flow using radial basis functions," *International Journal of Computational Fluid Dynamics*, vol. 16, no. 1, pp. 49–63, 2002.

[44] N. Bozkaya and M. Tezer-Sezgin, "The drbem solution of incompressible mhd flow equations," *International Journal for Numerical Methods in Fluids*, vol. 67, no. 10, pp. 1264–1282, 2011.

[45] S. H. Aydın and M. Tezer-Sezgin, "A drbem solution for mhd pipe flow in a conducting medium," *Journal of Computational and Applied Mathematics*, vol. 259, pp. 720–729, 2014.

[46] B. Pekmen and M. Tezer-Sezgin, "Drbem solution of incompressible mhd flow with magnetic potential," *Comput. Model. Eng. Sci*, vol. 96, no. 4, pp. 275–292, 2013.

[47] B. Pekmen and M. Tezer-Sezgin, "Drbem solution of mhd flow with magnetic induction and heat transfer," *CMES: Computer Modeling in Engineering & Sciences*, vol. 105, no. 3, pp. 183–207, 2015.

[48] H. Fendoğlu, C. Bozkaya, and M. Tezer-Sezgin, "Mhd flow in a rectangular duct with a perturbed boundary," *Computers & Mathematics with Applications*, vol. 77, no. 2, pp. 374–388, 2019.

[49] A. A. Darhuber and S. M. Troian, "Principles of microfluidic actuation by modulation of surface stresses," *Annu. Rev. Fluid Mech.*, vol. 37, pp. 425–455, 2005.

[50] M. Rivero and S. Cuevas, "Analysis of the slip condition in magnetohydrodynamic (mhd) micropumps," *Sensors and Actuators B: Chemical*, vol. 166, pp. 884–892, 2012.

[51] R. Peyret, *Spectral Methods for Incompressible Viscous Flow*. Springer Science & Business Media, 2013.

[52] O. D. Makinde and T. Chinyoka, "Mhd transient flows and heat transfer of dusty fluid in a channel with variable physical properties and navier slip condition," *Computers & Mathematics with Applications*, vol. 60, no. 3, pp. 660–669, 2010.

[53] P. Senel and M. Tezer-Sezgin, "Mhd flow in a circular pipe with arbitrarily conducting slipping walls," in *Journal of Physics: Conference Series*, vol. 1141, p. 012033, IOP Publishing, 2018.

[54] P. Senel and M. Tezer-Sezgin, "Drbem solution to mhd flow in ducts with thin slipping side walls and separated by conducting thick hartmann walls," *Computers & Mathematics with Applications*, 2019.

[55] M. Tezer-Sezgin and P. Senel, "Electrically driven mhd flow between two parallel slipping and partly conducting infinite plates," in *European Conference on Numerical Mathematics and Advanced Applications*, pp. 849–858, Springer, 2017.

[56] J. Hadamard, *Lectures on Cauchy's Problem in Linear Partial Differential Equations*. Courier Corporation, 2003.

[57] C. Aydin and M. Tezer-Sezgin, "Drbem solution of the cauchy mhd duct flow with a slipping perturbed boundary," *Engineering Analysis with Boundary Elements*, vol. 93, pp. 94–104, 2018.

[58] M. R. Bai, "Application of bem (boundary element method)-based acoustic holography to radiation analysis of sound sources with arbitrarily shaped geometries," *The Journal of the Acoustical Society of America*, vol. 92, no. 1, pp. 533–549, 1992.

[59] B.-K. Kim and J.-G. Ih, "On the reconstruction of the vibro-acoustic field over the surface enclosing an interior space using the boundary element method," *The Journal of the Acoustical Society of America*, vol. 100, no. 5, pp. 3003–3016, 1996.

[60] L. Marin, L. Elliott, P. Heggs, D. Ingham, D. Lesnic, and X. Wen, "An alternating iterative algorithm for the cauchy problem associated to the helmholtz equation," *Computer Methods in Applied Mechanics and Engineering*, vol. 192, no. 5-6, pp. 709–722, 2003.

[61] L. Marin, L. Elliott, P. Heggs, D. Ingham, D. Lesnic, and X. Wen, "Conjugate gradient-boundary element solution to the cauchy problem for helmholtz-type equations," *Computational Mechanics*, vol. 31, no. 3-4, pp. 367–377, 2003.

[62] L. Marin, L. Elliott, P. Heggs, D. Ingham, D. Lesnic, and X. Wen, "Comparison of regularization methods for solving the cauchy problem associated with the helmholtz equation," *International Journal for Numerical Methods in Engineering*, vol. 60, no. 11, pp. 1933–1947, 2004.

[63] L. Marin, L. Elliott, P. Heggs, D. Ingham, D. Lesnic, and X. Wen, "Bem solution for the cauchy problem associated with helmholtz-type equations by the landweber method," *Engineering Analysis with Boundary Elements*, vol. 28, no. 9, pp. 1025–1034, 2004.

[64] L. Marin, "A meshless method for the numerical solution of the cauchy problem associated with three-dimensional helmholtz-type equations," *Applied Mathematics and Computation*, vol. 165, no. 2, pp. 355–374, 2005.

[65] L. Marin and D. Lesnic, "The method of fundamental solutions for the cauchy problem associated with two-dimensional helmholtz-type equations," *Computers & Structures*, vol. 83, no. 4-5, pp. 267–278, 2005.

[66] A. Rap, L. Elliott, D. Ingham, D. Lesnic, and X. Wen, "Drbem for cauchy convection-diffusion problems with variable coefficients," *Engineering Analysis with Boundary Elements*, vol. 28, no. 11, pp. 1321–1333, 2004.

[67] D. Lesnic and G. Wake, "A mollified method for the solution of the cauchy problem for the convection–diffusion equation," *Inverse Problems in Science and Engineering*, vol. 15, no. 4, pp. 293–302, 2007.

[68] Z. Ranjbar and L. Eldén, "Numerical analysis of an ill-posed cauchy problem for a convection–diffusion equation," *Inverse Problems in Science and Engineering*, vol. 15, no. 3, pp. 191–211, 2007.

[69] L. Marin, L. Elliott, P. Heggs, D. Ingham, D. Lesnic, and X. Wen, "Dual reciprocity boundary element method solution of the cauchy problem for helmholtz-type equations with variable coefficients," *Journal of Sound and Vibration*, vol. 297, no. 1-2, pp. 89–105, 2006.

[70] D. Lesnic, "The decomposition method for cauchy advection-diffusion problems," *Computers & Mathematics with Applications*, vol. 49, no. 4, pp. 525–537, 2005.

[71] N. Alsoy-Akgün and D. Lesnic, "A numerical solution for an inverse natural magneto-convection problem," *Numerical Heat Transfer, Part B: Fundamentals*, vol. 63, no. 2, pp. 115–138, 2013.

[72] J. Chen, W. Han, and F. Schulz, "A regularization method for coefficient identification of a nonhomogeneous helmholtz equation," *Inverse Problems*, vol. 10, no. 5, p. 1115, 1994.

[73] F. Gylys-Colwell, "An inverse problem for the helmholtz equation," *Inverse Problems*, vol. 12, no. 2, p. 139, 1996.

[74] M. Burger and W. Mühlhuber, "Iterative regularization of parameter identification problems by sequential quadratic programming methods," *Inverse Problems*, vol. 18, no. 4, p. 943, 2002.

[75] L. Marin, L. Elliott, P. Heggs, D. Ingham, D. Lesnic, and X. Wen, "Parameter identification in helmholtz-type equations with a variable coefficient using a regularized drbem," *Inverse Problems in Science and Engineering*, vol. 14, no. 8, pp. 837–858, 2006.

[76] M. Tezer-Sezgin and C. Aydin, "Parameter identification in mhd duct flow cauchy problem using the drbem," in *Journal of Physics: Conference Series*, vol. 1141, p. 012032, IOP Publishing, 2018.

[77] R. Zheng, C. Coleman, and N. Phan-Thien, "A boundary element approach for non-homogeneous potential problems," *Computational Mechanics*, vol. 7, no. 4, pp. 279–288, 1991.

[78] A. G. Ramm, *Inverse Problems: Mathematical and Analytical Techniques with Applications to Engineering*. Springer, 2005.

[79] V. Kozlov, V. Maz'ya, and A. Fomin, "An iterative method for solving the cauchy problem for elliptic equations," *Comput. Maths. Math. Phys.*, vol. 31, no. 1, pp. 45–52, 1991.

[80] U. S. Mahabaleshwar, I. Pažanin, M. Radulović, and F. J. Suárez Grau, “Effects of small boundary perturbation on the mhd duct flow,” *Theoretical and Applied Mechanics, 44 (1), 83-101.*, 2017.

CURRICULUM VITAE

PERSONAL INFORMATION

Surname, Name: Aydın, Cemre
Nationality: Turkish (TC)
Date and Place of Birth: 18.07.1991, Ankara
Marital Status: Single
E-mail: cmr.metu@gmail.com

EDUCATION

Degree	Institution	Year of Graduation
B.S.	METU, Department of Mathematics	2014
High School	Fethiye Kemal Mumcu Anatolian High School	2009

PROFESSIONAL EXPERIENCE

Year	Place	Enrollment
2014-2018	METU, Department of Mathematics	Research Assistant

PROGRAMMING LANGUAGES

Matlab, C, C++

FOREIGN LANGUAGES

English (fluent)

PUBLICATIONS

1. C. Aydın, M. Tezer-Sezgin, *DRBEM solution of the Cauchy MHD duct flow with a slipping perturbed boundary* , Engineering Analysis with Boundary Elements, Vol. 93, pp. 94-104, 2018.

2. M. Tezer-Sezgin, C. Aydın *Parameter identification in MHD duct flow Cauchy problem using the DRBEM* , Journal of Physics: Conference Series, 1141, 2018.

3. C. Aydın, M. Tezer-Sezgin, *The DRBEM solution of Cauchy MHD duct flow with a slippingand variably conducting wall using the well-posed iterations* , An International Journal of Optimization and Control: Theories and Applications (IJOCTA), Vol.9, No.3, pp.76-85, 2019.

CONFERENCE PAPERS

1. C. Aydın, M. Tezer-Sezgin, *DRBEM Solutions of the Direct and Inverse Formulations of Cauchy Problem for the Magnetohydrodynamic Duct Flow*, Proceedings of the 17th International Conference on Computational and Mathematical Methods in Science and Engineering (CMMSE 2017), 4-8 July, 2017, Cadiz, Spain, pp. 154-165.

2. C. Aydın, M. Tezer-Sezgin, *DRBEM Solution of the Cauchy Problem for MHD Rectangular Duct Flow*, International Workshop on Mathematical Methods in Engineering (MME 2017), 27-29 April, 2017 Ankara, Turkey, pp. 47.

3. C. Aydın, M. Tezer-Sezgin, *The DRBEM Solution of the Cauchy MHD Flow in a Duct with one of the Walls is Slipping and Variably Conducting*, International Conference on Applied Mathematics in Engineering (ICAME 2018), June 27-29, 2018, Balikesir, Turkey, pp. 38.